PURJ (Sci.)

PANJAB UNIVERSITY RESEARCH JOURNAL (SCIENCE)

Vol. 73, 2023

PANJAB UNIVERSITY RESEARCH JOURNAL (SCIENCE)

VOL. 73, 2023

PANJAB UNIVERSITY RESEARCH JOURNAL (SCIENCE)
VOLUME 73, 2023

*The subscription of the journal may be sent in the form of a Bank Draft payable to **The Registrar, Panjab University, Chandigarh** and addressed to The Editor-in-Chief on the following address:*

Research Journal (Science)
Old Corresponding Building,
Panjab University, Chandigarh -160 014, (India)

The manuscripts for publication or any other enquiry is also to be addressed to the Editor-in-Chief.

Subscription fee:	**Inland**	**Foreign**
Annual Subscription:	Rs. 400/-	US $ 50
Life Membership:	Rs. 3000/-	US $ 250

Printed in 2024

CORRIGENDUM

(Pint Issue)

PANJAB UNIVERSITY RESEARCH JOURNAL (SCIENCE)

VOLUME 73, 2023

INSTALLATIONS AND FASHION EXHIBITS: A CONTEMPORARY COMMON GROUND OF ART, FASHION & TEXTILE

Prabhdip Brar and Bharti Sharma,
University Institute of Fashion Technology & Vocational Development, PU, Chd

ABSTRACT

With the infinite exploration in new media and materials, technical advancement, the boundaries and traditional definitions of art, craft, design, fashion, textiles have become harder to map and are expanding to different modes of visual presentation. This interesting space developed by interdisciplinary practices, is beyond the conventional definitions of Art and fashion as a practice and as a discipline. This paper is an exploration of these interdisciplinary practices in India in the field of textile, embroidery, fashion and art observed through the medium of installations and fashion exhibits.

INTRODUCTION

The domain of Art and Fashion, their effect and relationship, have been at the core of the research repertoire for long; however, the extant literature on these subjects has briefly touched upon the present interdisciplinary practice in the Indian context. This paper is an attempt to weave the stimulating unison of the two disciplines: Art and Fashion, and capture its metamorphosis into mediums like installations and fashion exhibits.

A gap was identified with theoretical literature in the exploration of this subject in context to the Indian domain and designers. The paper aims to explore and present these interdisciplinary dialogues and practices taking place in the contemporary Indian setting. Further the paper attempts to explore the intersection of Fashion and Art focusing on installation and exhibit pieces and their fluent transitions. These observations, explored through the practices of Indian fashion and textile designers in the past decade. This will widen the existing knowledge and document the visual vocabulary used by the contemporary practitioners of this style in India.

Art, Fashion and Installations

Through advancing cultures and the changing landscape of the society, the definitions of Art and Fashion have been reframed and continually evolved. Fashion has drawn on the iconography of its socio-cultural setting emerging as a cultural phenomenon, and so has art developed as a means of expression and aesthetic experience. Both disciplines guided by society, culture and the canons of art and aesthetics, have their share of differences and similarities. Geczy and Karaminas (2013) connect art and fashion in terms of their creation of imaginary worlds and their practice of utilizing a language of style to invigorate beliefs, perceptions, and ideas.Art historians, philosophers, critics and fashion experts have attempted to find answers and mark boundaries between the two, but have yet not arrived at any clear unequivocal definition to label this complex articulated symbiosis between the two.

Douglas et al. (2022) described art as a means to serve established systems of power. These systems, namely religion and the state, reciprocally rendered meaning, value and accessibility to art. These power structures in a profound way shaped and defined the content of artistic works.

The beginning of **art** was in the form of communicative icons and symbols, thereafter taken over by religion and orders of power. During the 19th century, guided by the artist‘s inherent urge for freedom from the limitations of history paintings and religious subject, modern movements like Impressionism, Fauvism, and Expressionism were born. Furthermore, the socio-political environment has time and again triggered and challenged the manifestation of creative expression and spirit among artists birthing numerous movements and isms throughout history.

Yuniya Kawamura deliberated that the term "fashion" is most commonly associated with clothing and styles of appearance. Although the word can be interpreted in various ways and forms, it is often used in a broad and ambiguous manner, as something associated with clothing fashion (as cited in Benton, 2012) .On the contrary, Valerie Steele questions why, one considers a classical Balenciaga evening dress, though produced within the fashion industry as a work of Art, when displayed on a pedestal or in a glass case in a museum (Geczy & Karaminas, 2013). In this context, Anne Hollander was often promoting the idea of fashion being an evolved part of visual art as much as painting and sculpture were, being a result of aesthetics experimentation and innovation. She suggests that an integral aspect of clothing is the creations of a strong

Corresponding author: drpbrar@pu.ac.in
Received: September 28, 2023, Accepted: December 20, 2023

visual impact that again links to the one created by visual art, which is often defined as the 'aesthetic' in art.

Installation is identified as a form that uses or occupies space. Also described as 'environments' these works not just engage, but immerse the viewers in itself and proceed to incorporate them as one of the key components of the works. Reflecting on the unified experiences, artist Ilya Kabakov further highlights the role of the viewer as the 'main actor', the focal point and the centre to which the installation gravitates to (Tate, n.d.). It is the viewer who is the part of the work and to whom the work is intended and addressed to. Speaking on the setting of an installation, Geczy & Karaminas (2019) state that the space can be a physical one in an architectural setting of a museum or can be more imaginative and ephemeral, beyond the conventional exhibition space. Installation in its true essence is both material and immaterial, rejecting the notion that art can only be perceived objectively or in isolation from its spatial, temporal and cultural context. They draw a parallel between installation and fashion objects. In their opinion installation art is primarily well-suited for showcasing fashion, especially in the contemporary era, as designers now experiment with increasingly advanced methods to present fashion items. These items are not standalone pieces but are instead part of a broader network of representations and narratives.

In the course of time, society has witnessed myriad connections, collaborations, similarities and parallels between these three, Art, Fashion and Installations. Highlighting the blurring perception of boundaries between museum exhibits and fashion Andy Warhol once prophesised, "All department stores will become museums, and all museums will become department stores".

Art and Fashion a dialogue begins

The link between Art and Fashion have been studied by researchers like Richard Martin in his works Fashion and Surrealism-1987 and Cubism and Fashion- 1998, Peter Wollen (1998) & Judith Clark (2014), Adam Geczy and Vicki Karaminas (2019) to name a few. They have tried to draw parallels between art and fashion exhibits; art movements and fashion, borrowing motifs and styles from each other yet maintaining their respective disciplines.

The convergence of the two in recent times is quite evident, especially by fashion exhibits marking their presence in spaces which were originally confined to showcasing art. Dutch fashion curator and theorist José Teunissen marks this steady shift to the 1960s emphasizing on the sustained blurring of art and fashion. The exhibition titled 'The Art of Fashion: Installing Allusions' (2009), curated by Teunissen and Clark, is an instance of an unequivocal dialogue between art and fashion, presenting fashion installations which also abandon the principle of wearable clothing. Judith Clark was a pioneer and one of the first fashion curator to introduce contemporary fashion into the gallery setting (Torres, 2017).

Figure 1: The Art of Fashion: Installing Allusions (2009)

(1) Hussein Chalayan Inertia collection (2) Nick Cave, Soundsuit

It's hard to point to the beginning of this dialogue between Art and fashion, but Stefania Ricci attempts to discover this through her curatorial exhibition titled, "Across Art and Fashion". She tries to capture the merging of the two worlds in the form of reciprocal inspirations, intersections and collaborations, from the experiences of the Pre-Raphaelites to those of Futurism and from Surrealism to Radical Fashion. Ricci (2016) writes about the exhibition curation, which in her opinion, began with the English Pre-Raphaelites and moved through the Viennese Secession led by Gustav Klimt and the Wiener Werkstätte, followed by Mariano Fortuny, while also acknowledging the innovative work of the Futurists. It then examined the contributions of artists involved in fashion, like Sonia Delaunay, as well as direct collaborations between artists and fashion designers, such as Thayaht with Vionnet and Dalí and Cocteau with Schiaparelli, continuing up to more recent partnerships. The focus is placed on designers who, inspired by art, transformed the fashion world, exemplified by Yves Saint Laurent's work with Mondrian. This theme is explored from diverse and multifaceted perspectives, such as, artists who offered alternatives to contemporary trends, those who collaborated with the fashion industry, fashion designers who sought the creativity of artists, and those who shared avant-garde ideas. Above all, it highlights how designers drew inspiration from art across various eras for their shapes and surfaces.

Having archived some of the greatest collaborations in art and Fashion through the 19th and 20th century, Cutler and Tomasello in their book 'Art + Fashion:

Collaboration and connections between icons' have captured the true flavour and essence of the term 'collaboration'. Having used this term collaboration to feature garments to public art installations, film to photography editorials. While making a selection of these collaborations out of infinite options, they state "But to exclude inspired work based on the narrow confines of a definition seemed as shortsighted, purposeless, and self-defeating as separating art and fashion" (Cutler & Tomasello, 2015).

Discussing the intermingling of these two disciplines, the work of American artist Jeff Koons 'inflatable bunny- 1986' saw itself moulded into a miniaturized rabbit pendant in platinum for Stella McCartney's collection. In 1951 on a four-page spread in Vogue magazine, the massive action paintings of Jackson Pollock, were photographed by Cecil Beaton not as an independent work of art but as a fluid backdrop for "Spring Ball Gowns". Adding to these encounters of Art and fashion is the non-objective neo plastic works of Mondrian, which complimented the mod style of the fashion industry. Mondrian works when used by Yves Saint Laurent, produced a Beatles-like fervour (Cutler & Tomasello, 2015).

Figure 2: Jeff Koons's "Rabbit", Photograph by John Lamparski / Getty

Figure 3: Rabbit – Collaboration with Stella McCartney

Japanese fashion designer Issey Miyake, a futurist creative artist and the originator of design that lies at the intersection of all media, practices and approaches, used the medium of installation to present his works. Explaining his work, Benton (2012) opined that, although many people considered him as an artist and his creations have been showcased in the carefully curated environment of museum installations, his creations are complete only when worn and vitalized by the human body. He takes inspiration from sculpture, dance, theatre, and his perspective on the human form. The likes of western Designers like Elsa Schiaparelli (The Lobster dress, 1937), Raf Simons (No Man's Land, 2019) and Henrik Vibskov, are some of the eminent practitioners of fashion's ongoing intersection with the art installations. These Liveable and breathable installations give visitors a new way to experience and appreciate fashion and also serve a purpose of immersive storytelling adding more integrity to these consumables.

Collaborations and connections between the two: Indian landscape

Today one finds a plethora of interactions between art and fashion in the work of Indian designers. Promoting these interdisciplinary practices in the Indian industry, one can find numerous designers and foundations in the present contemporary Indian art and design setting. This industry is not only experimenting with different mediums but foundations like Devi Art Foundation, Indian Art fair etc. are providing a platform for these interdisciplinary explorations.

Eminent designer- Gopika Nath identifies herself as a 'textile artist craftsman', beautifully illustrating the fluidity of disciplines, her works like the Stitch journals again reinfuses interdisciplinary practices. Another recent exhibition titled "Fracture: Indian Textiles, New Conversations" curated by Mayank Mansingh Kaul, Rahul Jain and Sanjay Garg illustrate the fluid interplay of art, fashion and textile. It is a project conceived by textile and fashion designers, textile craftspeople, graphic artists, and filmmakers to create art exhibits and installations using the medium of craft, embroideries and textiles of India. As explained by Mayank Mansingh Kaul, "The show also comes at a time when there is a need to create reflective writing and curatorial works on contemporary design in India, and with this we are trying to push museum-quality work in contemporary textiles which can be shown in a gallery-format" (Devi Art Foundation, 2015).

Figure 4: Interface- Series of Contemporary Chamba Rumalsby Swati Kalsi. Delhi Crafts Council.

Figure 5: Textile designer Meera Narula explores Phool Patti ka Kaam or Aligarh Kaam, a traditional north Indian embroidery technique.

Contemporary multidisciplinary designers like Swati Kalsi, Meera Narula, Rimzim Dadu, Gopika Nath and Meera Narula create installations, tapestry, journals and surface explorations developing these new media approaches. Péro's exhibit titled "Time to Love", in the Indian Art Fair 2020 is another example of the fashion exhibits; the brand "Pero" by Aneeth Arora wanted the audience to experience their production process and present it as an art form. Pero not only displayed their work in the form of garments and installations but went one step ahead with the performance, which Arora describes in his words, "The purpose of the exhibit is to involve people in the process of our garment making. We want them to be a part of the journey; hence we haven't used a lot of garments. Instead, you will find hanging textiles and buttons. It's all about (raising awareness) of the effort that goes in making the clothing. You feel the evolution when you see it all in its entirety".

Figure 6: Pero 'Time to Love' exhibition, in the Indian Art Fair 2020

Meaningful consumption

Another factor identified during the literature review was the unison of luxury fashion brands and contemporary new media art practices to attract, engage and offer immersive storytelling to the consumer. As stated in 'Fashion and Art', Geczy and Karaminas (2012) remark that as and when a fashion object is displayed in a museum or gallery, the value of that object being a commercially driven mass market product transforms from a consumable merchandise to a unique creative installation. This also strengthens the role of fashion of not only being confined to consumable merchandise, but also a new value system that identifies it as a collectable (Codignola, 2016). The consumer today demands for something intangible and meaningful that goes beyond a tangible luxury product and offers an experiential dimension. To address these demands, fashion finds a strategic solution in art. It is in the being of art, as described by Adam (2014) and Wagner & Wagner (2013), that it can emit an aura of originality, exclusivity, tradition, timelessness, and transcendence. This can also be counted as a reason for the traditional borders isolating fashion, culture, and art to become more fluid.

CONCLUSION

"My work is an amalgamation of both fashion and art,
and I exist within their fluid interface".
Nick Cave

The encounters of art and fashion have been around since the early 19th century and have exponentially grown in the contemporary times. Today artists and designers have marched forward beyond the confines of the limited definitions of various disciplines. Expressions in the form of art or fashion have grown beyond the material dimensions giving origin to the use of multidisciplinary mediums. Today the act of creation is led by collaboration; interplay and connections between multiply disciplines.

Figure 7: Akhila Krishnan, Naksha: Patterns in Space and Time, 2014

REFERENCES

Adam, G. (2014). *Big bucks. The explosion of the art market in the 21st century*. Lund Humphries.

Benton, A. (2012). *Fashion as Art/Art as Fashion: Is Fashion, Art?* [Master ‘s thesis, The Ohio State University]. The Ohio State University

Clark, J., Haye, A. D. L., & Horsley, J. (2014). *Exhibiting fashion: Before and after 1971*. Yale University Press.

Codignola, F. (2016). The Blending of Luxury Fashion Brands and Contemporary Art: A Global

Strategy for Value Creation. In A. A. Vecchi & C. Buckley (Eds.), *Handbook of Research on Global Fashion Management and Merchandising* (1st ed., pp. 50-76). Business Science Reference (an imprint of IGI Global). DOI: 10.4018/978-1-5225-0110-7.ch003

Cutler, E. P., Tomasello, J. (2015). *Art + Fashion: Collaborations and connections between icons.*

Chronicle Books.

Devi Art Foundation. (2015). *Fracture : Indian Textiles, New Conversations* [Exhibition catalogue]. Exhibited at New Delhi 21 Jan 2015 – 30 May 2015.

Douglas, S., Geczy, A. & Lowry, S. (Eds.). (2022). *Where Is Art?*.Routledge.10.4324/9781003037071-2

Geczy, A., & Karaminas,V. (2013). *Fashion and Art*. Bloomsbury Publishing.

Geczy, A., & Karaminas, V. (2018). *The End of Fashion: Clothing and Dress in the Age of Globalization*. Bloomsbury Publishing.

Geczy, A., & Karaminas, V. (2019). *Fashion Installation: Body, Space, and Performance.* Bloomsbury Publishing. 10.5040/9781350032545.0004

Marchetti, L. (2016). Fashion Curating. *European Academy of Design Conference Proceedings*. DOI:10.7190/ead/2015/161

Petrov, J. (2019) *Fashion, History, Museums: Inventing the Display of Dress*. London: Bloomsbury Academic. DOI:10.5040/9781350049024

Riley, A. (2022). *History of Fashion Installations as Art Exhibitions and Their Impact on the Public*

Impact on the Public's Perspective on Culture and Community [Master‘s thesis, Sotheby's Institute of Art]. digitalcommons.sia.edu

Ricci, S. (2016- 2017). *Across Art and Fashion* [Exhibition catalogue]. Exhibited at Salvatore Ferragamo 19 May 2016 - 7 April 2017.

Sbordone, M. A. (2020). Art and Fashion a New Approach. *Advances in Design, Music and Arts, 7th Meeting of Research in Music, Arts and Design* (pp.269-284). EIMAD. DOI:10.1007/978-3-030-55700-3_19

Tate. (n.d.). *Installation art* | Tate. Retrieved July 9, 2023 from https://www.tate.org.uk/art/art-terms/i/installation-art

Torres, L. (2017). Fashion in the Expanded Field: Strategies for Critical Fashion Practices. *Journal of*

Asia-Pacific Pop Culture, 2(2), 167-183. doi:10.5325/jasiapacipopcult.2.2.0167

Wagner, E., & Wagner, T. W. (2013). *Collecting art for love, money and more.* Phaidon

Wollen, P., & Gallery, H. (1998). *Addressing the Century - 100 Years of Art and Fashion*.

Hayward Gallery Publishing.

Yuli, B. (2010). *Fashion Design and Art Collaborations: An Investigation of the Collaborations*

Between Fashion Designers/Brands and Artists [Doctoral dissertation, The Hong Kong Polytechnic University, Institute of Textiles and Clothing (ITC)]

CHEMICAL ANALYTE INTERACTIONS OF METAL-FREE PHTHALOCYANINE THIN FILMS BY DIFFERENT VIBRATIONAL TECHNIQUES

Sukhwinder Singh
Principal Govt. Ranbir College, Sangrur, India

ABSTRACT

Thin films of Metal-free phthalocyanine have been deposited on KBr and glass substrates by thermal evaporation method and characterized by the X-ray diffraction and spectroscopic optical absorption techniques. The observed X-ray pattern suggests the presence of α crystalline phase of Metal-free phthalocyanine in the as-deposited thin films. Infrared spectra of thin films on the KBr pallet before and after exposure to the vapours of ammonia and methanol have been recorded in the wavenumber region of 400-1700 cm^{-1}. Shifts in the position of some IR and Raman bands in the spectra of exposed films have been observed. Some bands also show change in their intensity on exposure. The observed infrared bands also confirm the α crystalline phase. On vapour exposure change in the intensity of some bands is observed that may be attributed to its attachement towards hydrogen atom site of H_2Pc. Changes in the intensity of bands are interpreted in terms of the lowering of molecular symmetry from D_{2h} to C_{2v} due to formation of hydrogen bonds.

Key words: Metal-free phthalocyanine thin film, Chemical sensing, Infrared spectra, XRD spectrum, Optical absorption.

INTRODUCTION

Phthalocyanines (Pcs) are a class of organic semiconductors which have attracted much interest because of their high thermal and chemical stability, various synthetic modifications, ease of preparation of devices and reproducibility of experimental data. It is well known that Metal-free phthalocyanine (H_2Pc) and its complexes were used as photoconductors and absorb light on either side of blue-green region in the visible spectrum [1]. H_2Pc is a planar molecule having D_{2h} symmetry is found to exist in at least three polymorphic (α, β, γ) forms. The β-form is the most stable polymorph and a single crystal can be prepared by sublimation at 550^0C. These materials are generally P-type semiconductors and are stable towards chemical and heat. They are of great technological and fundamental interest, both because of their own properties and because of their similarity to other classes of compounds. The conductivity of these materials depends on the gaseous environment, and thus gas sensors based phthalocyanines have recently attracted considerable interest [2]. Optically-active phthalocyanines are grouped into several categories [3]. The eximious stability characteristics of Pc compounds have resulted in their extensive applications as chemical sensors [4], organic solar cells (OSCs) [5], as gas sensors [6], liquid crystal [7]. In very recent times, these compounds have been successfully tested for the detection of volatile organic compounds also by optical techniques [8]. Adsorption of gases on the surface of Pc thin films induces change in the electrical conductivity of Pc films [9]. In the gas sensing field, the electrical conductivity changes are induced in Pc thin films by adsorption of oxidizing or reducing gases on the surfaces. Hence, sensing properties of Pcs have been extensively studied by the electrical conductivity measurements. Detection of NO_2 gas down to 25 ppb concentration with a lead phthalocyanine film has been attained [10]. In order to understand the mechanism of sensing action, various spectroscopic techniques have also been employed [11-13]. In earlier studies, we have also reported the possibility of electron transfer from the methanol and ammonia to CuPc in order to explain the decreased conductivity of CuPc in the presence of these vapours [13,14]. In literature, there are few reports of Raman and infrared (IR) spectral studies of Pc thin films sensing [15–17]. However, vibrational spectroscopic techniques are not frequently used for the study of sensing properties of Pcs, though these techniques provide valuable data that can be used in the investigation of interaction between chemicals and Pc on molecular level. The vibrational frequency positions are sensitive to the sub-°A changes in bond length.

Corresponding author: ss8421462@gmail.com
Received: November 30, 2023, Accepted: December 15, 2023

Intensities of vibrational bands provide information about the orientational changes due to distortions in molecules. Moreover, IR absorption spectroscopy has also been used to identify the crystalline nature for both powder and thin films of Pc [18,19]. Despite being an important tool to study the material at molecular level, one probable reason for the lesser use of vibrational spectroscopy in the study of sensing properties of Pc thin films is that a large number of bands due to different fundamentals, overtones and combination vibrations are generally present in spectra. This makes deciphering information from spectra really difficult. However, recently reported density functional theory (DFT) based normal coordinate analysis of copper phthalocyanine (CuPc) and zinc phthalocyanine (ZnPc) [20-22] have made it possible to assign the observed IR bands accurately and gain insight into the bonding arrangements. Chemical vapors induced changes in the structure of Pc molecules, therefore, can be monitored with the help of IR and Raman spectroscopy. These changes depend on the nature of interacting chemical vapors/gases.

In the present work, we analyze the IR spectra of H_2Pc thin films, before and after exposure to the vapours of ammonia and methanol to investigate the effect of vapours on H_2Pc molecule by monitoring the changes in the spectra. Thin films are also characterized by X-ray diffraction (XRD) and optical absorption techniques.

EXPERIMENTAL

In the present study, H_2Pc powder (sublimed grade, dye content 99 %) from Aldrich, is used without further purification. Methanol and ammonia from Qualigens Fine chemicals, India, are used without further purification. Thin films of H_2Pc have been deposited on KBr and Corning 7059 glass substrates by vacuum evaporation technique by keeping substrate at room temperature and base pressure of $2x10^{-5}$ mbar, using a molybdenum boat. The films have been kept in the deposition chamber in dark for 24 hours to attain thermodynamic equilibrium [21]. The thickness of the film, used in the present study, is found $\approx$ 810 A° with a Surface Profiler Decktak 3030 ST. The IR spectra of the film deposited on the KBr substrate are recorded with a Perkin Elmer PE-Rx1 FTIR Spectrophotometer having spectral resolution of 1 cm^{-1}. The Raman spectra are recorded on a LabRam JY HORIBA HR 800 spectrograph equipped with the Olympus Bx41 microscope and ANDOR Model DU 420-0E-323 CCD detector. The measurements are carried out in a back scattering geometry with the incident light linearly polarized and scattered light was detected unpolarized. The excitation line at 488.0 nm is provided by an air cooled Ar+ laser. The UV-visible spectra were recorded on a HITACHI 330 UV-VIS-NIR Spectrophotometer having resolution of 0.07 nm. The crystalline nature of the thin films is characterized by using X-ray diffraction technique (Model: Philips PW 1610, Goniometer: Philips 1710, geometry configuration: $\theta - \theta$, detector: Cu Kα). Exposure of the thin films with each analyte vapour was done for 20 minutes in a desiccator under vacuum.

RESULTS AND DISCUSSION

The molecular structure of H_2Pc has a square-planar configuration with metal ion in its centre as shown in Fig. 1. The figure also shows the atom labeling scheme of the molecule. The molecule has an overall symmetry of D_{2h}, which can be inferred from the figure. Moreover, recent DFT calculations also resulted in the idealized D_{2h} point group symmetry for this molecule [23]. In present study, the H_2Pc thin films are characterized by optical, IR absorption and XRD spectroscopic techniques, as discussed below.

Optical absorption characterization

In the visible region of absorption spectrum of the as-deposited H2Pc thin film, we observe a broad Q band doublet at 610 and 691 nm [24] (figure 2). Intensity of the former band is more than the latter band. The Q-band is strongly localized on the Pc-ring, and is very sensitive to the environment of the molecule [25]. This band appears in the region between 620 nm and 700 nm. It can also be noticed that this band always shows the characteristic splitting (Davydov splitting) resulting from a dipole-dipole interaction in all thin films before and after annealing. The maxima in this region have been generally interpreted in terms of π-π^* transition between bonding and anti-bonding molecular orbital. The higher energy peak of the Q-band has been assigned to the first π-π^* transition on the Pc macrocycle [24]. The lower energy peak has been explained as a second π-π^* transition or as an excitation

peak or a vibration interval. The Q-band absorption was assigned to a π-π* transition from the highest occupied molecular orbitals (HOMO, □-orbitals) of eg symmetry [26]. This results in a doubly degenerate first excited state of ^1E_u symmetry. The split Q-band obtained for H_2Pc arises from its lower symmetry (D_{2h}) compared with that of planer MPCs (D_{4h}) and the consequent loss of degeneracy of the lowest unoccupied molecular orbitals (LUMO, □* -orbitals) orbital to produce Q_1 and Q_2 states.

XRD study

Figure 3 shows the XRD pattern of H_2Pc film. The film deposited at room temperature (305 K) are found to be amorphous in nature as shown in figure 3. We observe a broad diffraction band between 16 to 37^o suggesting, thereby, that most of the composition of thin film is amorphous. However, a peak at an angle of 6.67^o corresponding to d value = 13.280 Å is also observed. It arises due to (2 0 0) plane of α-crystallites belonging to the monoclinic symmetry [27,28]. Observed XRD pattern, therefore, suggests that H_2Pc is present with α-crystallites unit cell in the as-deposited thin film. The spacing of lattice planes of the crystallites and b axes are arranged parallel to the surface of the H_2Pc layer.

IR spectroscopic study

The IR spectra of H_2Pc thin film in 400-1700 cm^{-1} region under different experimental conditions are shown in figure 4. In order to simplify the assignment of observed IR bands, we assume that the film consists of H_2Pc molecules, since H_2Pc crystals are molecular solids. The molecule belongs to D_{2h} point group symmetry with 168 normal modes of vibrations. These vibrations can be broadly divided into two groups: one consisting of the in-plane vibrations of symmetry B_{1u}, B_{2u} and B_{3u} modes and are infrared active, while B_{1g} B_{2g} and B_{3g} and A_{1g} modes are Raman active. The A_u modes are vibrationally active. In the Raman spectra, we observe intense band of B_{1g} symmetry. Bands, which belong to the A1g and B_{2g} symmetry are also observed. We have utilized a simpler, qualitative approach to interpret the vibrational data of H_2Pc thin film on the basis of recently reported normal coordinate calculations [29-32]. These calculations along with the reported resonance Raman and IR studies of these complexes considerably simplify the assignment of vibrational bands of H_2Pc

The IR bands in 700-800 cm^{-1} region of the spectra of Pcs are often used to identify different polymorphs □, β, ε etc, because of their sensitivity to the crystal packing arrangements in thin films [33]. In the spectrum of as-deposited H_2Pc thin film before exposure (Fig. 4a), we observe bands at 712, 733 and 762 cm^{-1} with a shoulder at 771 cm^{-1}. The 712 cm^{-1} and 762 cm^{-1} bands can be can be assigned to C–H, N–H out-of-plane bending (doming) [32]. Band at 733 cm^{-1} has been assigned to N–H in-plane bending and has also contribution from isoindole stretching deformation [32]. The observed wavenumbers of these IR bands are in complete agreement with the reported positions of the bands of □- crystallites. Therefore, it is clear that □ crystalline form is present in the thin film. The presence of □ crystallite in the thin film is also supported by the appearance of unresolved bands at 863 and 871 cm^{-1}. Thus the observed IR band positions are in tandem with the XRD data. Kobayashi et al. [34] found intense bands in the range from 888 to 919 cm^{-1} what appears to be consistent with the metal ligands M–N, for Fe, Co, Ni, Cu, Zn, Pd and Pt series of phthalocyanines. In the present spectrum, the absence of such bands suggest that the sample under test does not contain any metal derivatives of phthalocyanines.

In the IR spectra of H_2Pc thin film exposed to different chemical vapours (Figs. 4b,c), we observe C-H bending modes at 712, 733 and 762 cm^{-1} with a shoulder at 772 cm^{-1}. These band positions match well with the corresponding bands in the IR spectrum of as-deposited H_2Pc thin film of □-phase. Hence, it is clear from the observed band positions that crystalline form of the thin film does not change on exposure to vapours. Therefore, it can be inferred from this observation that bonds orders are nearly identical in the □- H_2Pc films before and after exposure to the chemical vapours. However, in the presence of vapors, relative intensity of almost all bands e.g. at 1005, 1117, 1172, 1313, 1429,1451, 1502, 1535, 1628, and 1647 cm^{-1} is decreased with respect to the to C–H, N–H out-of-plane bending (doming) 712 cm^{-1}. It seems that the symmetry of H_2Pc molecules in the exposed thin film is changed from D_{2h}. Since the vapours used in the present study are well known coordinating chemicals, therefore, it is possible that vapour molecule attaches to the hydrogen atom site of the H_2Pc. Due to interaction of vapors, hydrogen atom moves out of plane and decrease the overall molecular symmetry from D_{4h} to C_{2v}. As a result

some bands may gain intensity due to relaxation of the selection rules for C_{2v} point group. For example, bands of the B_{1u} species in D_{2h} become IR active as they correspond to A_1 species in C_{2v}. On the other hand, some bands may loose their intensity also as observed by us. Intensity of the band at 1380 cm^{-1} s less than the intensity of as-deposited thin film and this band arises due to isoindole stretching and isoindole deformation and in-plane bending of C-H atoms [23]. Therefore, presence of this band with the reduced intensity in the spectrum of exposed thin film relative to the as-deposited also supports the coordination of vapour molecule to the hydrogen atom of H_2Pc. On exposure the position of most of the IR bands do not show any significant shift except small and negligible shifts only in few bands.

It is well known that H_2Pc is a p-type organic semiconductor. Ammonia and methanol forms hydrogen bond with hydrogen and nitrogen atom of H_2Pc. Methanol forms hydrogen bonds using oxygen atom while ammonia using nitrogen atom and methanol form more stable hydrogen bonds than ammonia and decreasing intensity of almost all the bands. Ammonia and methanol molecules have lone pair of electrons, which can be transferred to other electron accepting molecules such as H_2Pc. When ammonia or methanol is attached to the hydrogen atom site of H_2Pc, some electron density from the coordinating molecule is transferred to the H_2Pc. The increased electron density reduces the number of holes in the sample by occupying the vacant sites with concomitant decrease in the electrical conductivity of the H_2Pc material as reported by us elsewhere [35]. This further justifies our point that these chemical vapors attach at the out-of-plane coordination site of hydrogen atom. Therefore, on one hand, a decrease in the conductivity of the H_2Pc thin film is observed on exposure [35], on the other hand due to negligible change in the bond orders and bond lengths, IR bands do not show much shift in their positions but show quite appreciable change in their intensities.

Raman spectra

The Raman spectra of H_2Pc thin film under different experimental conditions are shown in figure 5 and 6. The observed bands and their assignments are listed in the respective figures. There are few differences in the spectra of H_2Pc thin films before and after exposure with the methanol vapours. Some bands show shift in their positions after exposure. Intensity of some bands also changes on exposure. The bands observed in between 1085 to 1230 cm^{-1} are most contributed from C-H in-plane bending vibrations, two of which are 1109 and 1123 cm^{-1} are found to contain benzene breathing vibration and one at 1165 cm^{-1} is found to contain the isoindole stetching vibration. The typical stretching vibration of the benzene nucleus in isoindole which corresponds to the peak observed at 1618 cm^{-1}. The bands at 1410 and 1432 cm^{-1} were described as isoindole ring stretches. Bands observed at 482, 566, 584 cm^{-1} and at 151, 685, 725, 1109, 1312 in the spectra of as-deposited H_2Pc thin film (figure 5a and 6a) show small but important upward shift of 2 cm^{-1} and 1 cm^{-1} respectively. Bands observed at 1339, 1410, 1432, 1538 cm^{-1} show downward shift of 2 cm^{-1} on exposure with the methanol vapours. These shifts indicates towards a slight increase in the bond order of H_2Pc molecule due to the □ back donation of electron density to the ring when methanol interacts with the hydrogen and nitrogen atoms of H_2Pc.

The relative intensity of bands at 151, 232, 482, 566, 685, 725 cm^{-1} and 1029, 1109, 1515, 1536, 1618 cm^{-1} are increased and decreased respectively on exposure with methanol. The bands at 353, 442, 878, 1063 and 1212 cm^{-1} disappear in the spectra of exposed H_2Pc. On the other hand, new bands at 181, 362, 409, 532, 864, 885, 916, 1117, and 1263 cm^{-1} appear after exposure. Also band at 1367 cm^{-1} in the as-deposited H_2Pc spectrum is due to pyrrole ring stretching. The appearance and disappearance of these bands and change in the relative intensity of the observed bands once again confirm the coordination of methanol vapours with hydrogen and nitrogen atoms of the H_2Pc. Small upward shift in the wavenumbers of Raman bands after exposure is due to the charge transfer from vapour molecules to the ring. Changes in the intensity of vibrational bands are due to the out-of-plane distortion of the ring, when vapour molecules attach to with hydrogen and nitrogen atoms of the H_2Pc.

Conclusions:

From the above discussion, it is clear that observed IR and XRD spectra show the presence of □ crystalline H_2Pc in the as-deposited thin films. When these films

are exposed with methanol and ammonia vapours, changes in the wavenumbers and intensity of some IR bands are observed. Relative intensity change of bands in the spectra of exposed films may be explained on the basis of hydrogen bond with hydrogen and nitrogen atom of H_2Pc thin film. Coordinated vapour molecule donates some of its charge to the Pc ring via hydrogen atom. This charge transfer is responsible for most of the changes in the wavenumbers of the IR bands. The coordination of vapour molecules also induces an out-of-plane distortion in the Pc ring by moving the hydrogen atom out of the mean Pc plane. Displacement of hydrogen atom lowers the symmetry of H_2Pc from D_{2h} to C_{2v}, which accounts for the intensity changes in the vibrational bands

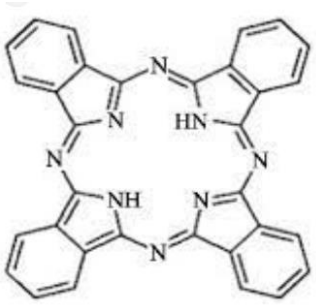

Figure 1: Structure and atom labeling scheme of H_2Pc

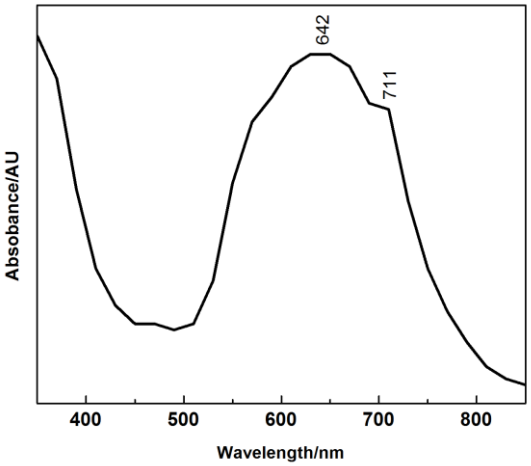

Figure 2: Optical absorption spectrum of the as-deposited H_2Pc thin film in 350-800 nm region.

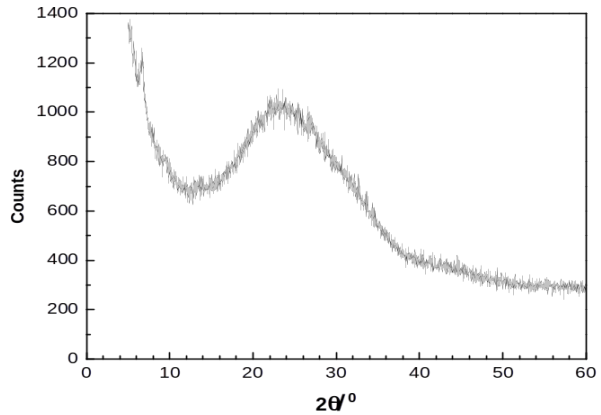

Figure 3: XRD pattern of H_2Pc thin film

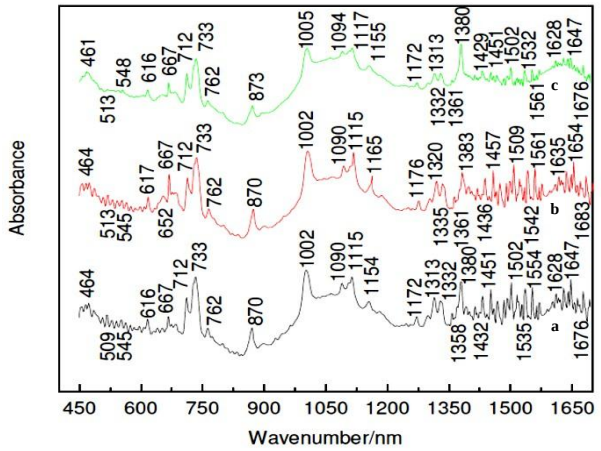

Figure 4: IR spectra of the H_2Pc thin films, (a) as-deposited; (b) exposed to ammonia; and (c) exposed to methanol in 400-1700 cm^{-1} region.

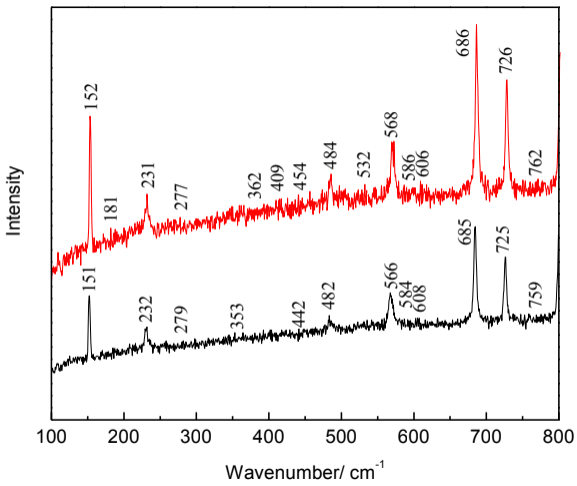

Figure 5: Raman spectra of the H_2Pc thin films, (a) as-deposited and (b) exposed to methanol in 100-800 cm^{-1} region.

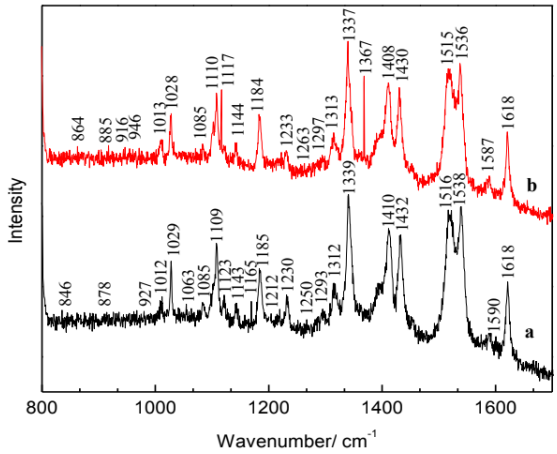

Figure 6: Raman spectra of the H_2Pc thin films, (a) as-deposited and (b) exposed to methanol in 800-1700 cm^{-1} region.

REFERENCES

A. R. Inigo, F. P. Xavier, G. J. Goldsmith. *Mater.Res. Bull.* **32 (5)** (1997) 539

R. A. Collins and K.A.Mohamad, 21 (1998) 154

A. C. C Bacilla, Y. Okada, S. Yoshimoto, M. K. Islyaikin, K. I. Koifman, N. Kobayashi, Bull. Chem. Soc. Jpn, **94** (**1)** (2021) 34.

Li XL, Y. Xiao, S. R. Wang, Y. H. Yang, Y. N. Ma, X. G. Li, Bull. Chem. Soc. Jpn **8**, (2019) 787

T. Miyata, S. Kawaguchi, M. Ishii and T. Minami, *Thin Solid Films* **425** (2003)255.

A. Suzuki, H. Okumura, Y. Yamasaki, T. Oku, Appl Surf Sci. **488 (**2019) 586.

T. A. Temofonte, K.F.Schoch, *J.Appl.Phys.* **65** (1989) 1625

B.A. Minch, W. Xia, C.L. Donley, R.M. Hernandez, C. Carter, M.D. Carducci, A. Dawson, D.F. O'Brien and N.R. Armstrong, *Chem. Mater.* **17** (2005) 1618.

J. Spadavecchia, G. Ciccarella, G. Vasapollo, P. Siciliano, R. Rella, *Sens. Actuators B* **100** (2004) 135.

F. I. Bohrer, C. N. Colesniuc, J. Park, I. K. Schuller, A. C. Kummeland W. C. Trogler, *J. Am.Chem. Soc.* **130** (2008) 3712.

T. A. Tomofonte, K.F. Schoch, *J. Appl. Phys.* **65** (1989) 1350.

T. V. Basova , E. K. Kol'tsov and I. K. Igumenov *Sens. Actuators B* **105** (2005) 259.

A. Mrwa, M. Friedrich, A. Hofmann and D. R. T. Zahn *Sens. Actuators B* **25** (1995) 596.

S. Singh S, S. K. Tripathi and G. S. .S Saini *Mater. Chem. Phys.* **112** (2008) 793.

S. Singh , G. S. S. Saini and S. K. Tripathi in V. K. Aswal , K. G. Bhusan and J. V. Yakhmi (Eds.), Proceedings of the DAE Solid State Physics Symposium, vol. 50 (2005) Prime Time Education, Mumbai 22, India, p. 445.

T.V. Basova, E.K. Kol'tsov and I.K. Igumenov, Sens. Actuators B 105 (2005) 259.

D. Battisti and R. Aroca, *J. Am. Chem. Soc.* **114** (1992) 1201.

A.Mrwa, M. Friedrich, A. Hofmann and D.R.T. Zahn, *Sens. Actuators B* **24/25** (1995) 596.

D. Li , Z. Peng Z, L. Deng , Y. Shen and Y. Zhou, *Vib. Spectrosc.* **39** (2005) 191.

D. R. Tackley, G. Dent and W. E. Smith, *Phys. Chem. Chem. Phys.* **2** (2000)3949.

Z. Liu , X. Zhang, Y. Zhang and J. Jianzhuang, *Spectrochim. Acta A* **67** (2007)1232.

S.K. Tripathi, A. Kumar, *J. Non-Cryst. Solids* **104** (1988) 229.

E. A. Lucia and F. D. Verderame, J. Chem. Phys. 48 (1968) 2674.

X. Zhang, Y. Zhang, J. Jiang, Spectrochimica Acta Part A 60 (2004) 2195

D. Eastood, L. Edwards and M. Gouterman, J. Mol. Spectrosc. 20, 281 (1966).

Q. Chen, D. Gu, J. Shu, X. Tang and F. Gan, Mater. Sci. Eng. B 25, 171 (1994).

J. J. Andre and J. Simon, Molecular Semiconductors (Springer-Verlag, Berlin, 1985).

G. Maggioni et al, Sens. Actuators B 127 (2007)150.

U. Ashida, N. Uyeda, E. Suito, Bull. Chem. Soc. Jpn 39 (1966) 2616

N. M. Amar, R. D. Gould, A. M. Saleh, Current Applied Physics 2 (2002) 455

B. Stymne, F.X. Sauvage, G. Wettermark, *Spectrochim. Acta* **35A** (1979) 1195

X.X. Zhang, Y.X. Zhang, J.Z. Jiang, Vib. Spectrosc. 33 (2003) 153–161.

Xianxi Zhang, Yuexing Zhang, Jianzhuang Jiang, *Spectrochimica Acta Part A* **60** (2004) 2195

J. H. Sharp and M. Lardon, *J. Phy. Chem* **72 (9)**(1968) 3230

T. Kobayashi, F. Kurokawa, N. Uyeda and E. Suito, *Spectrochim. Acta A* **26** (1970) 1305

S. Singh, G. S. S. Saini and S. K. Tripathi Recent Advances In Condensed Matter Physics N. I. T. Hamirpur Abs 37 (2009)

AEROBIOLOGY OF ANGIOSPERM POLLEN GRAINS ALLERGIC REACTIONS - A CASE STUDY OF BIHAR, INDIA

Naira Nayab* and MD Anzer Alam
Department of Botany, Jai Prakash University, Chapra, Bihar, India

ABSTRACT

Aeroallergens present in the air causes respiratory and naso-bronchial allergy namely asthma, rhinitis, and skin allergy. In the present work airspora found in the air of Doriganj were examined by volumetric air sampler during the year 2023. Pollination Calendar of 42 angiosperm plant species was prepared. Result suggested that species of family Asteraceae were the most dominant. Pollen grains of *Acacia auriculiformis*, *Holoptelea integrifolia*,*Cynodon dactylon*, *Ambrosia artemisiifolia*, *Parthenium hysterophorus*, *Lantana camara*,*Amaranthus spinosus*, and *Ageratum conyzoides* were found to be noteworthy in terms of their allergenic properties. Pollination calendar is beneficial for the natives in diagnosing and treating patients with various aeroallergic conditions.

Keywords: - Aeroallergens, Airborne particles, Angiosperms, Diseases, Pollinosis, Pollination calendar.

Introduction

Meier (1930) coined the term aerobiology to describe a project that involved the study of life in the air (Lancia et al 2021). Airborne biological materials are known as bio aerosols (Pepper and Gerba, 2015). Aerobiology involves two primary aspects: the first focuses on the spread of biological materials, while the second involves assessing the type and amount of these dispersed substances within biological systems. Gregory (1952) coined the term 'air spora' to describe the particles suspended in the air that originate from plants and animals. The air spora consists of viruses, bacteria, algae, microscopic fungi, fungal spores, moss and fern spores, pollen, small seeds, fragments from plants and animals, protozoa, tiny insects, and more. This research work emphasizes on the pollen grains of flowering plants and airborne fungal spores that are responsible for the allergic reactions experienced by the natives. The pollen is the most vital part in the flowering plants with a special structure and function (Knox et al, 1986). Figure-1 shows the schematic image of mature pollen grain of angiosperm plant species. Pollen grains released by seed plants are the primary origin of airborne allergens responsible for respiratory issues. The feeling of itching could be due to the mixing of some fungal toxins into the yellow substance, or due to certain pollen being allergenic (Bera et al. 2018). Allergen is an antigen capable of stimulating Type-I hypersensitivity reaction in atopic individuals through Immunoglobulin E (IgE) responses (Shamji and Durham, 2017). Allergic rhinitis (AR), allergic rhino-conjunctivitis, and asthma affect a significant share of the global population, with a higher prevalence in developed countries. It is estimated that over 300 million people worldwide suffer from asthma, while Allergic Rhinitis occurs in about 500 million people, out of which 200 million have asthma as co-morbidity (Sukhan, 2019). Pollen is the most common cause of these respiratory diseases, as more than 150 pollen proteins have been proved to cause allergic sensitization (Suanno, 2022). Tree pollen remains high in the list of allergens in the spring seasons. Its scattering completely depends upon different kinds of pollen grains, availability of water content, type of carbohydrate and other channels to avoid desiccation during pollen release (Pacini 2009). Pollen production is mainly affected by meteorological factors amongst which temperature, rainfall, wind speed and direction are the important concentration moderators (Lattore and Caccvari 2009). In recent age aeroallergens has become a huge public health problem globally. The swift growth of industries, interactions within the immune system and the gradual effects of climate change are contributing to the proliferation and worsening of respiratory conditions like rhinosinusitis and asthma. A common long-term health condition that greatly affects the people of Doriganj is asthma. The presence of airborne allergens in Doriganj is of greater importance concerning societal problems such as pollen allergies

Corresponding author: nayabnaira@gmail.com, alamanzer@gmail.com
Received: October 20, 2023, Accepted: December 23, 2023

and become one of the most serious health issues. *Broussonetia papyrifera* (paper mulberry), *Alternanthera pungens* (Khaki weed), *Ambrosia artemisiifolia*, *Cannabis sativa* (marijuana), *Eucalyptus globules* (gum trees or Stringybark trees), Grasses, *Cynodon dactylon. Plantago major* (great plantain), *Parthenium hysterophorus* are common sources of pollen and some tree species, including *Ailanthus excelsa*, *Holoptelea integrifolia*, Palm and oak, also produces highly allergenic pollens. There is no adequate information available about aeroallergens in Doriganj. This study uncovers the link between the impact of pollinosis and fungal spores causing environmental pollution due to pollen concentration in the climate of Doriganj. In this study pollination calendar of 42 angiosperm plant species found in the flora of Doriganj and its surrounding areas were made. Eight (8) fungal spores were also identified as allergenic.

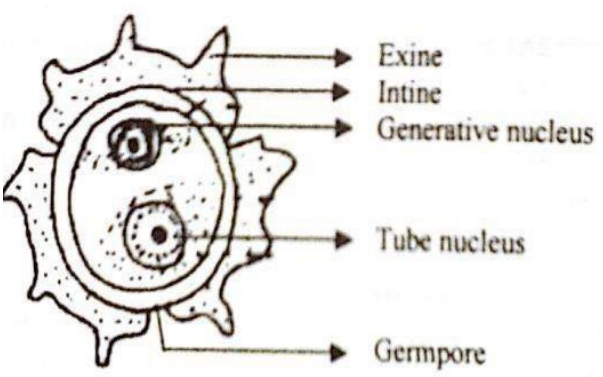

Source: https://qsstudy.com/describe-formation-structure-pollen-grain

Figure-1: Shows the schematic image of mature pollen grain of angiosperm species

MATERIALS AND METHODS SAMPLING SITE

Doriganj is 10 km. away from Chhapra town of district Saran, Bihar, India. It lies latitudinally of 25° 44' 0" North and longitudinally of 84° 50' 0" East. In the present study, the airborne spores and pollen trapping was done by using the Tilak Air Sampler (Tilak and Kulkarni; 1970). Four different locations in Doriganj (Bhairopur Nizamat, Doriganj Ghat, Doriganj chowk and Union bank road) were selected for monitoring biogenic allergens (Figure 2).

Source: https://www.veethi.com/places/Doriganj-map-114597.htm

Figure-2: Map of Study Areas within Doriganj

FIELD SURVEY

Periodic field visits were undertaken to observe the vegetation types and flowering seasons over a span of one year (2023). Plants were identified with the help of local people and other botanical resources. Key information such as habitat specifics, distribution patterns, cultivation methods, pollination mechanisms, flowering periods, and vernacular names were recorded. The flowering period is examined as the duration starting from the budding stage until the shedding of all flowers. Over a period of one year, detailed observations were recorded to create a comprehensive flowering schedule encompassing approximately 42 species across various habit types. This resource has provided pertinent details for easy detection of airborne pollen grains.

Meteorological Data

Data pertaining to meteorological conditions were gathered from the Indian Meteorological Department located in Patna. Table-1 provides information about the average seasonal fluctuations in meteorological parameters during the year 2023.

Table-1: Seasonal fluctuations in weather observed by the (PMD) during 2023

Parameters	Summer	Rainy	Winter
Mean Temperature ºC	33.15	30.25	18.30
Rainfall (mm)	3.20	6.80	1.0
Humidity (g.m-3)	57.5	80.42	20.5

Morphological Study Preparation of reference slides

The floral specimens gathered during the field survey were used to prepare reference slides of their pollen

grains following the method given by (Wodehouse, 1935). Approximately 20 slides were prepared as reference standards, aiding in the precise confirmation of different types of airborne pollen grains collected from the atmosphere.

Pollen morphology under microscopic observation

The reference slides prepared were examined under the compound microscope at magnifications of x1000. The aerial pollen grains were identified based on observations obtained during the study. The classification of size and shape categories based on Erdtman's (1952) proposed framework.

Preparation of a systematic guide to identify airborne pollen grains

It has been formulated by considering several morphological features. This key proved to be great tool in identification of air-born pollen grains.

Aerobiological Survey

Apparatus and its Applications

Samples were obtained using a volumetric Tilak A ir Sampler. The sampling process involved continuous operation of the air sampler, with its orifice projection tube maintained at a fixed height of one meter above the ground. To protect the apparatus from rain, it was covered with a polythene shield, which did not affect its sampling efficiency. This device, which is a cubical tin box, was powered by electricity and capable of providing continuous air sampling for eight days. Air was pulled into the sampler at a speed of five liters per minute and directed through a clear adhesive tape that covered a rotating cylinder coated with a thin film of petroleum jelly. This trap allowed for the collection of bio particles present in the air. The exposed cello tape was replaced after every 8 days and divided into 16 equal segments, each representing a 12-hour period of sampling, either during the day or night. These cello tape segments were then affixed to microscopic slides using glycerin jelly as a mounting medium. Macroscopic dust particles were removed with the help of a needle. The slides were gently heated using a flame to eliminate any moisture present. A cover glass measuring 18x18 mm is used to protect the materials. The slides were labeled with the respective locations and dates for identification purposes. The slides were now ready for observation under compound microscope x1000 magnification.

Spore and Pollen Analysis

The process of spore and pollen analysis includes identifying the unique morphological characteristics of spore and pollen grains through compound microscopic as well as a binocular microscope examination and comparison with reference slides. The identification of spores and pollens were performed by the method described by Faegri and Iverson in 1966.

Plant identification and Pollen preservation

A comprehensive knowledge of the distinct characteristics of pollen grains/spores and the indigenous plant species is crucial for precisely recognizing and detecting the dispersed spores and pollen particles in the air. One of the simplest and widely used methods of pollen preservation is air-drying pollen. After collection, pollen were spread on a clean surface or filter paper and allow to air dry. Once completely dried, store it in airtight containers or vials at low temperatures to prevent moisture absorption.

Preparation of Pollination Calendar

During the investigation, documented plants were categorized as mentioned in Table 5. Key information including family names, common names, botanical name, pollination methods, habitats, frequencies, and flowering periods were considered for the investigation. Plant population frequency is calculated by using the following formula.

Percentage Frequency = (Number of Sampling Units in which species occur) / (Total Number of Sampling Units Employed for the Study) ×100

RESULTS AND DISCUSSION

One year consistent field excursions were conducted and comprehensive information about the plant species within the Doriganj was documented. The study has unveiled the diverse species, encompassing a wide range of trees, shrubs, climbers, herbs, grasses. Regions predominantly sustained with cultivated crops such as *Triticum aestivum, Solanum tuberosum, Glycine max,* and *Zea mays.* Weeds like *Parthenium, Euphorbia,*

Alternanthera ficoides, Xanthium, Amaranthus, Argemone, Achyranthus, Lantana and *Datura* have also been recorded. Shrubs like *Ricinus* and *Calotropis* were prevalent in this region. Trees included *Ficus, Syzygium, Azadirachta, Tamarindus, Eucalyptus, Delonix, Melia, Peltophorum, Polyalthia, Spathodea. Mangifera.* Herbs like *Chrysanthemum, Ocimum, Catharanthus,* and *Dahlia* were also found. Pollen grains are dispersed into the air through diverse means during their transport. The classification of the plant species was done according to their mode of pollination as shown in Table-5. Out of 42 species, 30 belongs to entomophilous and rest from anemophilus mode. Grasses are anemophilous in nature. Most of the trees, shrubs, and herbs mentioned in Table-5 exhibited entomophily and anemophily mode of pollination. Out of the 42 plant species pollen grains of *Acacia penninervis, Holoptelea integrifolia, Cynodon dactylon, Ambrosia artemisiifolia, Parthenium hysterophorus, Lantana camara, Amaranthus spinosus, Ageratum houstonianum, Chenopodium album* were found to be allergenic. Out of these 42 species, 15 belong to trees, 7 to shrubs, 20 belongs to herbs and 1, belongs to climber. 7 are grown in gardens for their aesthetic value, 20 are grown for their edible fruits, and 15 are cultivated members. Plants such as,*Phoenix sylvestris, Parthenium hysterophorus, Amaranthus virdis, Argemone mexicana, Cyperus albostriatus, Eragrostis pilosa, Ipomoea alba,* and *Cassia tora* represent examples of indigenous or untamed vegetation. Allergenic significant plant species were also categorized on the basis of their mode of pollination. Airborne pollen grains were identified using direct microscopic methods. The identification of pollen grains was conducted by examining their morphological characteristics. The captured pollen grains varied in both size and morphology. During the one year sampling a total of 18 distinct types of pollen grains were identified. To distinguish pollen grains, factors such as dimensions, configuration, exine structure, whether they are simple or compound, as well as the type, quantity, and size of apertures were taken into account. The species have the smallest and the largest pollen grains. The pollen grains exhibit various shapes encompassing prolate, oblate, oblate spheroidal, spheroidal, prolate spheroidal, as well as sub-prolate and sub-oblate forms. Highest number of air-borne pollen grains was reported in the month of March and April. The second highest peak was observed during September and October. The observed peaks were found to align with the flowering seasons of plants with significant allergenic properties, namely grasses and trees. In September, the majority of grasses and certain herbs bloom, making a substantial contribution to the airborne pollen count. *Cassia fistula, Amaranthus viridis, Mikania micrantha, Zea mays* and *Parthenium* were found to be flower throughout the year. Grass pollen consistently prevailed in the air across all seasons. Table 2 illustrates the percentage distribution of different spore types in the air during three distinct seasons: summer, rainy, and winter. For instance, *Parthenium* spores were predominant during summer with 40.55%, while *Cladosporium* showed the highest prevalence during the rainy season at 26.20%. The varying percentages of different spore types across the seasons have indicated fluctuations in the composition of airborne spores. Table 3 presents the yearly mean concentration and percentage contribution of different spore types found in the air. *Cladosporium* exhibited the highest yearly mean concentration at 1449645 spores and contributed significantly with 65.80% to the total spore count. Alternaria follows with a concentration of 154,855, contributing 7.75%. Other spore types, such as *Parthenium*, *Aspergillus*, and *Helminthosporium*, also make notable contributions, while Chaetomium, Fusarium, and Ragweed contribute smaller percentages to the overall count. The table 4 illustrates the percentage distribution of various pollen types trapped during three different seasons: summer, rainy, and winter. Tree pollen constituted the highest proportion across all seasons, ranging from 82.8% to 85.65%, followed by Weeds (12.15-15.3%), Grass (3.32- 4.60%), and stable Unidentified Pollen (2.30-2.70%). Meteorological data, including temperature ranges, humidity, rainfall, and wind speed, was procured from the respective department. In Table 5 Pollination Calendar of Angiosperms present in Doriganj were given. The detail of the morphological characteristics such as exine structure, aperture types, and size range of various pollen types has also been described. Acacia: Polyad, Spheroidal, Granulate Exine, Porate Aperture, Size: 35x45 µm, Ageratum: Monad, Sub-oblate, Spinulate Exine, Colporate Aperture (3), Size: 19x22 µm, Argemone: Monad, Prolate Spheroidal, Finely reticulate Exine, Colporate Aperture (3), Size: 38x35 µm, Ailanthus:

Monad, Prolate spheroidal, Finely reticulate Exine, Colporate Aperture (3), Size: 30x28 µm, Cassia: Monad, Sub-Prolate, Finely reticulate Exine, Colporate Aperture (3), Size: 35x30 µm, Cheno-amaranthus: Monad, Spheroidal, Minutely Granulate Exine, Minutely Granulate Spines, Colporate Aperture (5), Size: 25x26 µm, Cymbopogon: Monad, Spheroidal, Psilate Granulate Exine, Prolate Aperture (1), Size: >50 µm, Clerodendon: Monad, Prolate, Reticulate Exine, Colporate Aperture (3), Size: 48x35 µm, Dalbergia: Monad, Prolate, Granulate Exine, Colporate Aperture (3), Size: 33x25 µm, Delonix: Monad, Prolate Spheroidal, Reticulate Exine, Colporate Aperture (3),

Size: 54x50 µm, Eucalyptus: Monad, Oblate spheroidal, Pislate Exine, Colporate Aperture (3), Size: 18x22 µm, Hibiscus: Monad, Spheroidal, Spinate Exine, Dimorphic Spines, Prolate

Aperture (5), Size: 114x115 µm, Holoptelea: Monad, Oblate Spheroidal, Granulate Exine,

Porate Aperture (3-5), Size: 25x28 µm, Parthenium: Monad, Spheroidal, Spinulate Exine, Colporate Aperture (3), Size: 16x16 µm, Phoenix: Monad, Oblate, Psilate Exine, Colpate Aperture (3), Size: 27x16 µm, Polyalthia: Monad, Spheroidal, Spinulate Exine, Inaperturate, Size: 30x30 µm, Syzygium: Monad, Oblate, Granulate Exine, Colporate Aperture (3), Size: 13x15 µm, Xanthium: Monad, Spheroidal, Spinulate Exine, Colporotate Aperture (3), Size: 22x23 µm.

Table-2: Seasonal % contribution of allergenic component in 2023

Spore Type	Summer	Rainy	Winter
Chaetomium	12.70	4. 26	11.12
Heliminthosporium	6.08	12.069	12.27
Alternaria	4.88	9.55	13.34
Aspergillus	5.18	9.96	8.56
Cladosporium	3.12	26.20	11.87
Parthenium	40.55	25.20	32.54
Fusarium	4.25	15.29	20.25
Ragweed	2.50	20.22	25.55

Table-3: Mean concentration and per cent contribution of different spore types

Spore Type	Yearly Mean Concentration	% Contribution
Chaetomium	12238	0.65
Heliminthosporium	35668	2.10
Alternaria	154855	7.75
Aspergillus	40470	3.04
Cladosporium	1449645	65.80
Parthenium	80246	5.12
Fusarium	10755	0.58
Ragweed	10865	3.5

Table-4 Seasonal variation of pollen grains/cm^2 (2023)

Pollen % Trapped	Summer	Rainy	Winter
Tree	82.95	85.65	82.8
Weed	14.50	12.15	15.3
Grass	4.20	4.60	3.32
Unidentified pollen	2.30	2.45	2.70

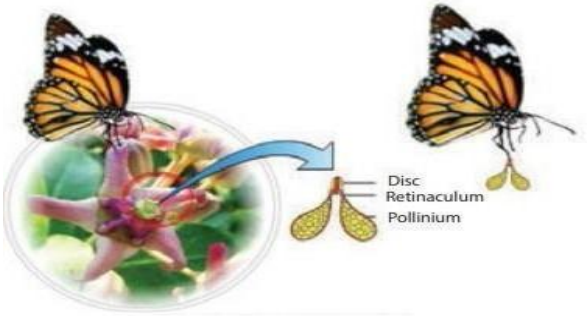

Source: https://www.brainkart.com/article/Agents-of-pollination_38201/

Figure 3: Entomophily pollination mechanism in *Calotropis.*

Source: https://www.pbs.org/wgbh/nova/article/dandelion-seed-flight/

Figure 4: Anemophily pollination mechanism in *Taraxacum officinale*.

Table-5 Pollination Calendar of Angiosperms present in Doriganj (2023)

S. N.	Name of the plants	Family	Habit	Frequency of Occurrence	Flowering period	Pollination mechanism
1	Ambrosia artemissifolia	Asteraceae	Herb	Frequent	July to Oct	Anemophilous
2	Acacia auriculiformis	Fabaceae	Tree	Frequent	Aug-Feb	Entomophilous
3	*Arachis hypogaea*	Fabaceae	Herb	Frequent	Feb-Mar	Entomophilous
4	*Achyranthes aspera*	Amaranthaceae	Herb	Abundant	Nov-Jan	Anemophilous

5	*Acorus calamus*	Acoraceae	Herb	Rare	May-Aug	Entomophilous
6	*Argemone Mexicana*	Papavaraceae	Herb	Common	Feb-June	Anemophilous
7	*Aerva lanata*	Amaranthaceae	Herb	Common	May-Oct	Anemophilous
8	*Ageratum conyzoides*	Asteraceae	Herb	Common	Nov-Feb	Anemophilous
9	*Alternanthera ficoidea*	Amaranthaceae	Herb	Common	Jan-Apr	Entomophilous
10	*Allium cepa*	Amaryllidaceae	Herb	Abundant	Nov-Feb	Entomophilous
11	*Alocasi a indica*	Araceae	Herb	Common	Mar-Jun	Entomophilous
12	*Aloe barbadensis*	Asphodelaceae	Herb	Rare	Oct-Dec	Entomophilous
13	*Alstonia scholaris*	Apocynaceae	Tree	Common	Oct-Jan	Entomophilous
14	*Alternanthera sessilis*	Amaranthaceae	Herb	Common	Dec-Mar	Anemophilous
15	*Amaranthus spinosus*	Amaranthaceae	Herb	Abundant	Jan-Dec	Anemophilous
16	*Amaranthus viridis*	Amaranthaceae	Herb	Abundant	Jan-Dec	Anemophilous
17	*Bauhinia acuminate*	Fabaceae	Shrub	Common	Sep-Feb	Entomophilous
18	*Cymbopogon citratus*	Poaceae	Herb	Common	Feb-Apr	Anemophilous
19	*Cassia fistula*	Fabaceae	Tree	Frequent	Jul-Sep	Entomophilous
20	*Cictrus maxima*	Rutaceae	Tree	Common	Feb-Aug	Entomophilous
21	*Cynodon dactylon*	Poaceae	Herb	Common	Jan-Dec	Entomophilous
22	*Datura metel*	Solanaceae	Shrub	Common	Dec- Mar	Entomophilous
23	*Delonix regia*	Fabaceae	Tree	Common	Mar-May	Entomophilous
24	*Euphorbia hirta*	Euphorbiaceae	Herb	Common	Jan-Dec	Entomophilous
25	*Eucalyptus globulus*	Myrtaceae	Tree	Frequent	Feb-Mar	Entomophilous
26	*Ficus religiosa*	Moraceae	Tree	Common	Apr- Aug	Entomophilous
27	*Holoptelea integrifolia*	Ulmaceae	Tree	Common	Feb- Mar.	Both, anemophilous, entomophilous
28	*Hibiscus rosa-sinensis*	Malvaceae	Shrub	Abundant	Jan-Dec	Entomophilous
29	*Ipomoea cairica*	Convolvulaceae	Shrub	Common	Jan-Dec	Entomophilous
30	*Lantana camara*	Verbenaceae	Shrub	Abundant	Jan-Dec	Entomophilous
31	*Mangifera indica*	Anacardiaceae	Tree	Common	Feb-May	Entomophilous
32	*Mikania micrantha*	Asteraceae	Weed	Common	Jan-Dec	Entomophilous
33	*Murraya koenigii*.	Rutaceae	Tree	Frequent	Mar-Apr	Entomophilous
34	*Parthenium hysterophorus*	Asteraceae	Herb	Common	Nov-Mar	Anemophily
35	*Phoenix sylvestris*	Arecaceae	Tree	Common	Jan-Apr	Entomophilous
36	*Solanum nigrum*	Solanaceae	Shrub	Common	Jan-Dec	Entomophilous
37	*Solanum tuberosum*	Solanaceae	Herb	Common	Aug-Dec	Entomophilous
38	*Triticum aestivum*	Poaceae	Herb	Cultivated	Jan- March	Entomophilous
39	*Tridex procumbens*	Asteraceae	Herb	Abundant	Nov-Apr	Anemophilous
40	*Vachellia nilotica*	Fabaceae	Tree	Abundant	Jun-Oct	Entomophilous
41	*Vernonia cinerea*	Asteraceae	Herb	Common	Nov-Mar	Anemophilous
42	*Zea mays*	Poaceae	Herb	Frequent	July-Sept	Entomophilous

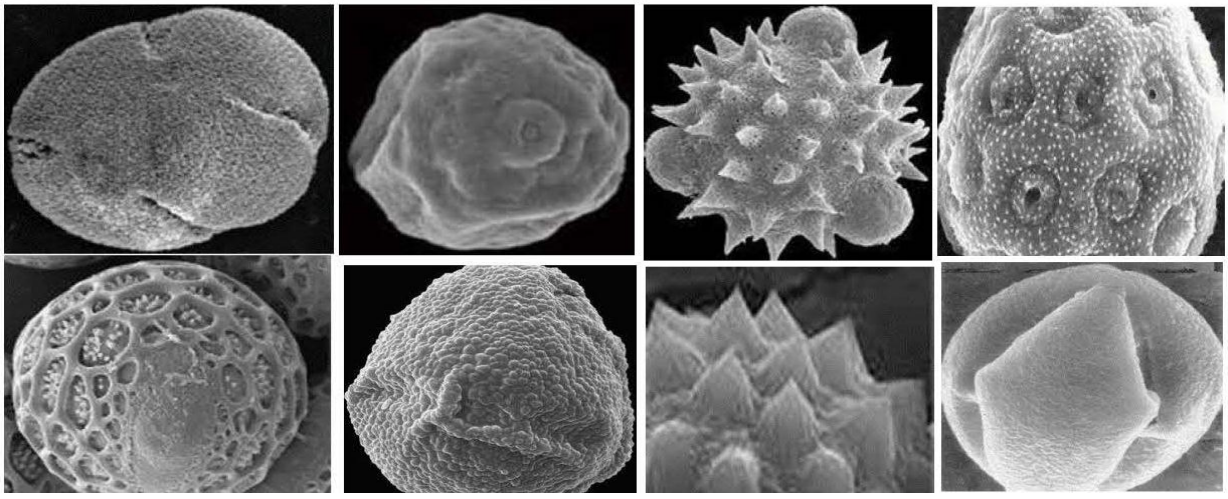

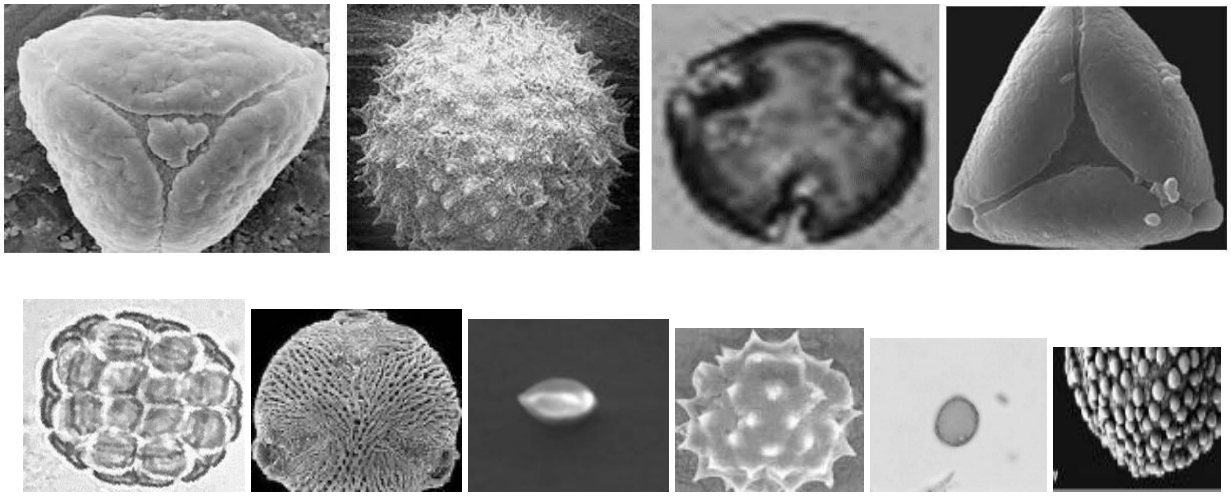

1 Argemone-mexicana, 2 Cymbopogon, 3 Ageratum, 4 Cheno-amaranthus, 5 Delonix, 6 Polyalthia,7 Xanthium, 8 Cassia, 9 Syzygium, 10 Hibiscus, 11 Dalbergia, 12 Eucalyptus, 13 Acacea, 14 Ailanthus, 15 Phoenix, 16 Parthenium, 17 Clerodendon, 18 Holoptelea.

Figure-5: Pollen Grain Morphology under Compound Microscope

CONCLUSION

A comprehensive plant survey was conducted in Doriganj and nearby regions over one year. This involved regular visits to observe vegetation types and flowering period. Sample were examined and identified by volumetric air sampler using various floras, and details of allergenic plants, including their botanical names, common names, families, flowering periods, pollination methods, frequency, and habits were recorded. A flowering calendar was prepared based on one year of observations. A year-long study of diverse flora revealed trees, shrubs, herbs, and crops like Wheat, Potato, and Maize. Weeds and allergenic plants, including *Parthenium*and*Amaranthus*, were identified. Pollination modes were entomophilous and anemophilous. Notably, *Acacia penninervis*, *Parthenium hysterophorus*, and others had allergenic pollens. Trees dominated, with 20% for aesthetics and 50% for edible fruits. Airborne pollen varied in shape, size, and peak months coincided with flowering seasons, notably grasses and trees in September-October. Spore composition fluctuated across seasons, with Cladosporium dominating at 65.80%. Tree pollens prevailed at 82.95%-85.65% across seasons, followed by Weed and Grass pollen, with a consistent unidentified pollen fraction. Understanding concentration patterns and estimating seasonal fluctuations in data can greatly aid in developing diagnostic and treatment approaches for patients with allergies in this region. The information recorded in Table- 5 is valuable as it provides insights into the diversity of plant species, their habits, and the mechanisms of pollination. This data is essential for ecological and botanical studies, as it helps researchers and professionals in these fields to gain a better understanding of the local flora and its impact on allergenic responses. Surveys in different regions found that only selected plant species release a significant amount of allergenic pollens into the environment. Morphological characteristics of pollen grains were identified with the help of reference keys. The study suggests that atmosphere of Doriganj contains diverse pollen types, potentially causing allergic responses in sensitive individuals. A local pollen calendar based on this data will aid area physicians. To prevent allergic reactions among the people of Doriganj, it is advised to avoid contact with allergenic pollen such as *Parthenium*, *Ageratum*, and *Argemone*.

REFERENCES

Bera, S. K., Tripathi, S., Gupta, S. C., and Bera, S. 2018. Pollen and spores in yellow rain from Lucknow, northern India. Palynology, 42(4): 504-515.

Davies, R. R. 1971. Air Sampling for Fungi, Pollens and Bacteria. In Methods in microbiology

Academic Press. Vol. 4: 367-404.

Erdtman, G. 1952. On pollen and spore terminology. Journal of Palaeosciences. 1: 169-176.

Erdtman, G. 1952. Pollen Morphology and Plant Taxonomy-Angiosperms. Almqvist and Wiksell, Stockholm, 539 p.

Faegri, K. 1966. Some problems of representivity in pollen analysis. Journal of Palaeosciences, 15((1-3), 135–140.

Ghufran, M.A., Hamid, N., Ali, A., and Ali, S.M. 2013. Prevalence of allergenic pollen grains in the city of Islamabad, Pakistan and its impact on human health. Pakistan Journal of Botany, 45(4): 87-90.

Gregory, P. H. 1952. Spore Content of the Atmosphere near the Ground. Nature, **170:**475- 477.

Knox, R. B., Williams, E. G., and Dumas, C. 1986. Pollen, pistil, and reproductive function in crop plants. Plant Breeding Reviews, 4: 9-79.

Lancia, A., Capone, P., Vonesch, N., Pelliccioni, A., Grandi, C., Magri, D., and D'Ovidio,

Latorre, F. and Caccavari, M. A. 2009. Airborne pollen patterns in Mar del Plata atmosphere (Argentina) and its relationship with meteorological conditions. Aerobiologia, 25: 297-312.

M. C. 2021. Research progress on aerobiology in the last 30 years: A focus on methodology and occupational health. Sustainability. 13(8): 1-20.

Malati, H.A. 2021. Study of air-spora over the groundnut fields in Nashik District of Maharashtra, India. Scholars Journal of Agriculture and Veterinary Sciences Scholars Journal of Agriculture and Veterinary Sciences 2 (1): 15-19.

Pacini, E. 2009. Pollination biology: Orchids pollen dispersal units and reproductive consequences. In Orchid Biology: Reviews and Perspectives, Dordrecht: Springer Netherlands. 185-218.

Pepper, I. L., and Gerba, C. P. 2015. Aero microbiology. In Environmental Microbiology (Third edition). Academic Press. 89-110.

Shamji, M. H., and Durham, S. R. 2017. Mechanisms of allergen immunotherapy for inhaled allergens and predictive biomarkers. Journal of Allergy and Clinical Immunology, 140(6): 1485- 1498.

Stephen, A. 2014. Pollen: A microscopic wonder of plant kingdom. International Journal of Advanced Research in Biological Sciences, 1(9): 45-62.

Suanno, C., Sandrini, S., Aloisi, I., De Nuntiis, P., Facchini, M. C., Del Duca, S., and Fernández-González, D. 2022. Airborne Pollen, Allergens, and Proteins: A Comparative Study of Three Sampling Methods. Sustainability, 14(19):11825.

Sukhan, V. S. 2019. Allergic rhinitis and asthma co-morbidity. Wiad Lek, 72(4): 622-626.

Wodehouse, R. P.1935. Pollen grains and worlds of different sizes. The Scientific Monthly, 40(1): 58-62.

REVIEW: UBIQUITINATION AND ITS ROLE IN HUMAN DISEASES

C Ratna Prabha
Biochemistry Department,
The Maharaja Sayaji Rao University of Baroda, Vadodara, Gujarat-390002

INTRODUCTION

Ubiquitination is necessary to regulate different physiological processes, including cell survival and differentiation, and innate and adaptive immunity. Ubiquitination is a protein posttranslational modification (PTM) and the second most common PTM after phosphorylation (1). It is involved in cellular functions like proteasomal degradation of proteins, receptor internalization, assembly of multiprotein complexes, intracellular trafficking, inflammatory signaling, autophagy, DNA repair and regulation of enzyme activity (2). The ubiquitination process is achieved by a cascade of enzymatic reactions carried out by three different types of enzymes that aid in covalently linking ubiquitin (Ub) to lysine residues on target proteins. These proteins are Ub-activating (E1), Ub-conjugating (E2) and Ub-ligating (E3) and they act sequentially on ubiquitin. E1 activates ubiquitin and transfers it to the E2 conjugating enzyme. Following this, E3 Ub ligases mediate isopeptide bond formation between the C terminus of Ub and a substrate lysine (3). Deubiquitinating enzymes (DUBs) are another group of enzymes that can remove Ub from the substrate and reverse the activity of Ub ligases (2). A tight regulation between all these enzymatic reactions is essential in maintaining cellular homeostasis.

Deregulation of ubiquitination is likely to be detrimental to cell functioning as it may lead to aberrant activation or deactivation of pathways, improper assembly of proteins, accumulation of misfolded proteins, or mislocalization of proteins. Several studies have shown the role of aberrant ubiquitination in the development of different human disease conditions, especially cancer. The majority of the evidence shows the defective activity of many E3 ligases to be the cause of human malignancies. With the increasing understanding of the complex mechanisms underlying this process, researchers have identified E3 ligases and DUBs as potential targets for the development of anti-cancer drugs (4).

This article describes, in brief, the ubiquitination process, the different components involved, and its role in different human disease development and progression.

Ubiquitin (Ub)

It is a small protein made of 76 amino acids, first identified by Gideon Goldstein et al. in 1975 (5). In humans, Ub is encoded by four genes: *UBB*, *UBC*, *UBA52*, and *RPS27A*. The UBA52 and RPS27A encode a single copy of Ub whereas the UBB and UBC genes encode polyubiquitin molecules.

Ubiquitination process

Ubiquitination is the process of tagging the ubiquitin molecule to a protein. It was first discovered by Goldknopf et al. 1977 that intracellular histones could be modified by ubiquitination. Later in 2004, Nobel Prize in Chemistry was awarded to Aaron Ciechanover, Avram Hershko and Irwin Rose for their significant contributions in the area of ubiquitination. The ubiquitin molecule brings about protein degradation in two ways, either through UPS or selective autophagy. The sequential activity of the three enzymes E1, E2 and E3 brings about the ubiquitination process (5) (Figure 1). E1 catalyzes the formation of a thioester bond between the active site Cys residue of E1 and the C-terminal carboxy group of Ub. There are only two E1 enzymes UBa1 and UBa6 encoded by the human genome (6). In the next step, E2 accepts the activated Ub due to the presence of a very conserved Ub-binding catalytic domain and helps E3 in transferring the Ub to the specific substrate (7). With the transfer of Ub, an isopeptide bond is formed between the lysine e-amino group of the substrate and the C-terminal carboxyl group of Ub. More than 600 E3 Ub ligases are encoded by the human genome, and these are important in substrate selection and achieving Ub linkage (8,9).

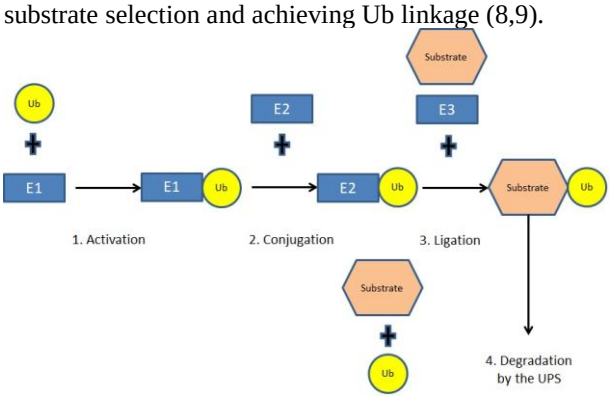

Figure 1: Ubiquitination process

Corresponding author: chivukula_r@yahoo.com
Received: November 30, 2023, Accepted: December 15, 2023

The type of ubiquitin conjugation with the substrate dictates the degradation pathway for that protein. There are three main types of ubiquitination linkages: monoubiquitination, polyubiquitination, and branched ubiquitination. Monoubiquitination is the attachment of a single Ub to a specific lysine residue of the substrate (10). Examples include the monoubiquitination of proliferating cell nuclear antigen (PCNA) in response to DNA damage repair by recruiting DNA polymerases (11). In other cases, monoubiquitination of membrane proteins may promote mitochondrial autophagy and peroxisome autophagy by modulating the interaction with the autophagy adaptor protein 62 (12). Polyubiquitination, on the other hand, involves the sequential conjugation of several ubiquitin moieties of variable length. There are different types of polyubiquitination depending on which of the seven lysine residues (K6, K11, K27, K29, K33, K48 and K63) is linked to the ubiquitin or it is through the amino-terminal methionine (13,14). Different polyubiquitination types are responsible for regulating different cellular processes. For instance, K11 polyubiquitination is involved in the cell cycle and trafficking events (15,16), whereas K27 polyubiquitination plays a role in mitochondrial autophagy (17,18). Branched ubiquitination is another type where there are several linkages present. For example, the mixed K11 and K63 linkages. These participate in the Epsin1-mediated endocytosis of major histocompatibility complex I (MHCI) (19,20).

The ubiquitin proteasomal system (UPS)

On accumulation of denatured or damaged proteins inside the cell, molecular chaperones of the heat-shock protein (HSP) family begin the first protective mechanism. They aid in the folding of de novo synthesized protein as well as refolding the denatured proteins. In events when this refolding is not successful, E3 ubiquitin ligases induce ubiquitination and select the damaged proteins for degradation (21). The co-chaperone carboxyl terminus of heat-shock cognate70 (HSC70)-interacting protein (CHIP) is one of the examples of E3 ligases that are involved in such processes (21). This process is highly regulated and if there is any discrepancy then it can lead to protein aggregation. These then form inclusion bodies that are subsequently delivered to the lysosome for autophagic degradation (22). Thus, several checkpoints ensure proper degradation and removal of the damaged misfolded proteins from the cell.

Ubiquitination and its involvement in different human diseases

Ubiquitination and cancer

Ubiquitination can promote both tumor-suppressing and tumor-promoting pathways, as Ub ligases have several substrates and depending on the nature of the substrate, a single Ub ligase can act as both an oncogene and as a tumor suppressor.

Regulating the stability of substrates that are marked for degradation is achieved by several Ub ligases. One of the best examples is the MDM2/p53 interaction. The MDM2 ligase ubiquitinates the tumor suppressor p53 and the SCF APC/C ligase complexes (23). This stabilizes cyclin-dependent kinases (CDK) and the cell cycle inhibitor p27 and controls the cell cycle progression (24). Hence, overexpression of MDM2 results in increased ubiquitination and subsequent degradation of p53. This affects the growth inhibitory function of p53, thereby leading to the development of cancer. Another example is of human papillomavirus (HPV) induced cervical cancer. Studies have shown that p53 levels are low in high-risk HPV-positive cervical carcinoma cell lines (25,26). Sheffner and colleagues have elucidated the mechanism of p53 inactivation in these cells. They have shown that the E6 oncoprotein encoded by the viral genome interacts with p53 and enhances UPS-mediated degradation of p53 by an E3-denoted E6-AP (E6-associated protein). Thus, removing p53 is possibly an essential mechanism by which high-risk HPVs induce malignant transformation. p27 is another tumor suppressor that acts as a cell-cycle inhibitor. There is a decrease in the p27 protein levels in several malignant conditions including gliomas, lymphomas, and cancer of the colorectum, prostate, uterine endometrium, and lung (27). The underlying mechanism for the reduced level of p27 is the overexpression of Skp2, the E3 enzyme that is responsible for the recognition and ubiquitination of p27. As a result, there is abnormally enhanced degradation of p27 by the UPS (28).

Ubiquitination is also known to regulate several key steps of the NF-κBsignaling pathway, one of the most important signaling pathways of cell survival and death (29). Aberrant NF-κB activation has also been observed in a variety of solid tumors (including prostate cancer, breast cancer, melanoma, pancreatic cancer and lung cancer) and in a number of hematopoietic cancers (including chronic myelogenous leukemia, multiple myeloma and Hodgkin's and non-Hodgkin's lymphomas) (30,31). One of the best examples of how failure in inflammatory response through NF-κBsignaling contributes to cancer development is in mucosa-associated lymphoid tissue (MALT) lymphoma, the most common extranodal non-Hodgkin's B cell lymphoma, which develops primarily in the mucosa of gastric tract and lungs. MALT1 regulates NF-κB pathways through its protease activity. This activity is itself regulated by monoubiquitination. MALT1 ubiquitination enhances its proteolytic activity, whereas a ubiquitination-deficient

mutant of MALT1 has low protease activity and impairs cellular survival (32).

Table 1: Examples of ubiquitination in human diseases

Disease name	Name of the ubiquitin/target protein involved	Suggested mechanism	Reference
Angelman syndrome	E3 ubiquitin ligase E6-AP	Reduces nuclear inclusions and accelerate polyglutamine-induced neurodegeneration	C.J. Cummings, Mutation of the E6-AP ubiquitin ligase reduces nuclear inclusion frequency while accelerating polyglutamine-induced pathology in SCA1 mice, Neuron 24 (1999)
Autosomal recessive Parkinson disease	Parkin (ubiquitin ligase)	Parkin is thought to act as a ubiquitin ligase through association with the ubiquitin-conjugating enzyme UbcH7.	H. Shimura, Familial Parkinson disease gene product, parkin, is a ubiquitin-protein ligase, Nat. Genet. 25 (2000) 3
Fanconi anemia	FANCL	A protein complex (the FA core complex) contains a subunit known as FANCL that contains a RING motif and likely helps in monoubiquitinylation of FACD2 and FANCI	Meetei AR, de Winter JP, Medhurst AL, Wallisch M, Waisfisz Q, Vrugt van de HJ, Oostra AB, Yan Z, Ling C, Bishop CE, et al.: A novel ubiquitin ligase is deficient in Fanconi anemia. Nat Genet. 2003, 35: 165-170. 10.1038/ng1241
Xeroderma pigmentosa	DDB2	UV-damaged DNA-binding protein complex UV-DDB, consists of DDB1 and DDB2. Altered DDB2 affects UV-DDB ligase activity, thereby affecting ubiquitination around damaged sites in the chromatin	Keeney, S., Chang, G.J. & Linn, S. Characterization of a human DNA damagebinding protein implicated in xeroderma pigmentosum E. J. Biol. Chem. 268, 21293–21300 (1993).
RIDDLE syndrome	Ub ligase RNF168	The genetic defect in the Ub ligase RNF168 results in radiosensitivity immunodeficiency dysmorphic features and learning difficulties	Stewart, G.S. et al. The RIDDLE syndrome protein mediates a ubiquitin-dependent signaling cascade at sites of DNA damage.
Huntington disease	TRAF6	Enhances aggregate formation by mediating atypical ubiquitination (Lys6-, Lys27- and Lys29-linked chains) of huntingtin	Zucchelli, S. et al. Tumor necrosis factor receptor-associated factor 6 (TRAF6) associates with huntingtin protein and promotes its atypical ubiquitination to enhance aggregate formation. J. Biol. Chem. 286, 25108–25117 (2011).
Incontinentiapigmenti	I-κB kinase complex (IKK) and NEMO	Truncated form of NEMO can no longer mediate NF-κB activation. Consequently, the transcription of pro-survival genes downstream of NF-κB pathways is blocked in incontinentiapigmenti, resulting in high sensitivity to TNF-stimulated apoptosis	Aradhya, S. et al. Atypical forms of incontinentiapigmenti in male individuals result from mutations of a cytosine tract in exon 10 of NEMO (IKK-γ). Am. J. Hum. Genet. 68, 765–771 (2001).
Von Hippel Lindau	pVHL	pVHL is part of the VCB–Cul2–VHL Ub ligase complex and is responsible for substrate recognition. Mutations in the VHL gene lead to stabilization of hypoxia-inducible factor-1α (HIF-1α), which stimulates rapid vascularization of tumors, thereby promoting tumor growth by ensuring nutrient and oxygen supply	Gnarra, J.R. et al. Mutations of the VHL tumour suppressor gene in renal carcinoma. Nat. Genet. 7, 85–90 (1994).

Another class of ubiquitination proteins is the Inhibitors of apoptosis-related proteins (IAPs) that bind and degrade apoptotic caspases. c-IAP1 and c-IAP2 have been linked to non-canonical NF-κBsignaling as they promote ubiquitination and proteasomal degradation of the NF-κB inducing kinase (NIK) (33). The genes encoding c-IAP1 and c-IAP2 are closely linked on the chromosome, and this region (11q21–q23 in humans) is amplified in a variety of human malignancies, including hepatocarcinoma, mammary carcinoma and medulloblastoma, and in the pancreatic, cervical, lung, oral squamous cell and oesophageal carcinomas (34).

Some cancers arise due to the increased activity of oncoproteins. One example is that of familial adenomatous polyposis which is a cancer predisposition syndrome associated with a variety of benign and malignant tumors. This is a genetic disorder inherited in an autosomal dominant manner and affected individuals have mutations in the *APC* gene (35). The APC protein is a positive regulator for beta-catenin, a major driver of numerous benign and malignant neoplasms. Thus, a defective APC results in the accumulation of beta-catenin and ultimately leads to constitutive pro-growth signaling(36).

A number of cases of breast and ovarian cancer have shown the presence of heterozygous mutations in the BRCA1 gene. The RING finger domain present in BRCA1 is common among many E3 enzymes. BRCA1 has shown E3 activity in cells and the substrates targeted by BRCA1 are BRCA1 itself and its counterpart for the E3 complex-BARD1. Mutation in the RING domain of BRCA1 abolishes the E3 activity of the BRCA1-BARD1 complex and possibly leads to breast cancer development (37,38).

Deubiquitinating (DUBs) enzymes in cancer

DUBs remove the Ub moieties from their substrates and can function as tumor-promoting proteins if their substrates act as promoters of cancer progression.

DUBs, such as A20, CYLD and BAP1, are tumor suppressors whose encoding genes are mutated in a number of human malignancies (39–41). A20 participates in the proinflammatory signaling pathway by interacting with proteins like TNF receptor-associated factor 2 (TRAF2), TRAF6 and nuclear factor NF-κB–essential modulator (NEMO). Deubiquitination by A20 removes Lys63 Ub chains from TRAF6 and the cell death protein RIPK1, thereby attenuating the NF-κBsignaling pathways. Thus, A20 inactivation can lead to unchecked NF-κB activity causing malignant transformation. Another example is that of USP1 and DUB3 which deubiquitinate inhibitors of DNA binding proteins in osteosarcoma and preserve the characteristics of mesenchymal stem cells (42). They also stabilize CDC25 to activate cell cycle progression (43).

Ubiquitin and neurodegenerative disorders

Neurodegenerative disorders like Parkinson's disease, Alzheimer's disease, and Huntington’s disease are a result of the toxic accumulation of protein aggregates that disturb cellular homeostasis and neuronal function. Studies have shown that deregulation of the Ub system can lead to aggresome formation and neurodegeneration.

Parkinson’s disease

Parkinson’s disease is characterized by the presence of Lewy bodies or protein aggregates consisting mainly of α-synuclein. Interestingly, ubiquitination seems to increase aggregation and neurotoxicity of α-synuclein in cultured human dopaminergic cells (44,45). Mutations in the Parkin gene have been linked to different forms of familial Parkinson’s disease. Parkin belongs to the family of E3 enzymes. Thus, a mutation in the Parkin gene results in a loss of its E3 enzymatic function (46,47). Parkin and PTEN-induced putative phosphatase 1 (PINK1) together cooperate in a pathway dedicated to the selective autophagic degradation of damaged mitochondria (mitophagy) (48,49). PINK1 activates Parkin through phosphorylation and subsequently ubiquitinates several outer mitochondrial membrane proteins, thus priming the damaged organelle for autophagic elimination (50). In contrast, the mitochondrial deubiquitinase USP30 can remove Ub moieties attached by Parkin to damaged mitochondria and block Parkin’s ability to drive mitophagy (51).

Alzheimer’s disease

Alzheimer’s disease is the result of the loss of neurons and synapses and alterations related to reactive processes. The typical aggregates found in this condition are extracellular β-amyloid plaques and intracellular neurofibrillary tangles consisting of hyperphosphorylated, ubiquitinated tau protein. The inhibition of the autophagy-lysosomal pathway and reduced efficiency of the UPS leads to the accumulation of tau in synaptic terminals of human Alzheimer’s disease brain samples (52). The selective autophagy adaptor p62 serves as a scaffold supporting tau polyubiquitination by TRAF6, promotes shuttling of polyubiquitinated tau to the proteasome, and is involved in the clearance of aggregated tau via the autophagic pathway (53). The UPS seems to be the predominant pathway for the clearance of monomeric soluble tau protein. UPS activity is, however, substantially inhibited by aggregated tau (54). Interestingly, studies in mice with transgenic tau expression have shown that amount of tau aggregates reduces by stimulation of autophagy (55).

Ubiquitin and diabetes

Interestingly, defects in the Ub system have shown to cause ligand-induced downregulation of the insulin receptor, decreased downstream signaling by insulin receptor substrate (IRS) proteins, and impaired biological response to insulin in mice and rats (56). Recently, a muscle-specific Ub ligase, mitsugumin 53 (MGM3) was identified that targets both the insulin receptor and IRS1 for Ub-dependent degradation.

MGM3 is overexpressed in insulin-resistance models, and diet-induced systemic insulin resistance is blocked by its depletion (57).

Excess degradation of misfolded but partially functional proteins by the UPS

All cells have developed complex stress responses to identify and destroy proteins that are misfolded. However, in instances where the misfolded protein has some residual functional activity, its degradation can lead to the development of a disease condition. Cystic fibrosis is an excellent example of this. It is an autosomal recessive disorder characterized by thick viscous secretions throughout the body, prominently in the lungs and pancreas. The CFTR gene encodes a chloride ion channel: cystic fibrosis transmembrane conductance regulator. The most common mutation reported in the CFTR gene that causes cystic fibrosis is delta F508 (58). This delta F508 mutant protein is recognized as misfolded and hence rapidly degraded by the UPS (59).

Table 2: Examples of drugs developed to target the ubiquitination system

Drug name	Target	Disease	Developmental stage
PR-171	Irreversibly inhibits the chymotryptic site of the proteasome	Multiple myelomas and non-Hodgkin's lymphoma	Phase 1
Salinosporamide A (NPI-0052)	Proteasome inhibition	Colon cancer	Phase 1
Bortezomib	Proteasome inhibition	Multiple myeloma	Approved
Carfilzomib (PR171)	Proteasome inhibition	Hematologic malignancies	Phase 3
AEG-35156	XIAP antisense	AML	Phase 2

CONCLUSION

The ubiquitination system is an important network that helps in the regulation of different cellular processes. In the last few decades, there has been a significant surge in studies directed to understand the underlying mechanism involving Ub in different signaling pathways. An emerging area of interest to scientists is the role of Ub in selective autophagy so as to develop therapeutic targets. Based on this knowledge, several drugs have been identified to target the different points in the pathway and modulate the autophagy process (Table 2). Many of these drugs are currently in clinical trials. As more information is deciphered from the ubiquitination process and with advancing technologies, it will help in the development of various strategies for the treatment of human diseases.

REFERENCES

Gross S, R Rahal, N Stransky, C Lengauer and KP Hoeflich. Targeting cancer with kinase inhibitors. J Clin Invest. 2015 May 1;125(5):1780–9.

Grabbe C, K Husnjak and I Dikic. The spatial and temporal organization of ubiquitin networks. Nat Rev Mol Cell Biol. 2011 May;12(5):295–307.

Hershko A and A Ciechanover. The ubiquitin system. Annu Rev Biochem. 1998;67:425–79.

Hoeller D and I Dikic. Targeting the ubiquitin system in cancer therapy. Nature. 2009 Mar 26;458 (7237):438–44.

Komander D and M Rape. The ubiquitin code. Annu Rev Biochem. 2012;81:203–29.

Ciechanover A, H Heller, R Katz-Etzion and A Hershko. Activation of the heat-stable polypeptide of the ATP-dependent proteolytic system. Proc Natl Acad Sci U S A. 1981 Feb;78(2):761–5.

Ye Y, Rape M. Building ubiquitin chains: E2 enzymes at work. Nat Rev Mol Cell Biol. 2009 Nov;10(11):755–64.

Varshavsky A. The ubiquitin system, an immense realm. Annu Rev Biochem. 2012;81:167–76.

Hershko A. Ubiquitin-mediated protein degradation. J Biol Chem. 1988 Oct 25;263(30):15237–40.

Rajalingam K and I Dikic. SnapShot: Expanding the Ubiquitin Code. Cell. 2016 Feb 25;164(5):1074-1074.e1.

Geng L, CJ Huntoon and LM Karnitz. RAD18-mediated ubiquitination of PCNA activates the Fanconi anemia DNA repair network. J Cell Biol. 2010 Oct 18;191(2):249–57.

Kwon YT and A Ciechanover. The Ubiquitin Code in the Ubiquitin-Proteasome System and Autophagy. Trends Biochem Sci. 2017 Nov;42(11):873–86.

Yau R and M Rape. The increasing complexity of the ubiquitin code. Nat Cell Biol. 2016 May 27;18(6):579–86.

Swatek KN and D Komander. Ubiquitin modifications. Cell Res. 2016 Apr;26(4):399–422.

Bremm A and D Komander. Emerging roles for Lys11-linked polyubiquitin in cellular regulation. Trends Biochem Sci. 2011 Jul;36(7):355–63.

Matsumoto ML, KE Wickliffe, KC Dong, C Yu, I Bosanac, D Bustos, et al. K11-linked polyubiquitination in cell cycle control revealed by a K11 linkage-specific antibody. Mol Cell. 2010 Aug 13;39(3):477–84.

Geisler S, KM Holmström, D Skujat, FC Fiesel, OC Rothfuss, PJ Kahle, et al. PINK1/Parkin-mediated mitophagy is dependent on VDAC1 and p62/SQSTM1. Nat Cell Biol. 2010 Feb;12(2):119–31.

Glauser L, S Sonnay, K Stafa and DJ Moore. Parkin promotes the ubiquitination and degradation of the mitochondrial fusion factor mitofusin 1. J Neurochem. 2011 Aug;118(4):636–45.

Kulathu Y and D Komander. Atypical ubiquitylation - the unexplored world of polyubiquitin beyond Lys48 and Lys63 linkages. Nat Rev Mol Cell Biol. 2012 Jul 23;13(8):508–23.

Boname JM, M Thomas, HR Stagg, P Xu, J Peng and PJ Lehner. Efficient internalization of MHC I requires lysine-11 and lysine-63 mixed linkage polyubiquitin chains. Traffic Cph Den. 2010 Feb;11(2):210–20.

Kubota H. Quality control against misfolded proteins in the cytosol: a network for cell survival. J Biochem (Tokyo). 2009 Nov;146(5):609–16.

Kopito RR. Aggresomes, inclusion bodies and protein aggregation. Trends Cell Biol. 2000 Dec;10(12):524–30.

Wade M, YC Li and GM Wahl. MDM2, MDMX and p53 in oncogenesis and cancer therapy. Nat Rev Cancer. 2013 Feb;13(2):83–96.

Sheaff RJ, M Groudine, M Gordon, JM Roberts and BE Clurman. Cyclin E-CDK2 is a regulator of p27Kip1. Genes Dev. 1997 Jun 1;11(11): 1464–78.

Werness BA, AJ Levine and PM Howley. Association of human papillomavirus types 16 and 18 E6 proteins with p53. Science. 1990 Apr 6;248(4951):76–9.

Scheffner M, K Münger, JC Byrne and PM Howley. The state of the p53 and retinoblastoma genes in human cervical carcinoma cell lines. Proc Natl Acad Sci U S A. 1991 Jul 1;88(13):5523–7.

Bloom J and M Pagano. Deregulated degradation of the cdk inhibitor p27 and malignant transformation. Semin Cancer Biol. 2003 Feb; 13(1):41–7.

Carrano AC, E Eytan, A Hershko and M Pagano. SKP2 is required for ubiquitin-mediated degradation of the CDK inhibitor p27. Nat Cell Biol. 1999 Aug;1(4):193–9.

Luo JL, H Kamata and M Karin. IKK/NF-kappaBsignaling: balancing life and death--a new approach to cancer therapy. J Clin Invest. 2005 Oct;115(10):2625–32.

Ben-Neriah Y and M Karin. Inflammation meets cancer, with NF-κB as the matchmaker. Nat Immunol. 2011 Jul 19;12(8):715–23.

Vucic D, VM Dixit and IE Wertz. Ubiquitylation in apoptosis: a post-translational modification at the edge of life and death. Nat Rev Mol Cell Biol. 2011 Jun 23;12(7):439–52.

Pelzer C, K Cabalzar, A Wolf, M Gonzalez, G Lenz and M Thome. The protease activity of the paracaspase MALT1 is controlled by monoubiquitination. Nat Immunol. 2013 Apr;14(4):337–45.

Varfolomeev E, JW Blankenship, SM Wayson, AV Fedorova, N Kayagaki, P Garg, et al. IAP antagonists induce autoubiquitination of c-IAPs, NF-kappaB activation, and TNFalpha-dependent apoptosis. Cell. 2007 Nov 16;131(4):669–81.

Zender L, MS Spector, W Xue, P Flemming, C Cordon-Cardo, J Silke, et al. Identification and validation of oncogenes in liver cancer using an integrative oncogenomic approach. Cell. 2006 Jun 30;125(7):1253–67.

Kinzler KW, MC Nilbert, LK Su, B Vogelstein, TM Bryan, DB Levy, et al. Identification of FAP locus genes from chromosome 5q21. Science. 1991 Aug 9;253(5020):661–5.

Munemitsu S, I Albert, B Souza, B Rubinfeld and P Polakis. Regulation of intracellular beta-catenin levels by the adenomatous polyposis coli (APC) tumor-suppressor protein. Proc Natl Acad Sci U S A. 1995 Mar 28;92(7):3046–50.

Ohta T and M Fukuda. Ubiquitin and breast cancer. Oncogene. 2004 Mar;23(11):2079–88.

Hashizume R, M Fukuda, I Maeda, H Nishikawa, D Oyake, Y Yabuki, et al. The RING heterodimer BRCA1-BARD1 is a ubiquitin ligase inactivated by a breast cancer-derived mutation. J Biol Chem. 2001 May 4;276(18):14537–40.

Dey A, D Seshasayee, R Noubade, DM French, J Liu, MS Chaurushiya, et al. Loss of the tumor suppressor BAP1 causes myeloid transformation. Science. 2012 Sep 21;337(6101):1541–6.

Bignell GR, W Warren, S Seal, M Takahashi, E Rapley, R Barfoot, et al. Identification of the familial cylindromatosis tumour-suppressor gene. Nat Genet. 2000 Jun;25(2):160–5.

Hymowitz SG and IE Wertz. A20: from ubiquitin editing to tumour suppression. Nat Rev Cancer. 2010 May;10(5):332–41.

Williams SA, HL Maecker, DM French, J Liu, A Gregg, LB Silverstein, et al. USP1 deubiquitinates ID proteins to preserve a mesenchymal stem cell program in osteosarcoma. Cell. 2011 Sep 16;146(6):918–30.

Pereg Y, BY Liu, KM O'Rourke, M Sagolla, A Dey, L Komuves, et al. Ubiquitin hydrolase Dub3 promotes oncogenic transformation by stabilizing Cdc25A. Nat Cell Biol. 2010 Apr;12(4):400–6.

Rott R, R Szargel, J Haskin, V Shani, A Shainskaya, I Manov, et al. Monoubiquitylation of alpha-synuclein by seven in absentia homolog (SIAH) promotes its aggregation in dopaminergic cells. J Biol Chem. 2008 Feb 8;283(6):3316–28.

Lee JT, TC Wheeler, L Li and LS Chin. Ubiquitination of alpha-synuclein by Siah-1 promotes alpha-synuclein aggregation and apoptotic cell death. Hum Mol Genet. 2008 Mar 15;17(6):906–17.

Tanaka K, T Suzuki, N Hattori and Y Mizuno. Ubiquitin, proteasome and parkin. BiochimBiophys Acta. 2004 Nov 29;1695(1–3):235–47.

Hattori N and Y Mizuno. Pathogenetic mechanisms of parkin in Parkinson's disease. Lancet Lond Engl. 2004 Aug 21;364(9435):722–4.

Chen Y and GW Dorn. PINK1-phosphorylated mitofusin 2 is a Parkin receptor for culling damaged mitochondria. Science. 2013 Apr 26;340 (6131):471–5.

Novak I. Mitophagy: a complex mechanism of mitochondrial removal. Antioxid Redox Signal. 2012 Sep 1;17(5):794–802.

Karbowski M and RJ Youle. Regulating mitochondrial outer membrane proteins by ubiquitination and proteasomal degradation. CurrOpin Cell Biol. 2011 Aug;23(4):476–82.

Bingol B, JS Tea, L Phu, M Reichelt, CE Bakalarski, Q Song, et al. The mitochondrial deubiquitinase USP30 opposes parkin-mediated mitophagy. Nature. 2014 Jun 19;510(7505):370–5.

Tai HC, A Serrano-Pozo, T Hashimoto, MP Frosch, TL Spires-Jones and BT Hyman. The synaptic accumulation of hyperphosphorylated tau oligomers in Alzheimer disease is associated with dysfunction of the ubiquitin-proteasome system. Am J Pathol. 2012 Oct;181(4):1426–35.

Wang Y, M Martinez-Vicente, U Krüger, S Kaushik, E Wong, EM Mandelkow, et al. Synergy and antagonism of macroautophagy and chaperone-mediated autophagy in a cell model of pathological tau aggregation. Autophagy. 2010 Jan;6(1):182–3.

Keck S, R Nitsch, T Grune and O Ullrich. Proteasome inhibition by paired helical filament-tau in brains of patients with Alzheimer's disease. J Neurochem. 2003 Apr;85(1):115–22.

Schaeffer V and M Goedert. Stimulation of autophagy is neuroprotective in a mouse model of human tauopathy. Autophagy. 2012 Nov;8(11):1686–7.

White MF. IRS proteins and the common path to diabetes. Am J Physiol Endocrinol Metab. 2002 Sep;283(3):E413-422.

Song R, W Peng, Y Zhang, F Lv, HK Wu, J Guo, et al. Central role of E3 ubiquitin ligase MG53 in insulin resistance and metabolic disorders. Nature. 2013 Feb 21;494(7437):375–9.

Riordan JR, JM Rommens, B Kerem, N Alon, R Rozmahel, Z Grzelczak, et al. Identification of the cystic fibrosis gene: cloning and characterization of complementary DNA. Science. 1989 Sep 8;245(4922):1066–73.

Ward CL, S Omura and RR Kopito. Degradation of CFTR by the ubiquitin-proteasome pathway. Cell. 1995 Oct 6;83(1):121–7.

FEELING THE STING: DENGUE SCARE

Dr. Rashmi Kohli
Department of Zoology, Postgraduate Government College for Girls, Sector-42, Chandigarh

ABSTRACT

Dengue fever is indeed a significant public health concern, particularly in more than 125 tropical and subtropical regions where flavivirus is transmitted by *Aedes aegypti or Aedes albopictus* mosquitoes while taking a blood meal. The term "dengue scare" commonly arises when there is an increase in reported cases of dengue fever within a community or region. While most dengue infections result in mild symptoms (such as fever, headache, muscle and joint pains), a small proportion of cases can progress to severe forms like dengue hemorrhagic fever (DHF) or dengue shock syndrome (DSS) all caused by four dengue virus (DENV) types (DENV-1, DENV-2, DENV-3, and DENV-4). Community response, public awareness along with fogging and larviciding are required to eliminate mosquito breeding sites.

Key Words: Dengue, *Aedes aegypti*, DENV, DSS.

INTRODUCTION

With an average of around 35 dengue patients seeking treatment every week at GMCH-32 in October, 2023 (Source: The Indian Express, 2nd November, 2023) it indicates a significant concern for the Tricity area. The information provided by Professor Sanjay Jain, the Head of the Department of Internal Medicine at PGI, regarding an increase in dengue cases in October, 2023 and the referral of more serious patients with very low platelets for hospitalization highlights the severity of the current situation.

Methodology and Research Done:

A survey of over 155 houses was done in Village Kajheri, Chandigarh to find out any stagnant water logging. A total of 370 containers, 110 Over Head Tanks, 72 coolers and 49 fridge trays were surveyed for stagnant water and the residents were instructed to decant the standing water in them. Notices were also issued to 2 of the Households.

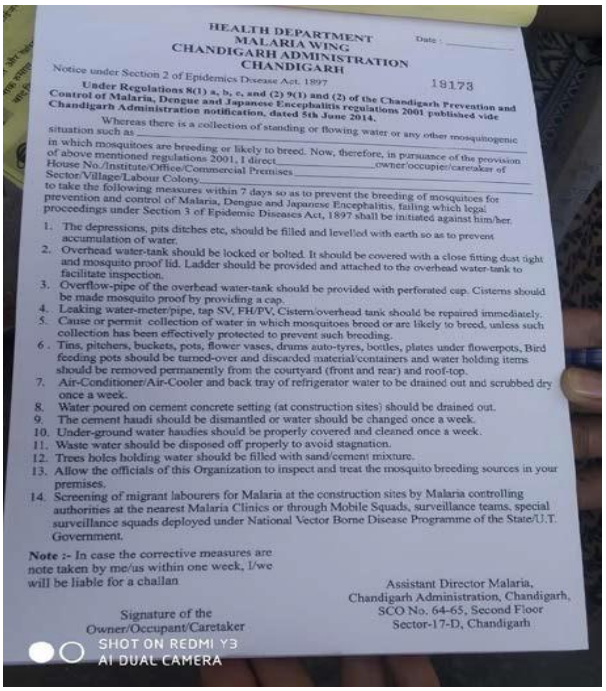
HEALTH DEPARTMENT
MALARIA WING
CHANDIGARH ADMINISTRATION
CHANDIGARH

Date : _____

Notice under Section 2 of Epidemics Disease Act, 1897 19173

Under Regulations 8(1) a, b, c, and (2) 9(1) and (2) of the Chandigarh Prevention and Control of Malaria, Dengue and Japanese Encephalitis regulations 2001 published vide Chandigarh Administration notification, dated 5th June 2014.

Whereas there is a collection of standing or flowing water or any other mosquitogenic situation such as _____ in which mosquitoes are breeding or likely to breed. Now, therefore, in pursuance of the provision of above mentioned regulations 2001, I direct _____ owner/occupier/caretaker of House No./Institute/Office/Commercial Premises _____ Sector/Village/Labour Colony _____ to take the following measures within 7 days so as to prevent the breeding of mosquitoes for prevention and control of Malaria, Dengue and Japanese Encephalitis, failing which legal proceedings under Section 3 of Epidemic Diseases Act, 1897 shall be initiated against him/her.

1. The depressions, pits ditches etc, should be filled and levelled with earth so as to prevent accumulation of water.
2. Overhead water-tank should be locked or bolted. It should be covered with a close fitting dust tight and mosquito proof lid. Ladder should be provided and attached to the overhead water-tank to facilitate inspection.
3. Overflow-pipe of the overhead water-tank should be provided with perforated cap. Cisterns should be made mosquito proof by providing a cap.
4. Leaking water-meter/pipe, tap SV, FH/PV, Cistern/overhead tank should be repaired immediately.
5. Cause or permit collection of water in which mosquitoes breed or are likely to breed, unless such collection has been effectively protected to prevent such breeding.
6. Tins, pitchers, buckets, pots, flower vases, drums auto-tyres, bottles, plates under flowerpots, Bird feeding pots should be turned-over and discarded material/containers and water holding items should be removed permanently from the courtyard (front and rear) and roof-top.
7. Air-Conditioner/Air-Cooler and back tray of refrigerator water to be drained out and scrubbed dry once a week.
8. Water poured on cement concrete setting (at construction sites) should be drained out.
9. The cement haudi should be dismantled or water should be changed once a week.
10. Under-ground water haudies should be properly covered and cleaned once a week.
11. Waste water should be disposed off properly to avoid stagnation.
12. Trees holes holding water should be filled with sand/cement mixture.
13. Allow the officials of this Organization to inspect and treat the mosquito breeding sources in your premises.
14. Screening of migrant labourers for Malaria at the construction sites by Malaria controlling authorities at the nearest Malaria Clinics or through Mobile Squads, surveillance teams, special surveillance squads deployed under National Vector Borne Disease Programme of the State/U.T. Government.

Note :- In case the corrective measures are note taken by me/us within one week, I/we will be liable for a chailan

Signature of the
Owner/Occupant/Caretaker

Assistant Director Malaria,
Chandigarh Administration, Chandigarh,
SCO No. 64-65, Second Floor
Sector-17-D, Chandigarh

Corresponding author: rashmi_kohli1@yahoo.com
Received: November 25, 2023, Accepted: December 25, 2023

DISCUSSION

The information provided by Dr. Suman Singh, the Director of Health Services in Chandigarh, highlights the significant impact of dengue in the Union Territory. With around 300 reported cases since January and 130 new cases in October, 2023 alone, it is evident that the situation requires careful attention and coordinated efforts.

The notable increase in dengue cases, especially in October, 2023 emphasizes the urgency of implementing effective measures to control the spread of the virus. The identification of the DENV2 strain as prominent underscores the importance of understanding the specific characteristics of the virus. The public needs to be informed about the symptoms of dengue, the importance of seeking medical attention promptly and measures to prevent mosquito breeding. Dr. Parvinder Chawla, Fortis, Mohali highlighted warning signs of dengue hemorrhagic fever or dengue shock syndrome. Persistent vomiting can be a symptom of severe dengue.

Additionally, acknowledging the efforts of the blood transfusion department, led by Dr. Ravneet Kaur, GMCH, Sector-32, Chandigarh and expressing gratitude to blood donors for their contributions can help foster a sense of community support and encourage continued participation in blood donation drives.

The significant increase in reported cases of dengue from 2022 to 2023, with 576 cases reported until October,23 in the latter year, indicates a notable change in the epidemiological situation. This rise in cases may be attributed to various factors, including environmental conditions, mosquito population dynamics and viral circulation.

Here's a breakdown of the monitoring recommendations:

1. **Duration of Hospitalization:** Closely monitoring patients for at least 48-72 hours in the hospital is essential. This duration allows healthcare professionals to observe the progression of the disease and promptly address any emerging complications.
2. **Monitoring Hemoglobin and Hematocrit Levels:** Regular monitoring of hemoglobin and hematocrit levels is crucial. Changes in these levels can provide valuable information about the patient's condition.
    - **Increase in Hemoglobin and Hematocrit:** An increase in hemoglobin and hematocrit levels on the second or third day of fever may indicate poor oral intake, suggesting dehydration. This information is valuable for adjusting fluid management and ensuring proper hydration.
    - **Falling Hemoglobin and Hematocrit:** A decrease in hemoglobin and hematocrit levels, especially when accompanied by clinical deterioration, suggests the possibility of internal bleeding. Internal bleeding is a severe complication of dengue and immediate hospitalization is necessary to address this critical situation.
3. **Clinical Assessment:** In addition to laboratory parameters, continuous clinical assessment is essential. Monitoring for signs and symptoms such as persistent vomiting, severe abdominal pain, bleeding manifestations, and changes in vital signs helps identify complications early on.
4. **Fluid Management:** Adequate fluid management is a key aspect of dengue care. Monitoring fluid intake and output, as well as adjusting fluid therapy based on the patient's response, is crucial in preventing dehydration and maintaining hemodynamic stability.

It is valuable to understand the nuances of **Patient Management** during different stages of the disease. Here's a summary of the key points:

1. **Decrease in Hemoglobin and Hematocrit with Improvement in Symptoms:** Hemoglobin and hematocrit levels may decrease during the critical phase due to plasma leakage into the interstitial space, leading to hemoconcentration. As the patient enters the recovery phase and begins to reabsorb the lost fluid, hemoglobin and hematocrit levels may normalize or even decrease slightly from their peak during the critical phase.
2. **Platelet Count Considerations:** Noting that a falling platelet count alone may not necessarily imply the need for hospital admission is a crucial point. Platelet counts can fluctuate during the course of dengue and admission may be warranted based on a combination of clinical symptoms, overall patient condition and laboratory results.
3. **Transfusion Threshold for Platelets:** The recommendation that platelet transfusion is typically reserved for cases where the count is below 10,000/cmm or there is evidence of active bleeding aligns with established guidelines. This approach helps ensure that platelet transfusions are administered judiciously and in cases where there is a clear clinical need.
4. **Evidence of Active Bleeding:** The emphasis on transfusing platelets when there is evidence of active bleeding from any site is a critical

consideration. This approach prioritizes interventions based on the clinical presentation and aims to address immediate threats to the patient's well- being.

The proactive measures taken by Dr. Suresh Bhonsle and the Health Department in Panchkula to check the spread of dengue are commendable. It is positive to note that a multifaceted approach has been adopted, involving community participation, awareness programs, cross-border meetings, deployment of teams in high-risk areas, inspections, breeding checks and surveillance.

Control Measures:

1. **Community Participation:** Community involvement ensures that dengue prevention efforts are sustained over time. When individuals are educated about the importance of eliminating standing water and maintaining clean surroundings, they are more likely to continue these practices even after official campaigns have ended.
2. **Awareness Programs:** Conducting awareness programs is an effective strategy to educate the public about dengue, its symptoms, preventive measures, and the importance of seeking timely medical attention. Well-informed communities are better equipped to take preventive actions.
3. **Cross-Border Meetings:** Collaborative efforts involving cross-border meetings indicate a regional approach to disease control. Dengue does not adhere to geopolitical boundaries, and cooperation between neighboring areas is essential for a comprehensive and coordinated response.
4. **Deployment in High-Risk Areas:** Targeted deployment of teams in high-risk areas, such as Kalka and Pinjore, demonstrates a strategic focus on locations with a higher incidence of dengue cases. This allows for more concentrated efforts to control mosquito breeding and implement preventive measures.
5. **Inspections and Breeding Checkers:** Regular inspections of homes, coupled with the deployment of breeding checkers, contribute significantly to identifying and eliminating potential mosquito breeding sites. Timely intervention in this regard is crucial to prevent the further spread of dengue.
6. **Surveillance:** Active surveillance is essential for monitoring the prevalence and distribution of dengue cases. Surveillance enables timely responses, targeted interventions, and the allocation of resources to areas with higher transmission rates.
7. **Results of Proactive Measures:** The mention of yielding positive results indicates that the proactive measures are making a tangible impact on controlling the spread of dengue. Continued efforts and adaptability in response strategies will be key to sustaining these positive outcomes.

Treatment:

These recommendations are in line with standard practices for dengue treatment and prevention. Here's a summary:

1. **No Specific Treatment:** There is no specific antiviral treatment for dengue, and care is primarily supportive.
2. **Fluids and Nutrition:** Adequate fluid intake is crucial to prevent dehydration, and a nutritious diet helps support the immune system during recovery.
3. **Bed Rest and Mosquito Net Use:** Patients are advised to get plenty of rest and use mosquito nets to prevent further transmission of the virus.
4. **Avoid Certain Medications:** Aspirin and non-steroidal anti-inflammatory drugs (NSAIDs) like ibuprofen (brufen) should be avoided due to the risk of bleeding. Paracetamol is recommended for managing fever and body ache.
5. **Monitoring at Home:** Monitoring fever, blood pressure, and pulse at home, whenpossible, helps in tracking the progression of the illness.
6. **Seek Medical Attention:** In case of fever, individuals should seek medical attention and get tested for dengue. Immediate hospitalization is advised for severe symptoms to address electrolyte imbalances and other complications.
7. **Platelet Monitoring:** Since dengue can lead to a decrease in platelet count, serial platelet estimation is recommended. Patients should be vigilant for signs of bleeding, such as from the gums, nose, or in stools.
8. **Hospitalization for Severe Cases:** Sudden and significant drops in platelet count may warrant hospitalization to manage complications and provide appropriate medical care.

Testing Site:

1. Dengue ELISA test (Ns1/IgM) is the recommended test for dengue and Rapid (Card) Tests are not recommended and may give unreliable results.
2. Free dengue testing facilities are available at:
   A.) Department of Virology, PGIMER
   B.) Department of Microbiology, GMCH-32C.) Department of Microbiology, GMSH-16D.)

Civil Hospital, Sector-45, Chandigarh E.) Civil Hospital, Sector-22, Chandigarh F.) Civil Hospital, Manimajra, Chandigarh

Conclusion:

1. **Existing Dengue Vaccine (Dengvaxia®):**
   - Dengvaxia is a tetravalent, live-attenuated dengue vaccine.
   - It is currently available for use and is intended for children 9 through 16 years oldwho have laboratory-confirmed previous dengue virus infection.
   - Dengvaxia is recommended for use in areas where dengue is endemic, includingcertain U.S. territories and freely associated states.
2. **Takeda's Dengue Vaccine:**
   - Takeda has a dengue vaccine available for children and adults in countries such asIndonesia, Thailand, Argentina, and Brazil.
   - Notably, it is mentioned that Takeda's dengue vaccine is not approved for use inIndia.
3. **Serum Institute of India's Dengusiil Vaccine:**
   - The Serum Institute of India (SII) is developing Dengusiil, a live attenuateddengue virus vaccine.
   - Following a successful Phase-I trial in Australia, the SII is set to begin Phase Iand Phase II trials for Dengusiil in India.
   - Dengusiil aims to be India's first indigenous dengue vaccine.
4. **Live Attenuated Vaccines and Immune Response:**
   - Live attenuated vaccines, like Dengusiil, are designed to induce both neutralizingantibodies and cell-mediated immune responses.
   - The protective immune response is expected to develop around four weeks aftervaccination.

References:

The Indian Express, Chandigarh, India, 2nd November, 2023.

Health Department, Chandigarh Administration, India.

Beasley, D. W. C. & Barrett, A. D. T. "The Infectious Agent." In *Dengue: Tropical Medicine: Science and Practice*, vol. 5, eds. G. Pasvol & S. L. Hoffman (London: Imperial College Press, 2008): 29–74.

National Institutes of Health. "How Dengue Virus Infects Cells." *NIH Research Matters* (2010).

World Health Organization. *Dengue: Guidelines for Diagnosis, Treatment, Prevention and Control.* Geneva: World Health Organization and the Special Programme for Research and Training in Tropical Diseases, 2009.

ALGAE AS A NUTRIENT SOURCE TO COMBAT DEFICIENCIES IN PREGNANT WOMEN

Sezal
University Institute of Engineering and Technology,
South Campus, Panjab University, Chandigarh-160014.

ABSTRACT

Algae are commonly found organisms who have been exploited by humans for centuries for their medicinal properties. Slowly as research advanced the other potentials of algae came to notice and they were soon incorporated in other industries. Algae have been into considerations regarding their huge advantages when applied as primary agriculture source. Nutrient based deficiencies are a common concern for pregnant women, which if left untreated might lead to adverse consequences of health for mother or fetus. Algal potential as a future food, its role as an efficient food additive and other commercial and environmental advantages of algae is discussed. Primary focus on the potential of algae or algae-based foods/nutraceuticals as a solution for efficient treatment of nutrient deficiencies in pregnant women is concerned. The future of algal industry, its potent advantages and probable challenges are also put to notice. The need for focused research regarding the same is also highlighted.

KEYWORDS: Nutrient deficiencies, Nutraceutical, Algal cultivation, Pregnancy, Health defects.

INTRODUCTION

Algae are one of the oldest organisms dating back to around 3 billion years and have since been some of the most common organisms inhabiting the Earth. They grow in variety of habitats including some extreme habitats. They grow in terrestrial environments and in both fresh and salt waters among aqueous habitats. Among the wide variety of marine life, approximately 90% of the species of marine flora are algae, which are responsible for about 50% of global photosynthesis (Tanna and Mishra 2019). Around 30,000 species have been scientifically described, but the real number might be much higher, with some estimates of it being at 1 million different species or more (Scieszka and Klewicka 2018). The individual algae classes (divisions), are distinguished primarily by the composition of their photosynthetic pigments, dominant habitat, cytological chemical and morphological aspects and products. The morphology and size of algae are highly variable. There are unicellular species measuring 3- 10 μm, and larger species measuring as much as 50-70m long (Scieszka and Klewicka 2018). On the basis of their size, a distinction is made between microalgae and macroalgae. Single- celled algae and cyanobacteria are together referred to as microalgae. Seaweeds are large algae termed macroalgae, categorized into three types according to their pigment content: red seaweeds (Rhodophyceae), green seaweeds (Chlorophyceae), and brown seaweeds (Phaeophyceae) . As photoautotroph organisms, algae are the starting point of most food webs in aquatic ecosystems.

Scientist have viewed algae as great source of food, feed and fertilizer production. They also show promising future as generator of biofuels, efficient removal of pollutants and heavy metals, wastewater treatment and its recycling. Algal sources have been used in production of cosmetics, gelling and thickening agents, functional foods and as dietary supplements. Algal bioresources with medicinal values are used to formulate nutraceuticals, many algal species containing bioactive compounds showing high antiviral, antibacterial, antioxidant, antimicrobial, neuroprotective, immunomodulating and anticancer action are exploited for their nutraceutical potential. However considering the enormous biodiversity of microalgae only a few of such medicinal specie like *Spirulina platendis* are recognised and used.

Studies have showed that algae contain important bioactive compounds and range of bioactive metabolites along with proteins, essential vitamins like Vitamin A,B12,D,E, carbohydrates, macronutrients, lipids, PUFAs, polysaccharides and pigments (Scieszka and Klewicka 2018). Prescribed consumption of specific algal sources have also proven to be of health benefits related to desirable growth, maintenance of bodily functions and prevention of adverse health conditions.

A healthy diet is an important determinant of health of both mother and offspring during pregnancy. The daily nutritional requirements of a women undergoes moderate increase during pregnancy where micronutrient requirements increase more than macronutrient needs (Marangoni et al. 2016). According to an Italian consensus, most prevalent nutrient deficiencies in pregnant women include iron, iodine, calcium, folic acid, vitamin D and DHA(Docosahexaenoic acid) (Marangoni et al. 2016). Other deficiencies of zinc, vitamins like vit A,B and E, copper, selenium and other nutrients might also affect. As a result of these deficiencies, many health

Corresponding author: sezalmittu@gmail.com
Received: September 28, 2023, Accepted: December 20, 2023

issues can be generated in the mother or fetus or both. Such issues may include abnormalities in growth or body composition, cardiometabolic, pulmonary or immune system related problems, neurodevelopmental or cognitive issues (Gernand et al. 2016).

The review discusses potential of algae in agriculture industry and subsequent advantages or disadvantages. Algae as a potential combat for treating nutrient based deficiencies in pregnant women is primarily discussed, its usage in nutraceuticals and additive foods both in enhancing medicinal or dietary capabilities is also reviewed. The future of algal bioeconomy is also discussed, algal advantages apart from its nutritional capabilities is also highlighted. The need for focused research and experimentations regarding algal potentials and its effects on pregnant women is also to be concerned.

ALGAE AS A NUTRIENT SOURCE:

Algae have been consumed by humans for various medicinal and nutritional needs. Traditionally, Asian countries have used seaweeds and microalgae majorly for food while the west preferred algal usage primarily in pharmaceutical or cosmetics. Algae are known to be nutritionally abundant sources and few also contain medicinal pigments that are exclusive to algal species. Microalgae and macroalgae (seaweed) are rich in proteins, soluble fibers and polysaccharides, lipids and polyunsaturated fatty acids, pigments, vitamins, and minerals. Apart from the nutritional estimation, method of consumption that enhances the impact of algal source consumed must also be discussed.

CARBOHYDRATES:

According to Escalante and Perez 2021, Seaweeds are considered sources of carbohydrates, mainly polysaccharides with total carbohydrate content ranging upto 76% on dry weight basis. Microalgae are slightly unexplored sources of carbohydrates although microalgal carbohydrates constitute good overall digestibility. Microalgal carbs contain upto 64% biomass on dry weight basis. Widely used for its polysaccharide extracts and beneficial carbohydrate substances, *Chlorella sp*. is widely produced despite its lower total carbohydrate contents.

Algal species like *Porphyridium sp.* and *Spirulina platensis* are also utilised due to their high sulphated carbohydrate contents.

DIETARY FIBERS:

Seaweeds are also known sources of soluble and insoluble dietary fiber. Seaweeds like *Fucus* and *Laminaria* have the highest insoluble dietary content, *Undaria pinnatifida* and *Porphyra*. *sp* have highest soluble dietary content (Escalante and Perez 2021).

LIPIDS AND FATTY ACIDS:

Lipids are group of molecules including fats, sterols, fat soluble vitamins and other substrates. Brown seaweeds sources have been analysed to be dominant sources of unsaturated fatty acids while red seaweeds show high saturated fatty acid content (Escalante and Perez 2021). Microalgae are proven sources of long chain PUFAs like EPAs(eicosapentaenoic acid), DHA (docosahexaenoic acid) and linolenic acids. Long chain acids like EPA and DHA are essential nutrients for human body yet we depend on microalgal sources since humans, animals or higher plants don't synthesize them. Algal Species like *Phaeodactylum* and *Nanochloropsis* are suitable producers of EPA while *Isochrysis* and *Schizochytrium* are dominant DHA suppliers along with producing other essential PUFAs (Escalante and Perez 2021).

PROTEIN:

Main reason for algal consumption since ancient times has been their rich protein content. Seaweed proteins are excellent sources of most amino acids, such as proline, alanine, glycine, arginine, and especially aspartic and glutamic acids. Considering their high protein content and amino acid composition, red seaweeds prove to be a highly productive sources of nutraceutical production (Wijesekara and Kim 2015). Microalgal species like *Arthrospira maxima, Scenedesmus obliquus* and *Spirulina(Arthrospira platensis)* are widely known protein rich substrates. Spirulina powder is very rich in protein containing 18 amino acids including all essential amino acids. Quality of some algal proteins is also superior to plant source proteins. *Porphyra tenera* contains upto 47% protein by dry mass which is comparable to protein estimates in soybean (Escalante and Perez 2021). Most seaweeds contain essentially all amino acids and hence preferred over plant sources that are rich in specific amino acids.

VITAMIN AND PIGMENTS:

Plants and microbes are major sources of high value pigments, though natural pigments from plants present problems such as instability against environmental conditions and seasonal unavalabilities. Algae are therefore promising sources of natural pigments like carotenoids, b- carotene, astaxanthin, fucoxanthin and phycobiliproteins. B-carotene is a prominent source of vitamin A, it is largely produced by *Dunaliella salina* specie that contains upto 14% dry weight carotene content. Astaxanthin is a strong antioxidant and is

produced commercially using algal species like *Haematococcus pluvialis (*Escalante and Perez 2021). Lectin and phycobiliproteins are two families of bioactive algal proteins which have been exploited for several industrial applications. Lectins are mostly extracted from macroalgal sources, while phycobiliproteins are typically isolated from microalgae. Sterols mainly represented by fucosterol, clionasterol, isofucosterol and cholesterol are the main nutritional constituents of marine seaweeds.

OTHER NUTRIENTS:

Studies on algal species have also proven algae to be rich sources of valuable minerals like sodium, potassium, phosphorous, manganese, iron, copper and zinc. Alga *Bracteacoccus minor* showed high iron concentration by dry mass which was higher than supplements from *Spirulina maxima*. *Chlorococcum humicola* was observed to be excellent supplement for zinc and cobalt while *Fasciculochloris boldii* showed promising magnesium contents. Alga *Tetradesmus acuminatus* was found to be moderate in both sodium and potassium contents (Santhakumaran et al. 2020).

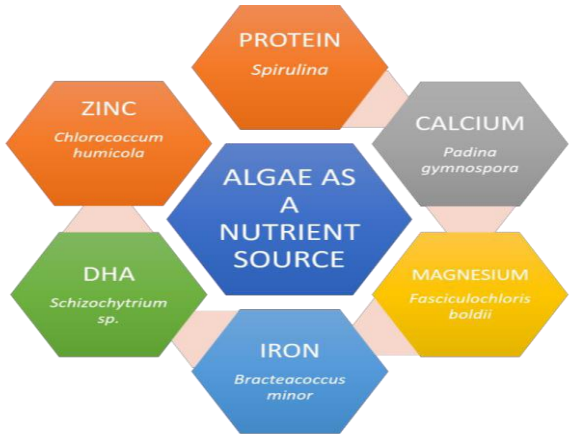

Figure 1: Depicting efficient algal sources of different nutrients. (Sources: Escalante and Perez 2021; Santhakumaran et al. 2020; Ramu et al. 2020).

ALGAL CULTIVATION FOR AGRICULTURE:

Presently, around 95% of the world's tonnage comes from seaweed farming, but only six species of macroalgae represent 96% of the world's production volume which include *kappaphycus, Eucheuma, Laminaria, Gracilaria, Undaria* and *Porphyra* (Hentati et al. 2020).

Present day agriculture is based primarily on terrestrial plants (Kuenz et al. 2020). With rising global population, decrease in fertile landmass and substantial environmental crisis, the behaviour and working of global agriculture must change drastically. Modern demands for an ideal agricultural source would include intensified agriculture on a flexible landmass(barren or non-arable) and feasible utilization of industrial waste products as manure. Algae can be cultivated on non-arable land, fermenters, photobioreactors and on open seas or oceans. According to estimates, around 5 million km^2 (0.3% of ocean surface) of seaweed production area should be adequate to produce biomass equivalent to all global agriculture annually (Ullmann and Grimm 2021). Microalgae too have been studied for having potential in agriculture, *Spirulina* as an example, is known to produce 10 times more biomass than corn hybrids (Ullmann and Grimm 2021). They are known to be genetically very diverse with varied biochemical potentials, yet presently microalgal production focuses on commercialising "low volume, high value" products. Modern biotechnological advancements also allow the use of algae to maximise the efficiency of a plant based agricultural economy thus expanding the potentials of algal cultivation. Experimentally, treatment of barley crop with an extract of *Ascophyllum nodosum* was proved to significantly improve the frost tolerance of barley during winters (Fleurence 2021). The use of algal biomass promotes the modernisation in terrestrial plant-based agriculture that is dependent on organic sources replacing potentially harmful chemical substrates.

It is important to note that despite of having immense potential as a feasible food source, algal cultivation for agriculture and its commercialisation has its own challenges. For obtaining higher yields of microalgal production, high energy expenditure is needed because electric energy is essentially needed to power basic microalgal functions that higher plants are capable of performing by themselves (Kuenz et al. 2020). Algal based products need to be marketed as "high volume, low value" products for them to be able to reach global and diverse population. Major concerns preventing such algal commercialisation include higher initial investments, lack of economic incentives by the authorities, limited research and funds, lack of latest technologies in the algae production sector.

The establishment of a sustainable algae industry would also generate more jobs and income, during the corona crisis the seaweed farming industry of Bali was rejuvenated and was successful in generating an income of 400USD monthly for workers (Ullmann and Grimm 2021). Small scale pond micro-farm systems could also help farmers make money independently, hence protecting product integrity and the farmer from exploitation. Coastline seaweed

farming could help prevent fertilizer run-off into aquatic ecosystems. Floating microalgae farming could provide regular essential cooling of the photobioreactor (Ullmann and Grimm 2021). Such intelligent multi-purpose algal production systems are devised but need to be studied on a commercial scale for efficient large scale implementation. A modern take in algal cultivation is the Absolute knowledge collection of algal strains and subsequent rigorous experimentations would ensure a multifaceted algal bioeconomy to bloom. According to Fabris et al., 2020, future cultivation technology (integrating knowledge about phenomics and synthetic biology advancements) would allow microalgal yield to increase dramatically in the coming years.

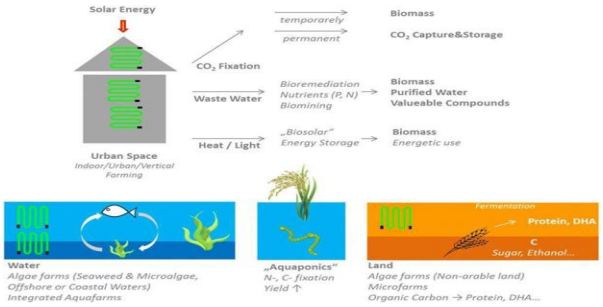

Figure 2: Potential of algae for a circular bioeconomy, landless food production and urban farming. (Source: Ullmann and Grimm 2021)

NUTRIENT DEFICIENCIES IN PREGNANT WOMEN:

Pregnant women are at increased risk of nutrient deficiencies because of higher nutritional needs of mother and the developing fetus. These deficiencies if severe and left untreated can cause problems to both or either the mother or fetus. Latest researches show that the period from conception to two years of birth are important determinants of adulthood diseases for an individual (Marangoni et al. 2016). These micronutrient deficiencies vary throughout pregnancy and their overdose is equally harmful as their underdose. The prevalence and intensity of such deficiencies differ across populations; their development status, dietary culture, food availability, societal norms are few of the determinant factors. North American vegetarian population is recommended to have more foods that are good sources of vitamin B12, Vitamin D, calcium and iron; the recommended intake of calcium is around 1200 mg/day which is 20% more than prescription for omnivores (Sebastiani et al., 2019). Although the recommendations for pregnancy might alter, but the impact of varied diets on nutrient reserves of the body is vastly accepted.

The RDAs (Recommended Dietary Allowances) are expert estimations for daily nutritional requirements of a population. In pregnancy the micronutrient requirements increase more than macronutrients (Marangoni et al. 2016). The RDA for pregnant women did not vary with that of non-pregnant women for nutrients like Vitamin D and E, whereas RDAs for iron, iodine, folate and Vitamin B6 sore to a 50% increase for pregnancy (Gernand et al. 2016). Nutritional needs surge during pregnancy but misinformed supplementation might affect adversely. Iron deficiency is the most common affecting estimated 40% pregnancies worldwide, considering which WHO has recommended iron supplementation for all women during pregnancies since 1950s (Tuncalp et al. 2019). Vitamin D deficiency during pregnancy is estimated to affect around 60% women in India (Tuncalp et al. 2016). Vitamin A deficiency affects 15% pregnant women in low income countries (Tuncalp et al. 2016).

	Acceptable micronutrients distribution range (AMDR)		
Nutrients (unit of measure/day)	Adult women	Pregnancy	Lactation
Vitamin A (mcg)	400-600	500-700	800-1,000
Vitamin B6 (mg)	1.1-1.3	1.6-1.9	1.7-2
Vitamin B12 (mcg)	2-2.4	2.2-2.6	2.4-2.8
Vitamin C (mg)	60-85	70-100	90-130
Thiamin (mg)	0.9-1.1	1.2-1.4	1.2-1.4
Riboflavin (mg)	1.1-1.3	1.4-1.7	1.5-1.8
Niacin (mg)	14-18	17-22	17-22
Folic acid (mcg)	320-400	520-600	450-500
Vitamin D (mcg)	10-15	10-15	10-15
Vitamin E (mg)	12	12	15
Vitamin K (mcg)	140	140	140
Calcium (mg)	800-1,000	800-1,000	800-1,000
Phosphorus (mg)	580-700	580-700	580-700
Magnesium (mg)	170-240	170-240	170-240
Iron (mg)	10-18	22-27	8-11
Zinc (mg)	7-8	9-11	10-13
Copper (mg)	0.7-0.9	0.9-1.2	1.2-1.6
Selenium (mcg)	45-55	45-55	59-70
Iodine (mcg)	150	220	290

Figure 3: Tabular representation comparing RDAs of adult women, pregnant women and lactating women. (Source: Mecacci et al. 2015).

Studies over south Asian countries (India, Bangladesh, Nepal) concluded prevalent zinc and Vitamin B12 deficiencies in pregnant women while 50-70% of pregnant women suffered vitamin E deficiency. In southern Nepal, only 4% of pregnant women were concluded to be on adequate nutrient levels. Evidence shows that around 80% of population does not meet the RDA for EPA and DHA, while DHA requirements increase to about 100mg during pregnancy and lactation, inferring that most pregnant women are prone to DHA deficiency (Marangoni et al. 2016). Iodine deficiency ranges from 17% in Oceania to 40 % in Africa (Gernand et al. 2016). A study on pregnant females aged between 20–40 years in certain parts of India were observed, around 42% were found to

have vitamin D deficiency and 14% had vitamin D deficiency in the first trimester itself of which around 63.63% of women with lower vitamin D reserves were vegetarians (Sebastiani et al. 2019). These nutrient deficiencies if ignored might have extreme consequences, hence specific care must be provided towards the cause and solution for combating these deficiencies.

HEALTH EFFECTS OF NUTRIENT DEFICIENCIES IN PREGNANCY:

Adequate nutrient intake promotes maternal health, proper fetal development and induces long term impacts on child's health. Nutrient deficiencies on the other hand produce adverse effects in mother, fetus, infant or adult child. These adverse effects could be antenatal (preceeding birth), birth defects or postnatal (post birth of offspring).

Protein demands increase progressively during pregnancy especially during the third trimester. In undernourished populations, protein intake is recommended to reduce risks of low birth weight neonates, SGA neonates and stillbirth prevention (Tuncalp et al. 2020). Iodine intake is necessary to promote production of fetal thyroid hormones during pregnancy that prevent hypothyroidism in fetus and newborns. Iodine deficiency is related to increased risk of spontaneous abortion, perinatal mortality and neurological disorders (Marangoni et al. 2016). Calcium RDAs for pregnant women are varied country wise, and for breastfeeding women. Calcium supplementations are recommended prior pregnancy to prevent pre-eclampsia complications (Tuncalp et al. 2020). Miscarriage is the unplanned spontaneous expulsion of underdeveloped fetus from the body, a major cause of which can be nutrient inadequacies. Severe zinc, copper, selenium, iodine and Vitamin E deficiencies are known to increase the risk of a miscarriage (Gernand et al. 2016). Adequate DHA content in breastmilk is proven to promote healthy cognitive development and visual activity in infants (Marangoni et al. 2016). Study depicts that abundant DHA and unsaturated fatty acids content shall improve the visual acuity, mental development and psychomotor skills of the fetus (Ramu et al. 2020). Iron demands increase drastically during pregnancy and immediately after postpartum. If iron reserves are deficient, it may increase risk of preterm delivery, post-partum hemorrhage, lower birth weight in baby and an increased risk of developing cardiovascular issues in adulthood is observed (Marangoni et al. 2016). Iron deficiency also increases the risk of abnormalities in the hippocampus development and brain energy metabolism (Gernand et al. 2016). Vitamin D importantly contributes in regulation of hormone secretion and embryonic implantation in pregnancy. In cases of inadequate consumption of vitamin D, associated risks include respiratory infections, allergic diseases, abnormal skeletal developments, preterm deliveries or low birth weight (Marangoni et al. 2016). Deficiencies in folate and Vitamin B12 reserves are studied to increase risk of fetal abnormalities, miscarriages, neural tube defects and cause disturbances in fertilization and embryo development (Gernand et al. 2016). Folic acid supplementation is also recommended to decrease risk of neural tube defects and congenital heart diseases, moreover promoting placental health (Marangoni et al. 2016). Deficiencies of other micronutrients including iron, zinc, copper, magnesium and Vitamins A and E have been postulated to affect organ structures of kidneys, pancreas and development of cardiometabolic diseases (Gernand et al. 2016).

Consumption of balanced diet is essential from the pre-conceptional period to ensure a healthy pregnancy. Due to increasing pollutants in the environment and addition of chemicals in food substances, the organic purity of food and based products is influenced. As a result, during pregnancies some women are recommended supplementations to cover up for what their available food diets can't provide. Nutraceutical supplementations must also be available to diverse economic populations to treat deficiencies efficiently. An estimate of 70% of the Indian population lives in rural areas and hence, interventions on the nutraceuticals is probable to cover only urban populations (Dudeja and Gupta 2017). Because of such economic disparities the occurrence of biased treatment of nutrient deficiencies amongst pregnant women might exist.

ALGAE AS A POTENTIAL COMBAT:

Nutrient deficiencies in pregnant women must be carefully examined before proposing any supplementation. Production of a single multi-nutrient supplement seems ideal but in practicality nutrient intakes and deficiencies amongst a population of pregnant women is subject to various factors and hence not consistent (Tuncalp et al. 2020). Although we do know from studies the RDAs for different nutrients as a generic prescription that promotes a healthy pregnancy. These RDAs might be met by either nutraceutical supplementation or specific food diets.

Processed food is nutritionally deficient and people are becoming aware of this. Not preferring pharmaceuticals, they now prefer natural substitutes probably because of its organic interactions with body (Dudeja and Gupta 2017). Algae have been used as an

additive in meat, bakery and dairy industry to enhance their quality. The addition of algae has increased nutritional abundance of meat, while overcoming its technical problems like lower salt content. Sea spaghetti, Wakame and Nori when added to meat supported increased contents of Manganese, Calcium, Magnesium and Potassium hence enhancing its nutritional value (Scieszka and Klewicka 2018). Cereal based products are commercially successful due to their high consumption and low cost, their lower nutritional abundance can be maximised by addition of bioactive rich algae. For example addition of algal species *Sargassum marginatum* and *Undaria pinnatifida*(Wakame algae) in pasta production were tested and proved to be beneficial (Scieszka and Klewicka 2018). Pasta is characterised by its lower protein contents which can be overcomed by addition of a suitable protein rich algae. Moreover the quality of bread was studied to increase by addition of known green algae (*Ulva lactuca* and *Laminaria*) (Scieszka and Klewicka 2018). Algae based products are also appreciated in the vegan market as a substitute for eggs. Dairy products like cheese are enriched with algae to increase their nutritional value and also help provide calcium through cheese in people who lack ability to digest it from casein (through ordinary cheese). Fermented seaweed sauce showed potential as a potent nutritional source and fermented seaweed extracts may be beneficial as therapeutic drugs (Scieszka and Klewicka 2018). Addition of algae in food products increases their nutritional versatility while preventing health damages from use of chemicals instead. Thus algae are ideal additives when discussed as nutraceuticals, therapeutics or functional foods. Challenges on incorporating algae in food includes its sharp green colour, powdered availability, conservational food habits and socio-ethnological barriers (Escalante and Perez 2021). Moreover, adequate importance must be given to the synergistic effects of algal additives; many Studies have depicted that synergistic combination of foods are an essential determinant in the prevention of chronic diseases (Natarajan et al. 2019).

Nutraceutical supplementation might seem like the best method to provide nutrient adequacy but also has side effects. Seaweeds were found to be a best source of supplementation during gestational period, without any side effects (Ramu et al. 2020). Alga *Padina gymnospora* was found to contain 820 mg /100g of calcium, which is competitive to the 1200 mg per day requirements of developing fetus; thus proving to be more beneficial than average dairy food supplementation of 305mg/100g (Ramu et al. 2020). Chlorella supplementation was found to dominantly decrease the risk of pregnancy associated edema, anemia, and proteinuria, hence it might be useful as a source of natural folate, vitamin B-12 and iron for pregnant women (Tang and Suter 2011). Ramu et al. 2019, conducted experiments on underexploited algal species of *Acanthophora spicifera, Gracilaria edulis, Padina gymnospora, Ulva fasciata* and *Enteromorpha flexuosa* to determine the nutritional contents of these species, the values were found to meet about 70% of vitamins need during pregnancy and lactation. According to experiments by Santhakumaran et al. 2020, 25 selected species of algae were found to contain abundant nutritional content. Alga *Bracteacoccus minor* was discovered as an efficient nutraceutical for iron which is a concerning nutrient in pregnancy. Alga *Chlorococcum humicola* was found to be promising supplement for zinc and copper requirements. Other algae also proved to be abundant carriers of magnesium, Calcium, zinc, copper and other discussed deficient nutrient w.r.t pregnancies. Alga *Tetrastrum komarekii* was also found to hold medicinal antioxidant activity. Antibacterial and antimicrobial activities of some of these researched algae were also found to be high. All such studies descriptively illustrate the nutraceutical potentials of algae. Further extended studies centralising pregnant women must be performed to extract complete potential of algae as a supplement.

Seaweed consumption was found to be inversely proportional to depression occurrence in pregnant Japanese women in a study regarding prevalence of depression in pregnant women (Tanna and Mishra 2019). In general, seaweeds were found to contain precise proportion of potassium required for essential blood plasma levels during pregnancy (Ramu et al. 2020). Extending studies regarding impacts of various algae on pregnant women would potentially derive many positive results. Although since pregnancy is a sensitive stage, any experimentation on the body must be carefully conducted, supported by enough studies and research before any recommendations. Algal potential is also highlighted in a clinical study where consumption of *Undaria* was found to lower the risks of breast cancer and mortality in women (Tanna and Mishra 2019). A 2014 study by Weiner, demonstrated safe carrageenan use for infant formula through studies (Tanna and Mishra 2019). Latest studies on various *Sargassum* polysaccharides found them to be of considerable anticoagulant, anticancer, antimicrobial, antiviral and anti-inflammatory potentials thus, nevertheless potent sources for enhancing disease immunity.

DISCUSSION AND FUTURE PROSPECTS:

Algal sources as discussed were studied to have immense potential as effective therapeutics, nutraceuticals, food or feed products or additives. These organisms have also shown applicative advantages

when used as biofuels, bioplastics, fertilizers, biorefineries, wastewater treatment, nutrient recycling, CO_2 biomitigation and has been used industrially to prepare gelling and thickening agents. Microalgae are capable of utilising carbondioxide as a substrate for production of its biomass, both organic and inorganic carbon forms, thus protecting the environment from acute global warming. According to study, production of 100t of algal biomass can fix about 183t of CO_2 (Kuenz et al. 2020). Thus promoting cost effective and efficient way of CO_2 biomitigation. According to studies, Microalgal biomass components such as carbohydrates, starch and lipids can be processed into bioplastics; plastic pollution can thus be reduced by efficient use of algae-based bioplastics (Fabris et al. 2020). Biorefinery is defined as process of sustainable production of bioenergy or bio by-products from biomass. Biorefinery of seaweed biomass is commercially feasible for production of animal feeds, food, biofertilizers, hydrocolloids and for its unique carbohydrate composition (Tanna and Mishra 2019). Algal cultivation could also help decrease the nutrient losses by binding non-renewable nutrients, thus preventing land infertility over the years (Ullmann and Grimm 2021).

Algae use minerals like nitrogen, phosphorous and sulfur alongside other important substrates to build biomass (Kuenz et al. 2020). Much of the wastewater excreted off industries has similar dominant effluents, therefore algae is used for cultivation on such wastewater where it utilises the waste effluents to grow thus cleaning up the wastewater. This wastewater management strategy is highly efficient due to its ability to recycle water and also promote cultivation. Although a drawback is the need of greater space as compared to conventional setup of wastewater treatment plants (Ullmann and Grimm 2021). Seaweeds also possess the ability to entrap heavy metals including Cadmium, Aluminium, Iron, and Arsenic; the majority of Arsenic in seaweeds is prevalent as arsenosugars which are known to very less toxic than inorganic Arsenic compounds which might be carcinogenic (Smyth 2021). Algal cultivation thus also promotes removal of heavy metals and some pollutants, thus influencing environmental cleaning (Scieszka and Klewicka 2018). Thus algae can be a potent mode of environmental friendly nutrient recycling and pollutant removal. Numerous studies discuss the cultivation of algae for biofuel production. Variety of biofuels can be obtained from algae like biomethane, biodiesel, bioethanol etc. Seaweeds are considered suitable sources of biofuel production due to their carbohydrate content of as high as 50% (Ullmann and Grimm 2021). Efficient biofuel production is linked to extraction of beneficial byproducts like pigments (chlorophyll, carotenoids) and other bioactive compounds that help balance high initial cost of cultivation (Ullmann and Grimm 2021). Increasing prices of oil and simultaneous depletion of fossil fuels are evident reasons to study algal biofuel production commercially. Integrating modern methods of synthetic biology, algae have been cultured to produce advance medicinal high value products, like Diatom *Phaeodactylum tricornutum* has been engineered to efficiently and successfully produce and secrete fully assembled antibodies (Fabris et al. 2020).

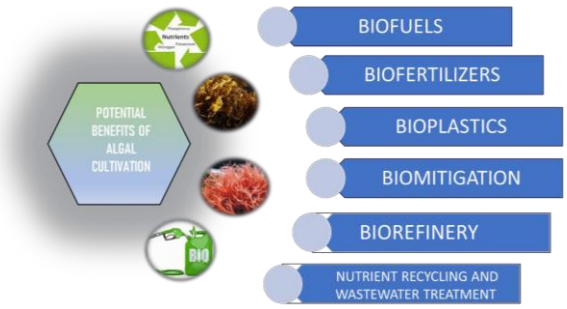

Figure 4: Various benefits of algal cultivation as a future bioresource.

A sustainable algae industry is probable to be multi-dimensional with respect to its market based functioning. Proposing Algal sources as food or supplementations for pregnant women requires rigorous study and multiple trials before prescribing them out in the market. Algal additives in foods must also be carefully processed with important concern towards pregnancy. Evident through studies, Synergic combinations of foods were of better help in relieving post- partum symptoms (Natarajan et al. 2019) Although algae have been consumed since centuries but definite algal interactions and mechanism still need thorough studies (Escalante and Perez 2021). Quantitative descriptions of nutrient and bio-pigment availabilities in algae have been studied but not in detail referencing to pregnancies. There also need to be detailed experimentations on digestibility of microalgae and its interactions with human metabolism (Escalante and Perez 2021). Further these studies need to expand their horizons towards pregnant women in specific, studying their impacts, side effects, efficiency, commercialisation and improvements clinically.

ACKNOWLEDGEMENT

All the authors acknowledge and thank their respective Institutes and Universities.

Author's contribution

All the authors contributed significantly.

Funding

This is a compilation written by its authors and required no substantial funding to be stated.

Disclosure statement

All authors declare that there exist no commercial or financial relationships that could, in any way, lead to a potential conflict of interest.

REFERENCES:

Ramu Ganesan, A., K. Subramani, M. Shanmugam, et al. (2020). A comparison of nutritional value of underexploited edible seaweeds with recommended dietary allowances. *Journal of King Saud University - Science*, *32*(1), 1206–1211.

Dudeja, P., & R. K. Gupta, (2017). Nutraceuticals. In *Food Safety in the 21st Century* (pp. 491–496). Elsevier.

Smyth, P. P. A. (2021). Iodine, seaweed, and the thyroid. *European Thyroid Journal*, *10*(2), 101– 108.

Fabris, M., R. M. Abbriano, M. Pernice, et al. (2020). Emerging technologies in algal biotechnology: Toward the establishment of a sustainable, algae-based bioeconomy. *Frontiers in Plant Science*, *11*.

Tang, G., & P. M. Suter, (2011). Vitamin A, nutrition, and health values of algae: Spirulina, chlorella, and dunaliella. *Journal of Pharmacy and Nutrition Sciences*, *1*(2), 111–118.

Hentati, F., L. Tounsi, D. Djomdi, et al. (2020). Bioactive polysaccharides from seaweeds. *Molecules*, *25*(14), 3152.

Sebastiani, G., A. Herranz Barbero, C. Borrás-Novell, et al. (2019). The effects of Vegetarian and Vegan diet during pregnancy on the health of mothers and offspring. *Nutrients*, *11*(3), 557.

Fleurence, J. (2021). Perspectives on the use of algae in agriculture and animal production. *Phycology*, *1*(2), 79–82.

Natarajan, T. D., J. R. Ramasamy, & K. Palanisamy, (2019). Nutraceutical potentials of synergic foods: A systematic review. *Journal of Ethnic Foods*, *6*(1).

Ścieszka, S., & E. Klewicka, (2018). Algae in food: A general review. *Critical Reviews in Food Science and Nutrition*, *59*(21), 3538–3547.

Tanna, B., & A. Mishra, (2019). Nutraceutical potential of seaweed polysaccharides: Structure, bioactivity, safety, and toxicity. *Comprehensive Reviews in Food Science and Food Safety*, *18*(3), 817–831.

Tuncalp, Ö., L. M. Rogers, T. A. Lawrie, et al. (2020). WHO recommendations on antenatal nutrition: An update on multiple micronutrient supplements. *BMJ Global Health*, *5*(7), e003375.

Gernand, A. D., K. J. Schulze, C. P. Stewart, et al. (2016). Micronutrient deficiencies in pregnancy worldwide: Health effects and prevention. *Nature Reviews Endocrinology*, *12*(5), 274–289.

Marangoni, F., I. Cetin, E. Verduci, et al. (2016). Maternal diet and nutrient requirements in pregnancy and breastfeeding. An Italian consensus document. *Nutrients*, *8*(10), 629.

Kuenz, A., D. Grimm, & G. Rahmann, (2020). Versatility of algae—exploring the potential of algae for nutrient circulation. *Organic Agriculture*, *11*(2), 251–260.

Ullmann, J., & D. Grimm, (2021). Algae and their potential for a future bioeconomy, landless food production, and the socio-economic impact of an algae industry. *Organic Agriculture*, *11*(2), 261–267.

Santhakumaran, P., S. M. Ayyappan, & J. G. Ray, (2020). Nutraceutical applications of twenty-five species of rapid-growing green-microalgae as indicated by their antibacterial, antioxidant and mineral content. *Algal Research*, *47*, 101878.

Wijesekara, I., & S.-K. Kim, (2015). Application of marine algae derived nutraceuticals in the food industry. In *Marine Algae Extracts* (pp. 627–638). Wiley-VCH Verlag GmbH & Co. KGaA.

Escalante, F. M. E., & D. A. Pérez-Rico, (2021). Advancements in algae in nutraceutical and functional food. *Recent Advances in Micro and Macroalgal Processing*, 506–536.

Mecacci, F., S. Biagioni, S. Ottanelli, & G. Mello, (2015). Nutrition in pregnancy and lactation: How a healthy infant is born. *Journal of Pediatric and Neonatal Individualized Medicine (JPNIM)*, *4*(2), e040236–e040236.

g-FACTOR MEASUREMENTS OF ISOMERIC STATES IN 135La

Neeraj Bansal[1], A. K. Bhati[2]*, R. Kumar[3], Anu Rathi[2], Ritu Rani[2]
[1] Department of Physics, Guru Nanak Dev University, Amritsar- 143005, INDIA.
[2] Centre for Advanced Studies in Physics, Panjab University, Chandigarh-160014, INDIA.
[3] Inter- University Accelerator Centre, JNU Campus, New Delhi- 100067, INDIA.

ABSTRACT

The g-factor of the one-quasiparticle isomeric state $\frac{11^-}{2}$ at 786 *keV* and the three- quasiparticle isomeric state ($\frac{23^+}{2}$) at 2738 *keV* in ^{135}La with reference to that of $\frac{19^-}{2}$ isomeric state in ^{137}La have been measured using the time-differential perturbed angular distribution technique. The nuclear reaction $^{128}Te(^{11}B, 4n\gamma)^{135}La$ was used to populate these isomeric states. The extracted $g\left(\frac{11^-}{2}\right)$ value, +0.146(3), corresponds to the configuration $\pi h_{\frac{11}{2}}$ with the admixture of $\pi\left(d_{5/2}/g_{7/2}\right)^1 \otimes 3^-$ while $g\left(\frac{23^+}{2}\right)$ value, +0.112(3), corresponds to the configuration $\pi h_{\frac{11}{2}} \otimes \nu h_{\frac{11}{2}}\left(s_{1/2}/d_{3/2}\right)^1$ with the admixture of $\pi g_{\frac{7}{2}} \otimes 3^- \otimes \nu h_{\frac{11}{2}}\left(s_{1/2}/d_{3/2}\right)^1$.

Keywords: g-factor, Time Differential Perturbed Angular Distribution, One- quasiparticle isomer, Oblate 3-quasiparticle isomer, Magnetic dipole band, Particle-vibration coupling.

INTRODUCTION

The nuclei in the mass $A \sim 130$ region characterized by γ-soft core, have been observed to exist in different shapes, i.e., symmetric (prolate ($\gamma = 0^0$) and oblate ($\gamma = -60^0$) and non-symmetric (triaxial, $\gamma = 30^0$), depending on the energy and the orbitals occupied by the valence nucleons, i.e quasiparticle configuration [1]. The interaction of the soft γ-core and the valence nucleons have been the topic of interest quite a long time to understand the large variety of structures and the exotic phenomenon, e.g. shape-coexistence, triaxiality, magnetic rotation (*MR*) bands and chiral bands etc. The nuclear structure calculations have predicted enhancement of triaxiality and reduction of quadrupole deformation (β) with increasing neutron number towards neutron shell closer N = 82 [2]. Such changes in the deformation parameters (β, γ) of the ground state influence the various nuclear properties across the isotopic chain, e.g,. type of the valence nucleon coupling scheme to the even-even core and hence the structure of the nuclear states. The interpretation of the energy level structure of odd-mass nuclei resulting from the complex combinations of the coupling of the quasiparticle and the collective degrees of freedom, at low excitation energies, have been challenging on both the theoretical and experimental fronts. The low-lying levels of odd-A La nuclei (57th. proton coupled to even-even Ba nuclei) have been analysed and understood based on the triaxial rotor-plus-particle (^{133}La) [3] and the weak coupling ($^{135,137}La$) models [4]. This is consistent with the observed gradual change from the rotational level structure (deformed region) to the vibrational level structure (near semi-magic ^{138}Ba) across the even-even Ba isotopic chain. The low-lying level studies of the even-even and even-odd nuclei, resulting from the beta-decay in this region, have indicated the sudden transition from the rotational to the vibrational level scheme when neutron number increases from N = 76 to 78. ^{134}Ba nucleus has attracted much attention for the possible phase transition, based on the spectroscopic signature, in the frame of reference of IBM model [5]. ^{134}Ba is nearly spherical and considered to be more vibrational class of nuclei. It is pertinent to look into the level structure of ^{135}La vis-a-vis neighbouring odd-A nuclei, i.e. ^{133}La and ^{137}La. In the present investigations, we have explored the nature of some of the isomeric states in ^{135}La through the magnetic moment measurements and removed the ambiguities in assigning the structure of the states [6]. These measurements are crucial in the transitional region to elucidate the single-particle and the collective nature of the nuclear states with respect to the neighbouring nuclei. Unfortunately, there is scant information on nuclear electromagnetic moments of La isotopes. The low energy structure of ^{135}La (Z = 57 and N = 78) has been analysed as the coupling of a valence proton to the excitations of the even-even core ^{134}Ba. The coupling of the available $2d_{5/2}$ and $1g_{7/2}$ single-particles to the core excitations yields positive parity levels, while the negative-parity states arise from the $1h_{11/2}$, proton coupling to the core excitations. In the present investigations, we have considered the $I^\pi = \frac{11^-}{2}\left(E = 786\ keV, T_{\frac{1}{2}} < 10\ ns\right)$ and the $I^\pi =$

Corresponding author: akbhati@pu.ac.in
Received: November 11, 2023, Accepted: December 4, 2023

$\left(\frac{23^+}{2}\right)\left(E = 2738\ keV, T_{\frac{1}{2}} = 28.4(8)\ ns\right)$ isomeric states in ^{135}La [6] for the g-factor measurements. The $\frac{11^-}{2}$ isomeric state, occurring all across the chain of odd-A La isotopes, is assumed to have single particle properties $\left(\pi h_{\frac{11}{2}}\right)$ and is a band head of a decoupled band. The analysis of the γ-ray transition probabilities (E1/E3) out of the $\frac{11^-}{2}$ isomeric states in $^{133,135,137}La$ have revealed the increasing trend of the collective admixture with A which makes it interesting to know the nature of $\frac{11^-}{2}$ isomeric state in ^{135}La through the static electromagnetic moment measurements. Previous experiments have displayed the g-factor and the spin value $\left(I = \frac{27^+}{2}, 0.003(15)\right)$ of the $I = \left(\frac{23^+}{2}\right)$ state [7] in ^{135}La. The assigned configuration $\pi g_{7/2} \otimes \upsilon\left[h_{11/2}\right]^2$ and the spin value, $I = \frac{27^+}{2}$ [7], of the $\left(\frac{23^+}{2}\right)$ isomeric state disagree with that of the in-beam γ-ray spectroscopy work, i.e. $\pi h_{11/2} \otimes \upsilon h_{11/2}\left(s_{1/2}/d_{3/2}\right)^1$ [6]. For a small g-factor value, 0.003(15), of the $\left(\frac{23^+}{2}\right)$ state [7] only a fraction of a Larmor precession pattern was observed with poor statistics which introduces much uncertainty in the results. The half-lives of the isomeric states are favourable to utilize the time differential perturbed angular distribution (*TDPAD*) technique in the presence of the high internal magnetic field in iron to observe the precession frequencies with better statistics and the reliable spin rotation pattern. Present measurements are motivated by the fact that the magnetic moment measurements exhibit the influence of the collective degree of freedom on the structure of the single particle predominated states.

EXPERIMENTAL DETAILS

The isomeric states in ^{135}La were populated by the heavy-ion reaction $^{128}Te(^{11}\mathrm{B}, 4n\gamma)^{135}La$ using a 60 MeV ^{11}B pulsed beam with 250 ns repetition period from the 15UD Pelletron accelerator facility *at Inter University Accelerator Centre, New Delhi*. The target was prepared from the isotopically enriched 500 μg/cm^2 ^{128}Te evaporated on 5.7 mg/cm^2 gold foil backed by 99.99% pure iron foil for the g-factor measurements. The recoiling ^{135}La ions were implanted into the ferromagnetic iron foil. The *Fe* foil was rolled to the desired thickness and annealed [8] to get the saturated internal magnetic field at the recoil implanted *La* ions for the g-factor measurements. The beam was stopped in *Ta* foil after the iron foil. The *Fe* foil was polarised by 0.2 *T* external magnetic field perpendicular to the beam-detector plane. The γ-rays from the respective isomeric states were detected by two $LaBr_3(Ce)\left(1\frac{1''}{2} \times 1\frac{1''}{2}\right)$ detectors placed at $\pm 135^0$ in a horizontal plane w.r.t. the beam at a distance of 20 cm from the target. The de-exciting γ-ray spectrum was monitored by a *HPGe* detector. For the calibration of the internal magnetic field at *La* in *Fe*, the $\frac{19^-}{2}\left(E = 1869.5\ keV, T_{\frac{1}{2}} = 342(25)ns, g = +0.246(6)\right)$ [9, 10, 11] isomeric state in ^{137}La was excited through the $^{130}Te(^{11}\mathrm{B}, 4n\gamma)^{137}La$ reaction using 55 MeV ^{11}B pulsed beam with 500 ns time interval. The ^{130}Te target was prepared through evaporation of enrich 250 μg/cm^2 ^{130}Te on 6 mg/cm^2 gold foil backed by the annealed iron foil. The partial level scheme of ^{135}La, showing the decay of the presently investigated isomers, is projected in Fig. 1.

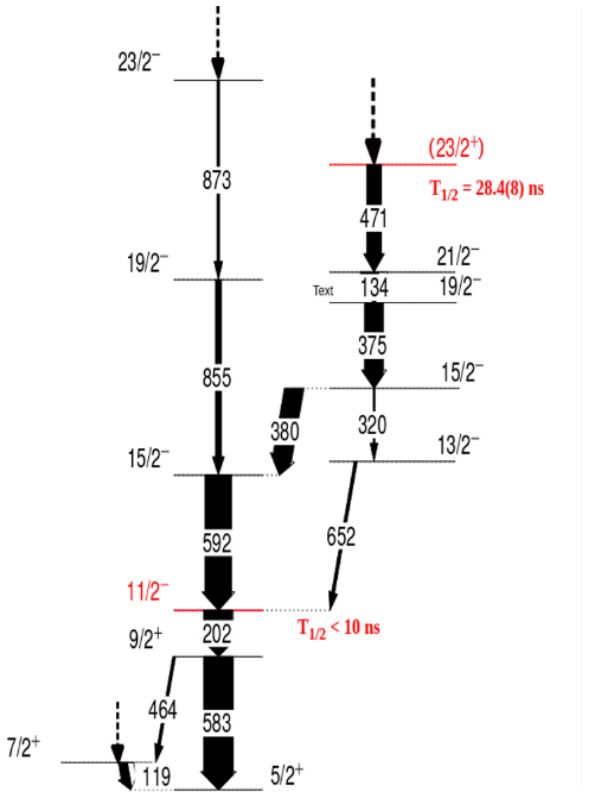

Figure-1: Partial level decay scheme of $\frac{11^-}{2}$ and $\left(\frac{23^+}{2}\right)$ isomeric states in ^{135}La (weak transitions are omitted).

DATA ANALYSIS AND RESULTS

The data were collected in the *LIST* mode with four parameters: the two energy and two time signals from the time to pulse height converter corresponding to each $LaBr_3(Ce)$ detector. In the off-line analysis of the list-mode data, following proper gain matching for the energy and time, two dimensional matrices of energy versus time were formed for each detector. These

matrices were then used to create the time gated energy spectra and the energy-gated time spectra for the system. As an illustration the typical delayed γ-ray energy spectrum of ^{135}La registered by *HPGe* detector is projected in Fig. 2.

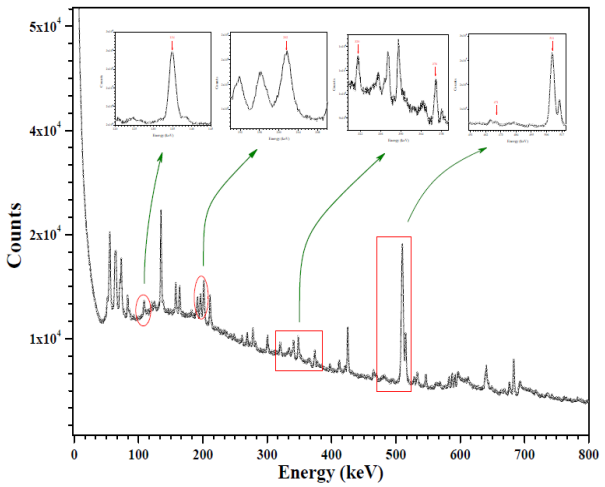

Figure 2: Delayed γ-ray energy spectrum of ^{135}La without background subtraction.

The exponential decay curve of the isomeric state is superimposed of the modulated intensity pattern due to the nuclear spin precession in the presence of the internal magnetic field in *Fe*. The time spectra of both the $LaBr_3(Ce)$ detectors were added after matching the time zero (T_0), normalization and background subtraction. The summed time spectra were *LSQ* fitted to the exponential decay to extract the half-life times of the corresponding states. The resulting decay spectra for the $\frac{11^-}{2}$ and $\left(\frac{23^+}{2}\right)$ isomeric states in ^{135}La are shown in Fig 3. The observed half-lifetime $T_{1/2}\left(\frac{23^+}{2}\right) = 27.7(4)$ ns, is in good agreement with the results of the previous measurement [6]. For the $\frac{11^-}{2}$ isomeric state, in addition to the direct decay component a small contribution from the decay of $\left(\frac{23^+}{2}\right)$ state was also considered in the *LSQ* fitting. The extracted half-life of the $\frac{11^-}{2}$ isomeric state $T_{1/2}\left(\frac{11^-}{2}\right) = 8.56(1)$ ns, measured first time, falls in the systematic of the $\frac{11^-}{2}$ isomeric state across the Z=57 isotopic chain. We have attempted to measure the lifetime of $\frac{21^-}{2}$ state also which was predicted to have the comparable value to that of $\left(\frac{23^+}{2}\right)$ [6].

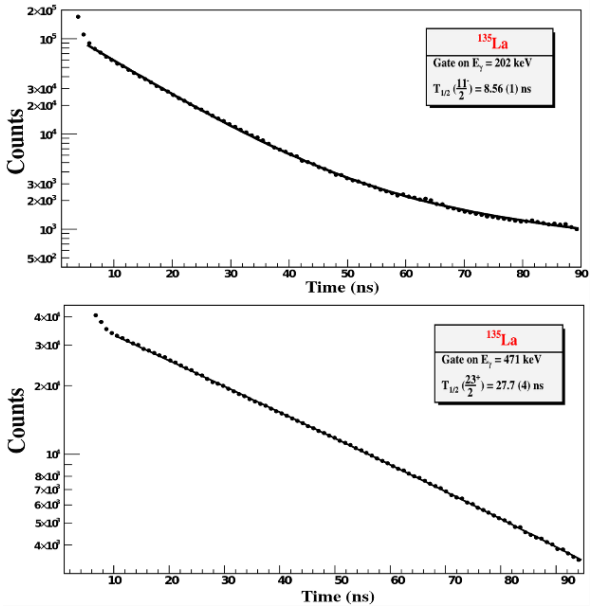

Figure 3: Summed time spectra with gates on γ-ray transitions from $\frac{11^-}{2}$ to $\left(\frac{23^+}{2}\right)$ isomeric states in ^{135}La. The solid curve shows the least squares fit to the data.

The decay and the spin rotation spectra (magnetic interaction) corresponding to the successive 134, 320, 380 and 653 keV gamma ray transitions from the $\frac{21^-}{2}$ state, see Fig. 1, are exactly the same in shape and bear the same value of half-life and Larmor frequencies as that of the 471 keV gamma ray from the $\left(\frac{23^+}{2}\right)$ state to the $\frac{21^-}{2}$. This reveals the half of the $I = \frac{21^-}{2}$ state is less than the time resolution of the detecting system (< 1.5 ns) and not comparable to that of the $\left(\frac{23^+}{2}\right)$ isomeric state. The life-time analysis of the corresponding isomeric states confirms the identification of gamma rays in the delayed γ-ray energy spectrum. In the presence of extra nuclear magnetic field e.g. internal or external or both, the nuclear spin precesses with Larmor frequency ω_L due to hyperfine interactions which causes the time dependent modulation of the γ-ray intensity. The modulated time spectra were used to form the intensity ratio for the g-factor measurements,

$$R_{exp}(t) = \frac{I(135^0,t) - I(-135^0,t)}{I(135^0,t) + I(-135^0,t)} \quad (1)$$

to extract the respective Larmor precession frequencies $\omega_L (= g\mu_N B/\hbar)$. Here $I(\theta,t)$ are the background subtracted and normalized time spectra at two angles $\pm 135^0$. The ratio function was *LSQ* fitted to the simple expression, $R(t) = A_2 * \cos\{2(\theta - \omega_L t)\} + \psi$ [12], for

the directly populated $\left(\frac{23^+}{2}\right)$ and $\frac{19^-}{2}$ isomeric states in ^{135}La and ^{137}La, respectively. The angular distribution coefficient A_2, ω_L, phase angle θ for the bending of beam and normalization factor ψ were kept free parameters. The experimental ratio functions $R(t)$ and corresponding *LSQ* fitted spectra are projected in Fig. 4.

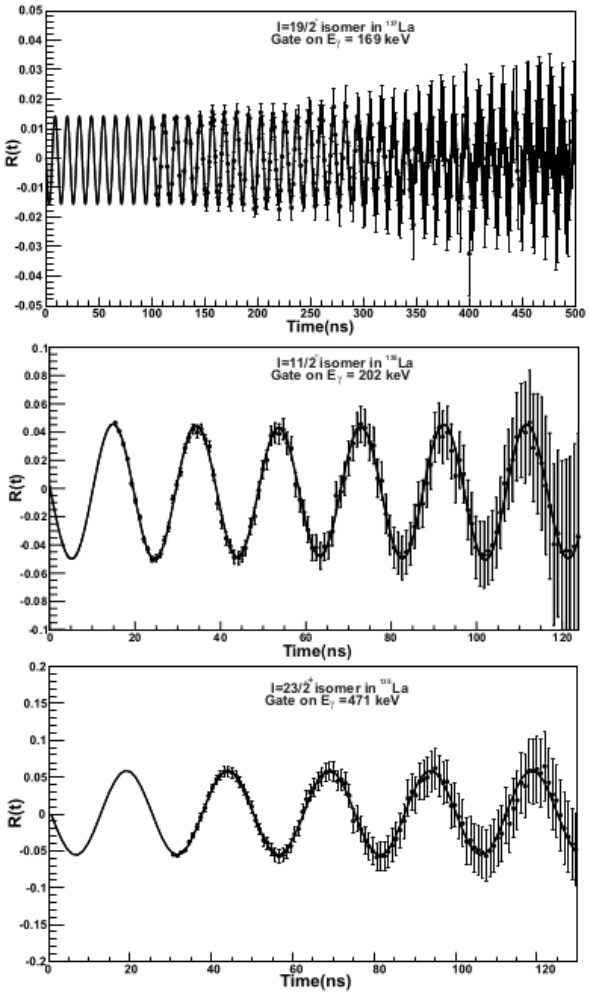

Figure 4: Spin rotation spectra of the $\frac{19^-}{2}$ isomeric state in ^{137}La and the $\frac{11^-}{2}$ and $\left(\frac{23^+}{2}\right)$ isomeric states in ^{135}La Nuclei implanted into the polarized iron at room temperature.

Within the *TDPAD* time window, no attenuation of the modulation amplitude has been observed in these measurements at room temperature, i.e. ions are implanted at unique sites and any possible relaxation time is expected to be much more than 500 ns. The Larmor precession frequencies for the $\left(\frac{23^+}{2}\right)$ and $\frac{19^-}{2}$ states are 124.9(4) M*rad*/s and 274.4(3) M*rad*/s, respectively. The extracted g-factor $\left(\left(\frac{23^+}{2}\right), ^{135}La\right)$, +0.112(3), with respect to the g-factor $\left(\frac{19^-}{2}, ^{137}La\right) = +0.246(6)$ [11] is free from any uncertainty of the effective magnetic field at the nucleus, provided the implantation conditions are same in both the nuclear reactions. The errors quoted are almost entirely due to the uncertainty in the g-factor of the $\frac{19^-}{2}$ state. As a byproduct, the extracted effective internal magnetic field $B_{in} = -23.2(6)$T at *La* in iron, using the known g-factor of the $\frac{19^-}{2}$ state, is within the range of the previous reported values, $B_{in} = 15(3) - 46(3)$T [13] and the sign is in confirmation with the theoretical predictions [14]. This is the first time that we are able to determine the sign of the internal magnetic field at *La* in *Fe*. The sign of the magnetic field and the g-factors were determined from the sense of rotation of the gamma-ray distribution pattern using the known sign of the anisotropy of the angular distribution function of the corresponding γ-ray transitions [15].

The theoretical ratio function $R(t)$ for the magnetic interaction was modified for the $\frac{11^-}{2}$ state by taking into account the side feeding from the $\left(\frac{23^+}{2}\right)$ isomeric state. The ratio functions were analysed using a *LSQ* fitting program based on the multilevel formulation [16] which takes into account side-feeding from the sequence of isomers. We have followed the two level analysis [17] for the small side-feeding from the $\left(\frac{23^+}{2}\right)$ state as per following expression,

$$R(t) = A(t)\cos\{2(\theta - \omega_L t)\} + A'(t)R_{cas}(t, \omega_{L1}, \omega_{L2}), \quad (2)$$

where $A(t)\cos\{2(\theta - \omega_L t)\}$ denotes the modulation pattern corresponding to the 202 keV γ-ray transition due to the direct population of $\frac{11^-}{2}$ level and $A'(t)R_{cas}(t, \omega_{L1}, \omega_{L2})$, corresponding to the side feeding from the $\left(\frac{23^+}{2}\right)$, state. The presence of two frequencies $\omega_{L1}\left(\frac{11^-}{2}\right)$ and $\omega_{L2}\left(\frac{23^+}{2}\right)$ in the expression produces beat pattern as shown in Fig. 4. In the analysis, the extracted side-feeding fraction comes out to be the same as that in the lifetime analysis of the $\frac{11^-}{2}$ state. The *LSQ* fitted values of the Larmor precession frequency $(\omega_{L1})$for the $\frac{11^-}{2}$ state is 162.5(2) M*rad*/s. This shows the 25% enhancement of the Larmor frequency of the $\frac{11^-}{2}$ state with respect to that of the $\left(\frac{23^+}{2}\right)$ state and the g-factor so obtained is 0.146(3).

DISCUSSION

The ^{135}La nucleus is considered to be a nearly spherical nucleus. The single particle effects are expected to play important role in the g-factors of the excited states. The $\frac{11^-}{2}$ and the $\left(\frac{23^+}{2}\right)$ isomeric states in ^{135}La nucleus have been assigned pure one quasiparticle, $\pi h_{11/2}$, and three quasiparticle (3-qp), $\pi h_{11/2} \otimes \nu h_{11/2}(s_{1/2}/d_{3/2})^1$, configurations, respectively [6, 15]. The g-factor of a multi-particle configuration, within the framework of the shell model, is expressed by the additivity relation,

$$g(I_1 \otimes I_2; I) = \frac{1}{2}(g_1 + g_2) + \frac{1}{2}(g_1 - g_2) \times \frac{I_1(I_1+1) - I_2(I_2+1)}{I(I+1)} \quad (3)$$

The effective g-factors of the constituent single quasiparticle and 2-qp states are inserted from the ref. [18] to get a rough estimate of the experimental g-factor values. The corrections due to residual interactions, e.g., core polarization, for different configurations have been completely neglected in these extreme single-particle calculations. The experimental and the estimated g-factor values are listed in Table 1. The measured g-factors, +0.112(3) and +0.146(3), of the $\left(\frac{23^+}{2}\right)$ and $\frac{11^-}{2}$ states, respectively, are reduced as compared to the estimated values. It apperas that the measured g-values are not corroborated by the above configurations completely, i.e., as pure shell model states. The configurations of the low and middle spin states in ^{135}La have been analysed based on various coupling schemes of the single quasiproton with the coexisting two-quasiparticle excitations and the vibrational bands in ^{134}Ba core. An interplay between the core excitations is expected to give additional structures. Further, the pure two-quasiparticle excitations of the core are not supported by the particle transfer reactions [19] also, which points to the presence of collective components in the wavefunction of the states. We shall consider the configuration of each state separately.

The measured g-factor value, +0.112(3), of the $\left(\frac{23^+}{2}\right)$ isomeric state is in disagreement with the magnitude, 0.003(15), and the sign corresponding to the adopted maximum aligned configuration, $\pi g_{7/2} \otimes \nu(h_{11/2})^2$, by Levon et al. [7]. The configuration is expected to have negative g-factor. Earlier, Leguillon et al [6] have proposed the 3-qp state I = $\left(\frac{23^+}{2}\right)$ as the coupled state of $h_{11/2}$ proton to the 5^- core (^{134}Ba) state with $\nu h_{11/2}$ $(s_{1/2}/d_{3/2})^1$ configuration, i.e. 3-qp configuration $\pi h_{11/2} \otimes \nu h_{11/2}(s_{1/2}/d_{3/2})^1$. The empirical g-factor of the 3-qp configuration is overestimated as compared to the present value, Table1, which exhibit the presence of the admixture of collective nature in the wavefunction.

The $\left(\frac{23^+}{2}\right)$ isomeric state de-excites through 471 keV E1 transition to the opposite parity $21^-/2$ state with $\pi g_{7/2} \otimes \nu h_{11/2}(s_{1/2}/d_{3/2})^1$ configuration. The 5^- core state has also been observed to decay through E1 and E3 transitions to the ground band in ^{134}Ba [20] and the g-factor of the 5^- state in ^{136}Ba [21] has shown the presence of octupole-coupled component in the wavefunction. We may, therefore, postulate the participation of octupole vibrations in the excitation of the $\frac{21^-}{2}$ state to the $\left(\frac{23^+}{2}\right)$ isomeric state. The configuration of the $\left(\frac{23^+}{2}\right)$ state is modified to have a component corresponding to the octupole correlations built over the $\frac{21^-}{2}$ state, i.e. $\frac{21^-}{2} \otimes 3^- \rightarrow \pi g_{7/2} \otimes 3^- \otimes \nu h_{11/2}(s_{1/2}/d_{3/2})^1$. We, therefore, propose the admixture of spin-flip combination, $\pi g_{7/2} \otimes 3^- \otimes \nu h_{11/2}(s_{1/2}/d_{3/2})^1$, to account for the coupling to octupole vibrations. In the absence of any theoretical calculation, the collective octupole vibrations are expected to have a g-factor near Z/A. We have assumed g = 0.37 as the average of the experimental g-factor value of the first 2^+ excited states in ^{134,136}Ba [22] isotopes for the octupole vibrations. The g-factors of the octupole-vibration-coupled spherical configurations are listed in Table 1. The estimated g-factor of the $\left(\frac{23^+}{2}\right)$ state lies in between 0.06 to 0.49 depending on the fraction of the pure multi-quasiparticle component and the octupole correlation component to the wavefuntion of the state, see Table 1. The wavefunction of the $\left(\frac{23^+}{2}\right)$ state can be written as,

$$|(23^+/2)\rangle = \alpha\,|\pi\, h_{\frac{11}{2}} \otimes \nu\, h_{\frac{11}{2}}\left(s_{\frac{1}{2}}/d_{\frac{3}{2}}\right)^1\rangle + \sqrt{(1-\alpha^2)}\,\big|\pi\, g_{\frac{7}{2}} \otimes 3^- \otimes \nu\, h_{\frac{11}{2}}(s_{\frac{1}{2}}/d_{\frac{3}{2}})^1\rangle \quad (4)$$

Recently, Laskar et. al. [23], have reported the g-factor value, -0.049(3), of the $\left(\frac{23^+}{2}\right)$ isomeric state employing the time differential perturbed angular distri bution (*TDPAD*) technique in the presence of high external magnetic field [23]. In a stark contrast, both the sign and magnitude of the g-factor measured by us, differ with respect to the precisely measured vanishingly small negative g-factor, $-0.049(3)$ [23]. The measured g-factor, $-0.049(3)$, has been assigned to the $\pi d_{5/2} \otimes \nu\left(h_{11/2}\right)^{-2}$ configuration with small admixture of $\pi g_{7/2} \otimes \nu\left(h_{11/2}\right)^{-2}$ in the wavefunction based on the *LSSM* calculations [23]. This signifies the absence of definite information about the implantation site of the

recoil ions and the associated hyperfine magnetic field in the ferromagnetic host Fe [13]. The positive parity of the $\pi d_{5/2} \otimes \nu(h_{11/2})^{-2}$ wavefunction, affirmed by the g-factor, establishes the positive parity of level. The intra band gamma-ray transition analysis of the I = $\frac{11^-}{2}$ decoupled band has been consistent with the single-particle $\pi h_{11/2}$ character while the small g-factor value, ~10% as compared to the single-particle g-factor value, suggests the presence of configuration mixing in the wavefunction. The measurements of the reduced E1 and the E3 gamma-ray transition probabilities out of the $\frac{11^-}{2}$ states in ^{133,135,137}La nuclei have revealed the presence of octupole correlations and the increasing trend of the admixture of the type $(\pi d_{5/2} \otimes 3^-)\frac{11^-}{2}$ in the wavefunction of the $\frac{11^-}{2}$ state towards the N = 82 shell closer [24, 25, 26, 27]. It is imperative to consider the octupole vibration coupling terms in the structure of $\frac{11^-}{2}$ state which is consistent with the g-factor measurements in ^{133}La [28]. The $\frac{11^-}{2}$ isomeric states decays to the second excited state, I = $\frac{9^+}{2}$, of the I = $\frac{5^+}{2}$, ground band through E1 transitions. The $\frac{9^+}{2}$ level is a mixture of the and configurations because of the near degeneracy of the $(2d_{5/2} \otimes 2_1^+)$ and $(2g_{7/2} \otimes 2_1^+)$ orbitals. We may, therefore, purpose mainly the admixture of $1g_{7/2} \otimes 3^-$ and $2d_{5/2} \otimes 3^-$ configurations to the wavefunction of the $\frac{11^-}{2}$ level to account for the enhanced E1 transitions, as suggested by Van Hise et al. [29]. The g-factor of the octupole phonon coupled configurations, $1g_{7/2} \otimes 3^-$ and $2d_{5/2} \otimes 3^-$ are tabulated in Table 1. Assuming that there is no other contribution, e.g. the quadrupole phonon coupling, e.g. in the $\frac{9^+}{2}$ the wavefunction of the $\frac{11^-}{2}$ state can be expressed as,

$$|(11^-/2)\rangle = \alpha\,|\pi\, h_{\frac{11}{2}} + \sqrt{(1-\alpha^2)}|\pi\, d_{\frac{5}{2}}/g_{\frac{7}{2}} \otimes 3^-\rangle \quad (5)$$

The estimated g-factor value can be in between 0.5 and 1.17 depending on the fraction of the octupole coupled configurations and differ considerably from the experimental value +0.146(3). This shows the complex nature of the state and the breakdown of particle-core coupling scheme. It seems that $\frac{11^-}{2}$ state is largely collective in nature with minor contribution from the single-particle $\pi h_{11/2}$ wave function. The discrepancy between the predicted and the experimentally observed g-factor values may arise as we are limited to the elementary shell structure analysis and treating the quasiparticle and the collective degrees of freedom as independent for the qualitative discussion. Extremely large basis is required for the treatment of a collective vibrational state in the conventional shell model approach which is cumbersome process for the theoretical calculations. Additional contributions due to core polarisation effects and Coriolis coupling, depending on the admixture terms, have to be considered in the theoretical calculations.

Spin value (I^π)	Configuration	g^{a}_{cal}	g_{exp}
$\frac{11^-}{2}$	$\pi(g_{\frac{7}{2}} \otimes 3^-)_{\frac{11}{2}^-}$	+0.5	0.146(3)[b]
	$\pi(d_{\frac{5}{2}} \otimes 3^-)_{\frac{11}{2}^-}$	+0.8	
$\frac{23^+}{2}$	$\pi(h_{\frac{11}{2}} \otimes \nu(h_{\frac{11}{2}} \otimes s_{\frac{1}{2}})_{6^-}$	+0.387	0.112(3[b])
	$\pi(h_{\frac{11}{2}} \otimes \nu(h_{\frac{11}{2}} \otimes d_{\frac{3}{2}})_{6^-}$	+0.490	
	$\pi(g_{\frac{7}{2}} \otimes 3^-) \otimes \nu(h_{\frac{11}{2}} \otimes s_{\frac{1}{2}})_{6^-}$	+0.06	
	$\pi(g_{\frac{7}{2}} \otimes 3^-) \otimes \nu(h_{\frac{11}{2}} \otimes d_{\frac{3}{2}})_{6^-}$	+0.141	
$\frac{27^+}{2}$	$\pi g_{\frac{7}{2}} \otimes \nu(h_{\frac{11}{2}})^3_{10^+}$	+0.031	

Table 1: Calculated and experimental $g-$factors of the states.

[a]The effective single particle $g-$factors adopted in the calculations [18]:
i) for protons : $h_{\frac{11}{2}} = 1.17$; $g_{\frac{7}{2}} = 0.72$; $d_{\frac{3}{2}} = 1.33$; $d_{\frac{5}{2}} = 1.38$,
ii) for neutrons : $h_{\frac{11}{2}} = -0.2$; $g_{\frac{7}{2}} = 0.24$; $d_{\frac{3}{2}} = 0.44$; $d_{\frac{5}{2}} = -0.33$; $s_{\frac{1}{2}} = -1.76$.
[b]Present Work

The present analysis suggests the inclusion of effects associated with the coupling of the particle to the surface vibrational modes of the core, i.e., collective admixtures are important. The coupling of the octupole vibrations has been observed to influence the g-factor of the states in the transitional nuclei [30].

CONCLUSION

The g-factor of the $\frac{11^-}{2}$ and $\left(\frac{23^+}{2}\right)$ states in ^{135}La have been measured using the *TDPAD* technique. The assigned configurations are at variance with that of the previous measurements and the theoretical considerations. We have observed the presence of octupole coupled component in the wavefunction of both the states. The appreciable reduction in the g-factor of the $\frac{11^-}{2}$ isomeric state in ^{135}La with respect to ^{133}La is attributed to the change in the nature of the low lying levels from the rotational to vibrational

ACKNOWLEDGEMENT

The authors wish to thank the accelerator crew, particularly Dr. S. Chopra, Mr. R. Joshi and Mr. P. Barua, for the stable pulsed beam and continuous support at Inter University Accelerator Centre during the experiment. We acknowledge the financial assistance by the PURSE and the UGC IUAC.

REFERENCES

E.S. Paul, D.B. Fossan, Y. Liang, R. Ma, N. Xu, Phys. Rev. C 40 (1989) 1255.

J. Yan, P. von Brentano, A. Gelberg, Phys. Rev. C 48 (1993) 1046.

J. Meyer-Ter-Vehn, Nucl. Phys. A 249 (1975) 111.

A. de-Shalit, Phys. Rev. 122 (1961) 1530.

R.F. Casten, N. Zamfir, Phys. Rev. Lett. 85 (2000) 3584.

R. Leguillon, H. Nishibata, Y. Ito, C.M. Petrache, A. Odahara, T. Shimoda, N. Hamatani, K. Tajiri, J. Takatsu, R. Yokoyama, E. Ideguchi, H. Watanabe, Y. Wakabayashi, K. Yoshinaga, T. Suzuki, S. Nishimura, D. Beaumel, G. Lehaut, D. Guinet, P. D. D. Curien, A. Astier, T. Konstantinopou-los, T. Zerrouki, Phys. Rev. C 88 (2013) 044309.

A.I. Levon, O.F. Nemets, V.A. Stepanenko, V.P. Chepak, Bulletin of the Academy of Sciences of the USSR, Physical series 40 (1976) 125.

P. Maier-Komor, K.H. Speidel, A. Stolarz, Nucl. Instr. and Meth. A 334 (1993) 191.

E. Browne, J.K. Tuli, Nuclear Data Sheets 108 (2007) 2224.

J.J. Valiente-Dobon, P.H. Regan, C. Wheldon, C.Y. Wu, N. Yoshinaga, K. Hi gashiyama, J.F. Smith, D. Cline, R.S. Chakrawarthy, R. Chapman, M. Cromaz, P. Fallon, S.J. Freeman, A. Gorgen, W. Gel-letly, A. Hayes, H. Hua, S.D. Langdown, I.Y. Lee, X. Liang, A.O. Macchiavelli, C.J. Pearson, Z. Podolyak, G. Sletten, R. Teng, D. Ward, D.D. Warner, A.D. Yamamoto, Phys. Rev. C 69 (2004) 024316.

O.C. Kistner, M.H. Rafailovich, J.W. Noe, S. Vajda, Bulletin of the American Physical Society 27 (1982) 728.

H. Frauenfelder, R. Steffan, Alpha-Beta and Gamma-ray spectroscopy, edited by K. Sieghbahn (North Holland Amsterdam) 2 (1965) 997.

G.N. Rao, Hyp. Ints. 24-26 (1985) 1119.

D. Torumba, P. Novak, S. Cottenier, Phys. Rev. B. 77 (2008) 155101.

J.R. Leigh and K. Nakai and K.H. Maier and F. Puhlhofer and F.S. Stephens and R.M. Diamond, Nucl. Phys. A 213 (1973) 1.

O. Hausser, T.K. Alexander, J.R. Beene, E.D. Earle, A.B. McDonald, F.C. Khanna, I.S. Towner, Nucl. Phys. A 273 (1976) 253.

M. Ionescu-Bujor, E. A. Iordachescu, D. Plostinaru, G. Pascovici, Nucl. Phys. A 272 (1976) 1.

T. Lonnroth and S. Vajda, Z. Phys. A 317 (1984) 215.

H. Kusakari, K. Kitao, S. Kono, Y. Ishizaki, Nucl. Phys. A 34 (1980) 206.

T.Morek, H. Beuscher, B. Bochev, D.R. Haenni, Z. Phys. A 298 (1980) 267.

M. Ohshima, S. Hayashibe, N. Kawamura, Y. Itoh, M. Fujioka, T. Ishimatsu, Hyp. Ints. 7 (1979) 103.

J.M. Brennan, M. Hass, N.K.B. Shu, N. Benczer-Koller, Phys. Rev. C 21 (1980) 574.

Md. S. R. Laskar, S. Saha, R. Palit, S. N. Mishra, N. Shimizu, Y. Utsuno, E. Ideguchi, Z. Naik, F. S. Babra, S. Biswas, S. Kumar, S. K. Mohanta, C. S. Pal shetkar, P. Singh, and P. C. Srivastava, Phys. Rev. C 99 (2019), 014308.

E.A. Henry, N. Smith, P.G. Johnson, R.A. Meyer, Phys. Rev. C 12 (1975) 1314.

E.A. Henry, R.A. Meyer, Phys. Rev. C 12 (1975) 1321.

E.A. Henry, R.A. Meyer, Phys. Rev. C 13 (1976) 2063.

E.A. Henry, R.A. Meyer, Phys. Rev. C 18 (1978) 1814 12.

C. Gerschel, N. Perrin, L. Valentin, Journal de Physique 34 (1973) 753.

J.R. van Hise, G. Chilosi, N.J. Stone, Phys. Rev. 161 (1967) 1254.

P. Thakur, V. Kumar, A.K. Bhati, S.C. Bedi, R.P. Singh, R.K. Bhowmik, A.E. Stuchbery, Phys. Rev. C 74 (2006) 034329

FORM IV
(See rule 8)

1.	Registration No.	:	ISSN-0555-7631
2.	Place of Publication	:	Old Correspondence Building Panjab University, Chandigarh – 160014 (India)
3.	Periodicity of Publication	:	Annual
4.	**Publisher's & Editors' Name**	:	
	Editor-in-Chief	:	Professor G.S.S. Saini
	Nationality	:	Indian
	Editor	:	Professor Desh Deepak Singh
	Nationality	:	Indian
	Address	:	Research Journal (Science) Room No. 28-29, Old Correspondence Building, Panjab University, Chandigarh- 160014 (India)
5.	Printer's Name	:	Mr. Jatinder Moudgill
	Nationality	:	Indian
	Address	:	Manager Panjab University Printing Press Chandigarh – 160 014.
6.	Name and address of the Individuals who own the newspaper and partners or shareholders holding more than one percent of the total capital.	:	Panjab University, Chandigarh

Professor G.S.S. Saini , hereby declare that the particulars given above are true to the best of my knowledge and belief.

Professor G.S.S. Saini
Editor-in-Chief

PANJAB UNIVERSITY RESEARCH JOURNAL (SCIENCE)

LIFE MEMBERSHIP FORM

Name _____

Qualification _____

Area of Specialization _____

Present Designation _____

Address: (Tick the address on which you would like to receive the journal.
Local members would receive the journal by hand)

i. Office _____
_____

ii. Residence _____
_____

Telephone (O) _____
(R) _____
(Mobile) _____
Fax _____
Email. _____

Payment Mode:

(Only local cheques are acceptable. Draft to be drawn in favour of
The Registrar, Panjab University, Chandigarh

If by cheque/Draft:
Cheque/D.DNo. _____ Date _____ Amount_____
Name of the Bank: _____

Date _____
Place: _____

SIGNATURES

Subscription fee:

	Inland	**Foreign**
Life Membership:	Rs. 3000/-	US $ 250
Annual Subscription:	Rs. 400/-	US $ 50

Send to: The Editor-in-Chief
Research Journal (Science)
Old Correspondence Building
Panjab University, Chandigarh-160014(India)

INSTRUCTIONS FOR AUTHORS

Panjab University Research Journal of Science (PURJS) is an international peer-reviewed journal covering wide-range of research activities in all disciples of science.

PURJS provides opportunity to scientists, engineers and medical experts to publish original full research articles, rapid communications, state-of-the-art reviews in all disciplines of the science, engineering and medicine.

JOURNAL POLICY: It is PURJS policy to publish only original and unpublished research work, therefore, PURJS does not wish to receive any papers on research work that has already been reported in parts or contains already published text, data, figures, tables or other illustrations or any copyright materials whatsoever that has been submitted or accepted for publication either in a journal or conference proceedings elsewhere in any form, in print or in electronic media. When submitting a manuscript, authors should make a full statement to the Editors that the research work contained in their manuscript is completely original and unpublished. If redundant or duplicate publication is attempted or occurs authors should expect immediate editorial action to be taken including prompt rejection of the submitted manuscript. Submission of any manuscript that contains redundant or duplicate publication of the same or very similar research work violates the policies of this journal

ETHICAL COMPLIANCE: Research papers reporting animal or clinical studies should, where appropriate, contain a statement that they have been carried out with animal or human ethics committee approval. All scientific studies should be carried out in accordance with the relevant national and local guidelines. Each author(s) warrants that his or her research institution has fully approved the protocol for all scientific studies involving animals or humans and that all experiments of any kinds were conducted in compliance with ethical and humane principles of research after ethics committee approval.

SUBMISSION OF MANUSCRIPT: Authors are requested to read PURJS policy before submitting their manuscript to Editors. Authors are encouraged to submit high quality original research work that has not been published or nor under consideration by other journals or conference proceedings elsewhere. Authors should submit manuscript electronically as a Microsoft Word file to the Editor-in-Chief. Authors are highly encouraged to submit manuscript electronically as a MS Word file (preferred) or a PDF file to save time for the reviewing process.

Authors should submit a list of SIX (6) potential referees accompanied with their complete mailing address, telephone, fax and email address, who may be contacted for reviewing the manuscript though refereeing, is done by anonymous reviewers selected by the Editor-in-Chief or Editor. (The selection of the reviewer is the discretion of Editors –in-chief and reviewers may not necessarily be from the list provided).

MANUSCRIPTS - The manuscripts should be typewritten (double spaced) with ample margins.

Page 1 should contain only title of manuscript, author(s) name(s) and affiliation(s), a short running title (abbreviated from the title) not exceeding 40 characters, name & complete mailing address of the person to whom correspondence should be addressed.

Page 2 should contain an abstract not exceeding 150 words. The abstract should contain no illustration or reference to the figures, tables, or authors. The abstract should be followed by 3-4 key words.

Rest of the content also continue from this page and should be described under Headings, Introduction, Results and Discussions. Acknowledgements should be inserted at the end of the text before References.

SHORT COMMUNICATION: A short communication should be a record of completed short investigation giving details of new methods or findings. It should not exceed 4 to 5 typed pages with an Abstract followed by Key words. Body of the text should not have any separate title, like Abstract, Materials and Methods, Results and Discussion except the Acknowledgements and References.

REFERENCES:

While citing references in the text it should conform to the following style:-

Adherence of *E. coli* to intestinal mucosal surface...pathogenesis (Beachey, 1981). According to Arnoldi (1976), these feathers....

The references at the end of article should be in alphabetical order and presented as follows:-

Ahuja, D.B. 1990. Population dynamics of mustard aphid, Lipaphis erysimi (Kalt.) on Indian mustard Brassica juncea. Indian J. Plant Protection, 18 : 233-235.

Bener, A. and F.C. Erk. 1979. The analysis of whorls on specific fingerstips with respect to sex, bilateral asymmetry and genetic relationship. Ann. Hum. Biol., 6 : 349 - 356.

Buskrik, E.R., K.L. Anderson, and J. Brozek. 1956. Unilateral activity and bone and muscle development in the forearm. Res. Quart., 27 : 127-131.

Jain, S.K. 1986. Orchid Wealth of India. In: Biology, Conservation, and Culture of Orchid
s (Ed.S.P.Vij) pp. 319-22. Affiliated East - West Press (New Delhi).

ILLUSTRATIONS: The illustrations, preferably be in the form of text-figures, should also be submitted electronically. All figures whether photographs or drawing, must be numbered in single series (Fig. 1, 2, 3.etc.). The figures should be arranged and numbered in the order in which they are referred to in the text. The figures or photographs (plates) submitted for publication must not be less than 300 DPI. The ratio of length & width of the full figure plate must necessarily be in proportion to the page size of the journal i.e. 23 cm x 18 cm. Figures must carry magnification bars.

Legends to figures should be typed on a separate sheet of paper to be inserted after References. Abbreviations used for the figures should be given in an alphabetical order after the legends.

TABLES: Tables 1, 2, 3 should be single-spaced on separate page and numbered. Each table must bear a short descriptive heading.

PROOFS: Page proof will be sent to corresponding author.

Manuscripts and Correspondence should be addressed:

Editor-in-Chief
Research Journal of Science
Old Correspondence Building
Panjab University,
Chandigarh. 160 014 (India)
Telephone: 0172-2534376
E.mail : resjoursci@pu.ac.in

Published by :
EDITOR-IN-CHIEF
Research Journal (Science)
Panjab University, Chandigarh-160 014
INDIA

www.puchd.ac.in

ISSN-0555-7631